Molecular logic gates

Koskela, Suvi Jonna Mikaela

Award date:
2003

Awarding institution:
University of Bath

MOLECULAR LOGIC GATES

submitted by Suvi Jonna Mikaela Koskela

for the degree of PhD

of the University of Bath

2003

Suvi Koskela

ProQuest LLC
789 East Eisenhower Parkway
P.O. Box 1346
Ann Arbor, MI 48106-1346

Abstract

Many complex life processes depend on simple cations and anions. Protons are involved in bioenergetics, sodium and potassium in membrane potential generation and calcium ions in intracellular signalling. Anions, like phosphate and fluoride, also play important roles in different chemical as well as biological systems, therefore making their detection fundamental. Fluoride is present in biological fluids and tissues, especially in bone and teeth. Fluoride is also released during the hydrolysis of some substances used as chemical weapons such as sarin and determination of the fluoride concentration can be used to quantify the concentration of the nerve agent.

Two series of sensors, with naphthalene and pyrene as fluorophores, have been prepared and evaluated. The sensors consist of a fluorophore and two receptor units; a benzocrown ether (cation receptor) and a boronic acid (fluoride receptor). Fluorescence spectroscopy studies have shown that the pyrene sensor with boronic acid and either benzo-15-crown-5 or benzo-18-crown-6 ether as receptors give significant fluorescence changes upon complexation in methanol with potassium fluoride. Potassium chloride and potassium bromide cause no change in fluorescence intensity, which shows that the fluorescence cannot be switched on unless both receptors are bound to their respective species (potassium cation to the crown ether unit and fluoride anion to the boronic acid unit). The fluorescence of a model compound, which does not have a crown ether unit to bind the cation, does not change when potassium fluoride is added. These results confirm that the sensors behave as AND logic gates, i.e. both receptors of the sensor have to be bound to their substrates to give an output.

The sensors' interaction with fluoride in chloroform has also been evaluated. All the sensors investigated have shown spectral changes upon addition of tetrabutylammonium fluoride in chloroform. The breaking of a weak boron-nitrogen bond by fluoride in these molecules is proposed to explain the spectral behaviour.

Abstrakt

Många komplexa livprocesser är beroende av enkla katjoner och anjoner. Protoner deltar i bioenergi, natrium och kalium i generationen av membran potential och kalcium i intracellular signallering. Anjoner, till exempel fosfat och fluorid, spelar också en viktig roll i olika kemiska och biologiska system, därmed är också detektion av dem fundamental. Fluorid finns i biologiska vätskor och vävnader, speciellt i ben och tand. Detektion av fluorid i dricksvatten är viktigt p.g.a. allvarliga hälsoskador vid överdosering. Fluorid utsöndras också under hydrolys av kemiska vapen, som till exempel sarin, och bestämning av fluorid koncentrationen kan användas till att kvantisera koncentrationen av nervgasen.

Två olika serier av sensorer med naftalen och and pyren som fluoroforer, har framställts och evaluerats. Sensorerna består av en fluorofor och två receptorer; en kroneter (katjon receptor) och en boronisk syra (fluorid receptor). Undersökning med fluoresens spektroskopi har visat att sensoren med dessa receptorer och pyren som fluorofor bildar komplex med kaliumfluorid i metanol och signallerar detta genom att fluoresera. Kaliumklorid och kaliumbromid orsakar ingen förändring i fluoresens intensiteten, vilket visar att fluoresensen kan inte kopplas på ifall inte båda receptorerna är bundna till respektive substrat (kalium katjonen till kronetern och fluorid anjonen till boronisk syra). Fluoresens intensiteten av modell molekyler ändras inte då kaliumfluorid tillsätts. Dessa modellmolekyler har ingen kroneter som binder katjonen. Dessa resultat bekräftar att sensorerna beter sig som AND logic gate, d.v.s. båda receptorerna måste vara bundna till respektive substrat för att ge respons.

Sensorernas interaktion med fluorid joner i kloroform har också undersökts. Alla undersökta sensorer visade avtagande av fluoresens då tetrabutylammoniumfluorid tillsattes. Detta spektroskopiska beteende kan förklaras med brytning av en svag bor-kväve bindning.

Tiivistelmä

Monet monimutkaiset luonnonprosessit riippuvat yksinkertaisista kationeista ja anioneista. Protonit osallistuvat bioenergiikkaan, natrium ja kalium membraani potentiaalin kehitykseen ja kalsium ionit solujen väliseen signalointiin. Anionit, kuten fosfaatti ja fluoridi, näyttelevät myös tärkeää osaa eri kemiallisissa sekä biologisissa systeemeissä. Fluoridia esiintyy biologisissa nesteissä ja kudoksissa, erityisesti luussa ja hampaissa. Fluoridia vapautuu myös eräiden kemiallisten aseiden, esimerkiksi sariinin, hydrolyysissä. Täten fluoridi konsentraation määritystä voidaan käyttää hermoagenssin kvantitointiin.

Kaksi sensorisarjaa, naftaleeni ja pyreeni fluorofooreina, on syntetisoitu ja määritetty. Sensorit koostuvat fluorofoorista ja kahdesta reseptori osasta; bensokruunueetteri (kationi reseptori) ja boronihappo (fluoridi reseptori). Fluoresenssi spektroskopia tutkimukset ovat osoittaneet että sensori, joka koostuu näistä reseptoreista ja pyreeni fluorofoorista, tuottaa huomattavan fluoresenssi muutoksen muodostaessa kompleksin metanolissa kaliumfluoridin kanssa. Kaliumkloridi ja kaliumbromidi eivät tuota muutosta fluoresenssi intensiteetissä, mikä osoittaa että fluoresenssia ei voi kytkeä päälle elleivät molemmat reseptorit ole sitoutuneet (kalium kationi kruunueetteri osaan ja fluoridi anioni boronihappo osaan). Mallimolekyylien fluoresenssi intensiteetti ei muutu kaliumfluoridia lisätessä. Näillä mallimolekyyleillä ei ole kruunueetteriosaa joka sitoo kationin. Nämä tulokset vahvistavat että sensorit käyttätyvät kuten AND logic gate, eli molemmat sensorissa olevat reseptorit tulevat olla sitoutuneet substraattiin antaakseen tuloksen.

Sensoreiden ja fluoridin vuorovaikutusta kloroformissa on myös tutkittu. Kaikki tutkitut sensorit ovat tuottaneet spektroskooppisia muutoksia kun tetrabutyyliammonium fluoridia on lisätty kloroformissa. Tämän spektroskooppisen käytöksen on ehdotettu johtuvan molekyylin heikon boori-typpi sidoksen katkaisusta fluoridin sitoutuessa.

Acknowledgements

There are many people I would like to thank for their help and encouragement during these three years. First of all I would like to thank my supervisor Dr Tony James for giving me this great opportunity of doing a PhD in the first place and for his continuous help and support. Thanks also go to the past and present members of BART (Boronic Acid Research Team) for their help and team spirit: Dr Christopher Cooper, Dr James Hartley, Dr Christopher Ward, Dr Karine Frimat, Dr Susumu Arimori, Dr Giuseppe Gonsiglio, Laurence Bosch, Marcus Phillips, Yolanda Perez, Rachel Green and Mike Thatcher. I am also very grateful to Professor Thomas Fyles for helping me with my tricky graphs during the last months of my PhD.

I also wish to thank Beckman-Coulter, Universities of Birmingham and Bath for funding my PhD. I wish to thank the analytical and technical staff at both universities for their expertise.

I wish to thank all my friends at Birmingham and Bath universities. Thank you to Lucile, Jodi and Alex for our wine and cake evenings and for making my year in Birmingham so memorable. Thanks go to all the people in my lab, past and present, Cath 'Beyonce', Steve 'Le Fleur', Steve Hillier, Rachel, Phil and Mike for the strong coffee (who made it?), chats and dancing in the lab to Madness. Big thanks should also go to the 'coffee and crossword group': Chris, Kelly, Diane, Fleur, Duncan, Steve and Mike for the relaxing lunch breaks every day. Also big thanks to Diane, Marcus, Mike, Steve Flower, Michael and Steve who proofread my thesis! And I also wish to thank everyone at the Organic Department.

Enormous thanks and all my love go to my parents and my grandma for all the support and encouragement and for helping me out when the money's been tight. Ett enormt tack till min mamma för oändlig stöd och hjälp under alla mina skol- och studieår! Suuret kiitokset isilleni jatkuvasta mielenkiinnosta ja tuesta, hyvistä neuvoista sekä rahallisesta avusta koko opiskeluni aikana! Kiitokset mummilleni korvaamattomasta tuesta ja uskosta sekä rahallisesta avusta!

And finally, a huge big massive thank you to Steve for supporting me through hard times and for helping and advising especially during these last few months. Tack stora gröna randiga byxor,

I love you!

In loving memory of my grandfather

I kärt minne av min morfar

Kurt-Erik Rafael Grönqvist

(1920-2003)

Table of Contents

Abbreviations

AIBN	2,2'-Azobisisobutyronitrile
Ar	Aryl
br	Broad
CI	Chemical ionisation
δ	Chemical shift
d	Doublet
D	^{2}H
Δ	Heat
dec.	Decomposed
DMSO	Dimethylsulphoxide
e^-	Electron
EF	Enhancement factor
EI	Electron impact ionisation
ESI	Electrospray ionisation
EtOAc	Ethylacetate
FAB	Fast atom bombardment
g	Gram
h	Hours
hν	Light
HOMO	Highest occupied molecular orbital
HPLC	High performance liquid chromatography
HRMS	High-resolution mass spectrometry

I_F	Intensity of fluorescence emission
ICT	Internal charge transfer
IR	Infra-red
J	Coupling constant
K_a	Association constant
K_d	Dissociation constant
λ	Wavelength
lit.	Literature
LUMO	Lowest unoccupied molecular orbital
m	Multiplet
m-	*Meta-*
Me	Methyl
MeCN	Acetonitrile
MHz	Megahertz
mmol	Millimole
mM	Millimolar
mV	Millivolt
mp	Melting point
MS	Mass spectrometry
m/z	Mass to charge ratio
Naph	Naphthalene
NBS	*N*-bromosuccinimide
NMR	Nuclear magnetic resonance
nm	Nanometer
o-	*Ortho-*
p-	*Para-*

PET	Photoinduced electron transfer
Ph	Phenyl
ppm	Parts per million
Py	Pyrene
rt	Room temperature
s	Singlet
st	Strong
t	Triplet
*t*Bu	Tertiarybutyl
THF	Tetrahydrofuran
TLC	Thin layer chromatography
TFA	Trifluoroacetic anhydride
UV	Ultraviolet
v/v	Volume for volume
w/w	Weight for weight

1 *Introduction*

"Oh! Piglet," said Pooh excitedly, "we're going on an Expedition,

all of us, with things to eat. To discover something."

"To discover what?" said Piglet anxiously.

"Oh! Just something."

A. A. Milne

1.1 Fluorescent chemosensors

Sensors have long been important to detect the presence of different chemically or biologically important species. A sensor is a device, which gives a signal upon guest binding (Figure 1).

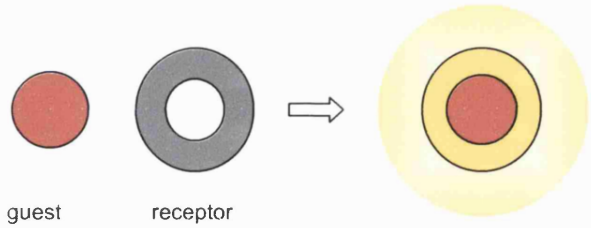

Figure 1. The action of a sensor: Signalling results when a guest binds to a receptor.

The phenomenon of molecular fluorescence possesses many features which make it particularly suitable for real-time, and real-space monitoring of atomic and molecular events.[1] The molecular basis means that it can report on the nanoscale if properly targeted. The active molecules can be easily "smuggled" into dynamic living systems, which then act as unwitting hosts. The fluorescence can be easily switched "off" and "on"; the fluorescence mechanism is slow enough that it can be switched "off" by competing chemical processes. It is also possible to arrange for switching "on" because quenching mechanisms are also influenced by chemical processes. Hence a two-state digital action is feasible.

Figure 2 describes the fluorescence principle and the various absorption and emission processes, which can occur in a molecule.[2]

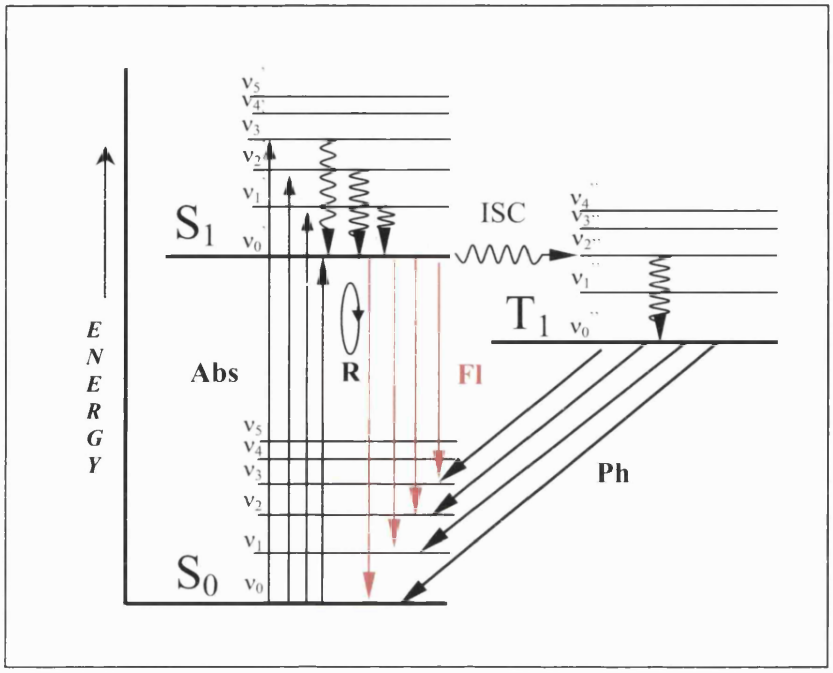

Figure 2. A molecular energy level diagram showing absorption (Abs), resonance emission (R), fluorescence (Fl), intersystem crossing (ISC) and phosphorescence (Ph).

The singlet ground electronic state of a molecule is represented as S_0. The first excited state and the first triplet state are represented by S_1 and T_1, respectively. Each electronic level has a series of vibrational states, labelled ν_1, ν_2, ν_3,... The most probable and intense emission is the resonance emission (R), which results from re-emission of absorbed light energy (Abs) (transition between ν_0' and ν_0). Fluorescence (Fl) is the emission, which results from the return from a higher energy level to a lower one at a longer wavelength (lower energy). The difference in energy in fluorescence corresponds to radiationless decay. This energy is lost in collisions with other atoms or molecules as kinetic energy of motion or in excited vibrational states in other particles. Phosphorescence (Ph) is the result of the emission from a triplet to a singlet state and because it is a forbidden transition it

will only occur very slowly requiring up to 1 second or even longer. The fluorescence emission, however, is allowed and is a very rapid transition, requiring less than 10^{-8} seconds to occur.

Compounds incorporating a binding site, a fluorophore, and a mechanism for communication between the two are called fluorescent chemosensors.[3] Fluorescent photoinduced electron transfer[4] (PET) sensors generally consist of a fluorophore and a receptor linked by a short spacer as seen in Figure 3.[5-7] A fluorophore is a molecule, which is able to fluoresce: anthracene, pyrene and naphthalene are examples of fluorophores. The changes in redox potential of the receptor upon guest binding can alter the PET process and generate changes in the fluorescence allowing switching "on" and "off".[6]

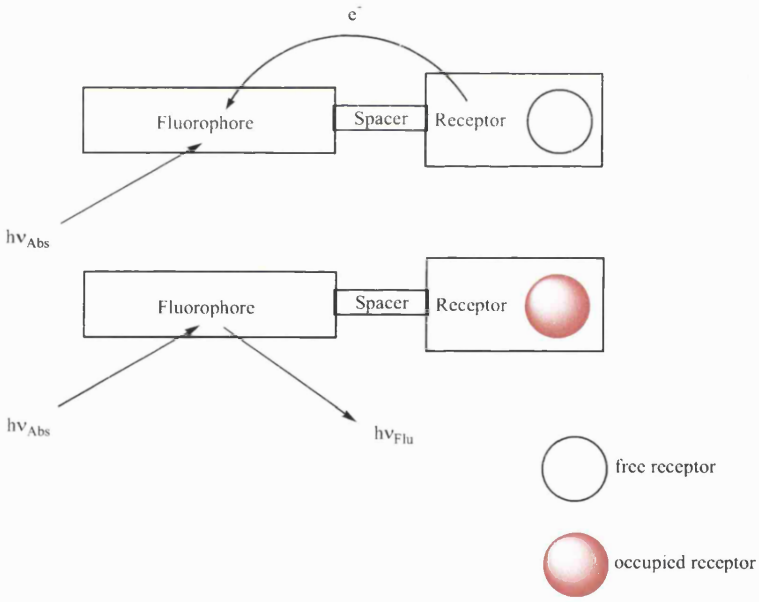

Figure 3. Schematic diagram of a fluorescent 'Off-On' sensor.

An example of an 'Off-On' sensor is depicted in Figure 4.[8] The fluorophore of the sensor is anthracene and two diethylamino units act as receptors for protons. At pH

values above 9 the diethylamino units participate in PET with the anthracene fluorophore and the sensor remains non-fluorescent. At pH values below 5, binding of protons inhibits the PET process and switches on the fluorescence.

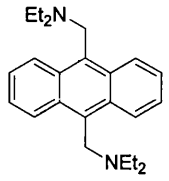

Figure 4. Example of an 'Off-On' fluorescent PET sensor.

The fluorescence can be switched "off" by the PET process. The PET process, in turn, can be suppressed by the entry of a guest into the receptor, which is then able to "switch on" the fluorescence. Further clarification on the PET process is possible in the terms of frontier orbital energy diagrams in Figure 5 and Figure 6.

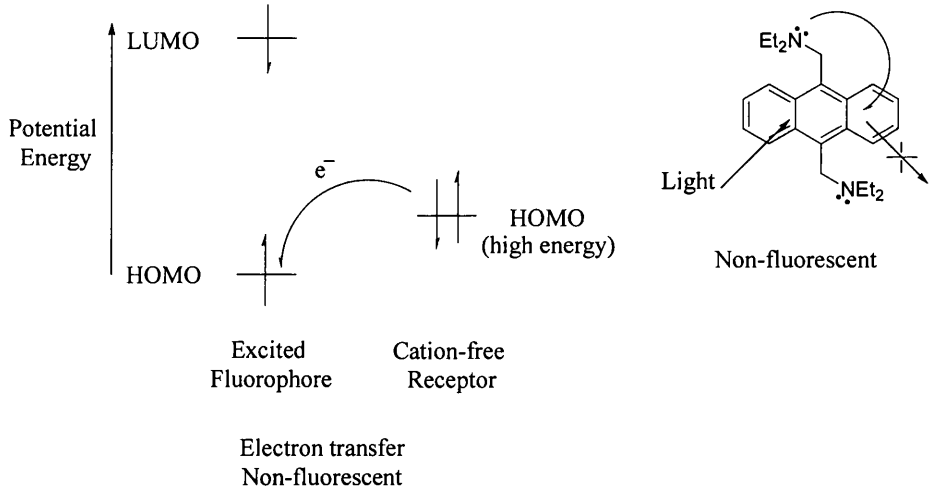

Figure 5. Frontier orbital energy representation of photoinduced process in an 'Off-On' signalling system and corresponding molecular example when cation-free.

When the receptor is free PET occurs to the lower HOMO of the fluorophore as shown in Figure 5.[9] Since the electron in the LUMO cannot return to the HOMO,

fluorescence will not take place. In the molecular example PET is occurring from the nitrogen lone pair in the amine to the anthracene fluorophore, which quenches the fluorescence. However, when the sensor is bound to its target (Figure 6), the energy of the HOMO of the receptor is reduced. Therefore PET cannot occur and fluorescence can take place.

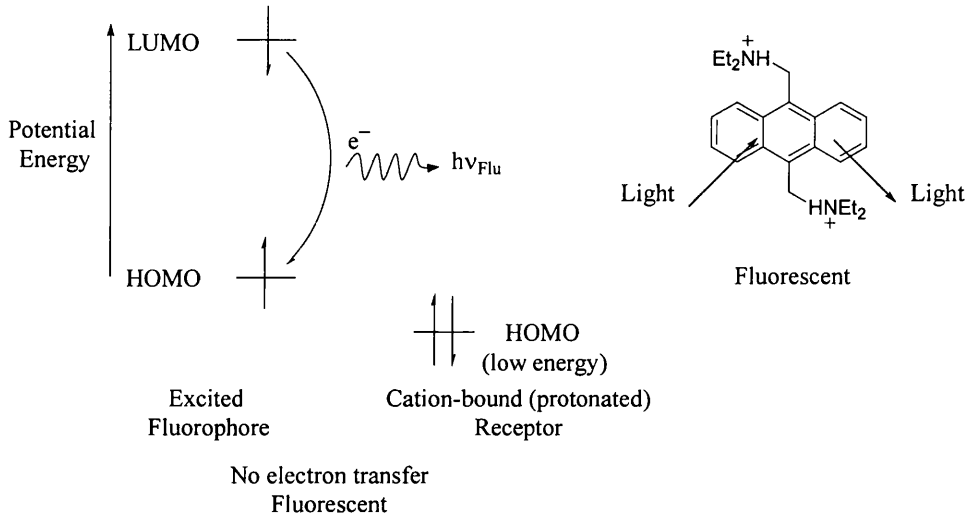

Figure 6. Frontier orbital energy representation of photoinduced process in an 'Off-On' signalling system and corresponding molecular example when cation-bound.

'On-Off' sensors are the opposite of the 'Off-On' sensor discussed above. As seen in Figure 7, when the receptor of the sensor is unoccupied there is no PET occurring and the sensor fluoresces. When the receptor is occupied there is a significant change in the situation. For simplicity a cationic target is considered. The electrostatic attraction will enable an electron to be transferred into the cation-bound receptor from the photoexcited fluorophore.[10]

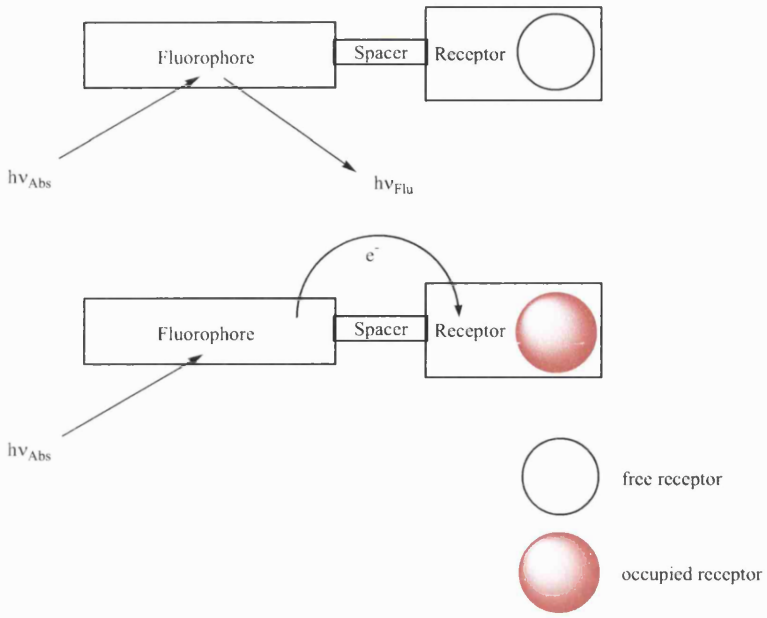

Figure 7. Design of 'On-Off' fluorescent PET sensor.

An example of an 'On-Off' fluorescent PET sensor is depicted in Figure 8.[11] The nitrogen of the pyridine ring is the proton acceptor and the delocalised 15-atom pi-electron system is identifiable as the fluorophore. The electron that originates from the fluorophore only has to cross a single spacer carbon atom before it arrives to the proton-bound receptor. This results in the "off"-switching of the blue-green fluorescence observed at pH values <7.

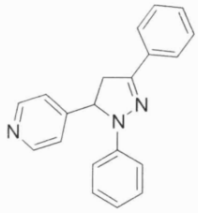

Figure 8. Example of an 'On-Off' fluorescent PET sensor.

When the receptor is free the molecule is able to fluoresce. The PET process can be amplified by the entry of a guest into the receptor, which is then able to "switch off" the fluorescence. Further clarification on the PET process in 'On-Off' systems is shown in terms of frontier orbital energy diagrams in Figure 9 and Figure 10.

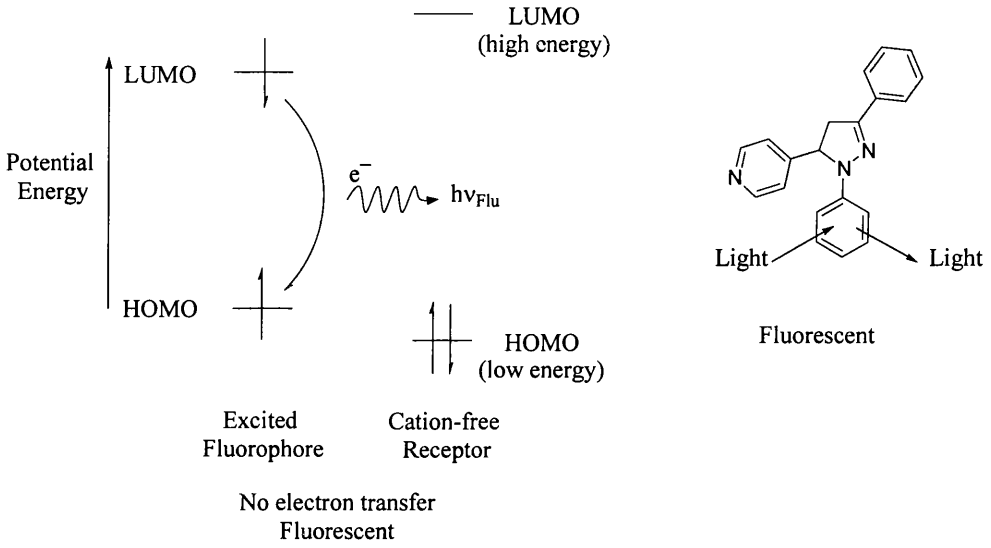

Figure 9. Frontier orbital energy representation of photoinduced process in an 'On-Off' signalling system and corresponding molecular example when guest-free.

In 'On-Off' systems, when the receptor is free, the LUMO of the receptor has higher energy than the LUMO of the fluorophore and the PET does not occur (Figure 9). This allows the electron to return to its HOMO and fluorescence takes place.

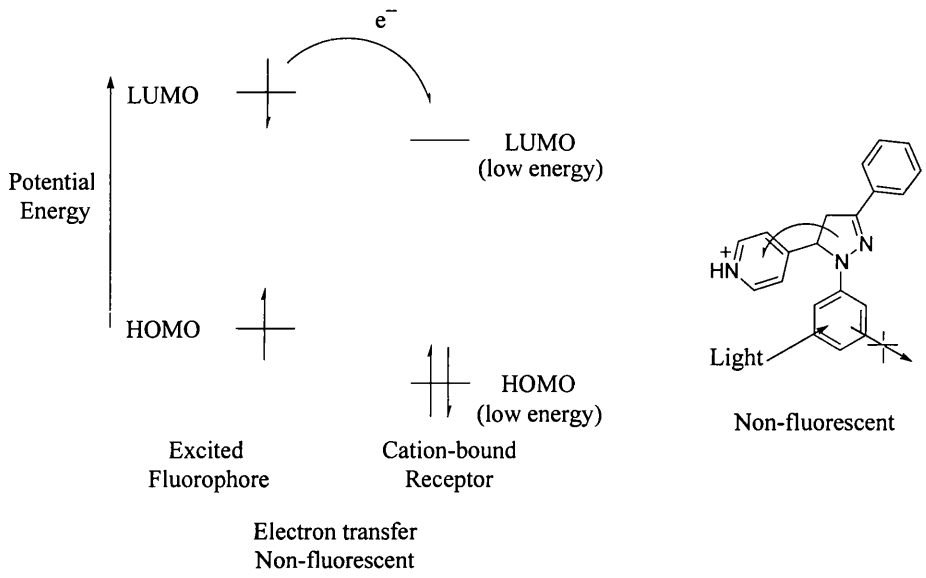

Figure 10. Frontier orbital energy representation of photoinduced process in an 'On-Off' signalling system and corresponding molecular example when cation-bound.

When the host is occupied, the fluorescence signal is switched 'off' by PET from the LUMO of the fluorophore to the LUMO of the receptor (Figure 10). Since the electron in the excited state cannot return to the HOMO of the fluorophore, fluorescence will not take place.

Other fluorescent systems also exist, for example charge transfer and electronic energy transfer systems. There is an excellent review by de Silva *et al.* on these and other fluorescent systems.[12]

Boronic acids in fluorescent systems

Michaelis and Becker first synthesized phenylboronic acid as long ago as 1882.[13] Kuivila was the first to study the binding between the diols of saccharides and boronic acids in 1954 and postulated the formation of a cyclic ester.[14,15] This was confirmed in 1959 by Lorand and Edwards. Boronic acids readily and reversibly form cyclic esters with diols in aqueous basic media. The most common interaction is with 1,2- and 1,3-diols of saccharides to form five- and six-membered rings respectively *via* two covalent bonds in nonaqueous or basic aqueous media. The rigid, vicinal *cis* diols of saccharides form more stable cyclic esters than simple acyclic diols such as ethylene glycol.[6]

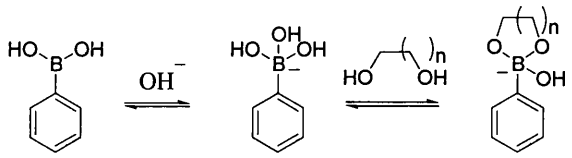

Scheme 1. Complexation of saccharide with boronate anion.

Boronic acids only bind strongly with saccharide in water at pH values high enough to create a boronate anion as shown in Scheme 1. To overcome this disadvantage fluorescent sensors using amines have been designed. The neighbouring group participation of the amine group lowers the working pH of the sensor molecule and also provides an electron-rich centre for PET to occur.[1,6,8,9,16] When saccharides form cyclic boronate esters with boronic acids, the acidity of the boronic acid is enhanced and therefore the Lewis acid-base interaction between the boronic acid and the tertiary amine is strengthened (Figure 11).

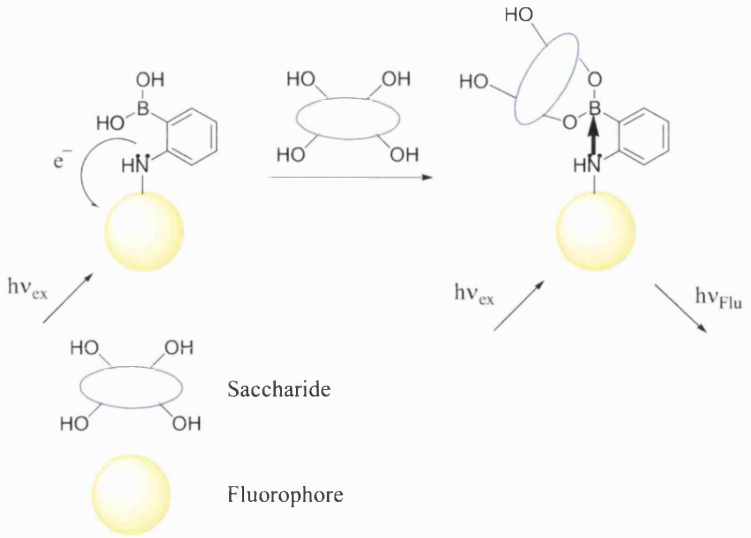

Figure 11. Neighbouring group participation of nitrogen with boron.

The strength of this acid-base interaction modulates the PET from the amine (acting as a quencher) to the fluorophore as shown in Figure 5 using frontier orbital energy diagrams.[9] When the sensor is free, PET occurs from the amine to the lower energy level of the fluorophore. Since the electron in the excited state cannot return to this lower energy level, fluorescence will not take place. However, when the sensor is bound to its target the Lewis acid-base interaction between the boronic acid and the amine is strengthened, PET cannot occur and fluorescence can take place.

Fluorescent sensors where boronic acid and amine interact to give photoinduced electron transfer (PET) have received much attention.[17-23] An advantage with fluorescent sensors for saccharides is the inherent sensitivity of the fluorescent technique. Because only small amounts of a sensor are required (typically 10^{-6} M), the synthetic costs of such sensors can be offset. Moreover, fluorescence spectrometers are widely available and inexpensive.

Molecular logic gates

Molecular logic gates follow the Boolean logic operations.[24] These rely on the binary 'yes-no', '1-0', or 'true-false' concept. The function of a logic gate can be read in a truth table. The simplest logic gate is the 1-input YES logic operation, where for an input 1 there is an output 1. The first column corresponds to the possible input and the operation being performed (positive (1) or negative (0)) can be read in the second column.

Input	Output
1	1
0	0

Figure 12. Truth table for YES logic operation.

Sensors designed as the 'Off-On' sensor, as depicted in Figure 3, behave like YES logic gates i.e. they are 'switched on' for a positive input. The applications of molecular logic gates in molecular digital computing are of considerable current interest.[25,26]

There are a variety of different logic gates, for example NAND, NOR, INH and XOR,[27-33] but only two types OR and AND will be discussed here.

OR logic gates

The OR gate provides a true output when any of its inputs are true. This means in chemical terms that whenever the multiple chemical inputs independently produce an output the molecule can be regarded as an OR logic gate. In other words OR logic gates do not have chemoselectivity.

a. **OR logic gate**

Input 1	Input 2	Output
0	0	0
0	1	1
1	0	1
1	1	1

b.

Figure 13. (a) Truth table and (b) physical electronic symbol of an OR logic gate.

Figure 14 shows an example of an OR logic gate for potassium or rubidium ions.[34]

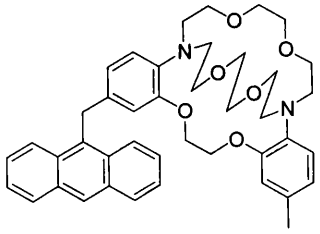

Figure 14. Example of a molecular OR logic gate.

This sensor has poor selectivity for cations and can bind to either potassium or rubidium ions. The cation-induced enhancement of the fluorescence is due to the suppression of a fast photoinduced electron transfer. Addition of either potassium

or rubidium to the sensor in Figure 14 in methanol enhances the fluorescence by similar factors (EF 9.4 and 10.6 respectively).

AND logic gates

The AND gate provides an output only when all inputs are true; i.e. the AND logic gates require two inputs to produce a fluorescence output. The nature of an AND gate is illustrated in Figure 15a.

a. **AND logic gate**

Input 1	Input 2	Output
0	0	0
0	1	0
1	0	0
1	1	1

b.

Figure 15. (a) Truth table and (b) physical electronic symbol for an AND logic gate.

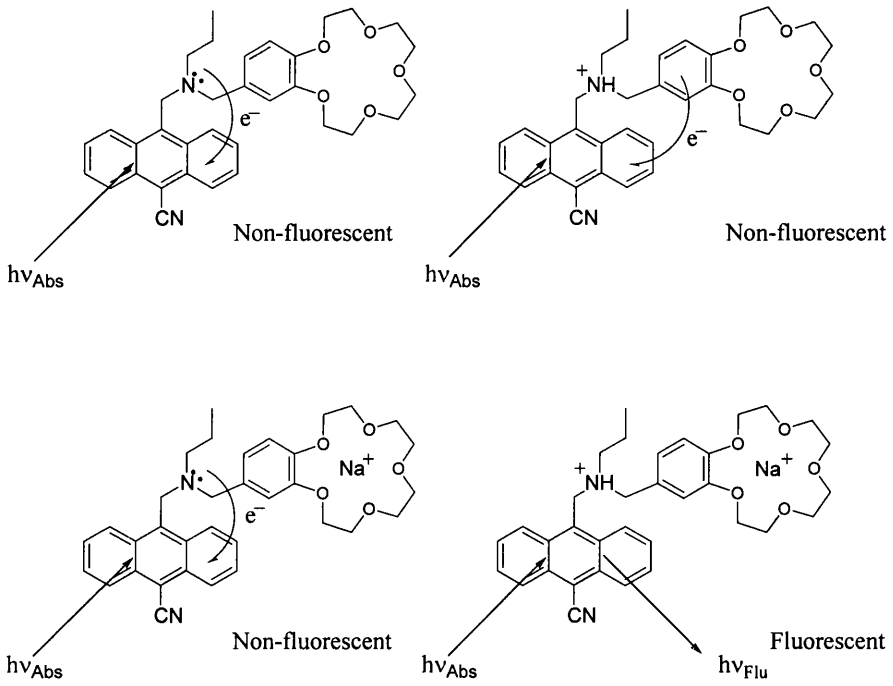

Figure 16. Example of a molecular AND logic gate.

De Silva and co-workers were first to design a molecular AND logic gate (Figure 16) in 1993. The molecule is based on 'fluorophore-spacer$_1$-receptor$_1$-spacer$_2$-receptor$_2$' format in Figure 18, with anthracene as the fluorophore and benzo-15-crown-ether and a tertiary amine as the receptors.[35] This molecule requires both Na^+ and H^+ input, to produce a fluorescence output. The fluorescence quantum yield ϕ_F increases from 0.011 to 0.068 and the enhancement factor goes up to 6.0.

Other examples of AND logic gates are depicted in Figure 17. The molecule in Figure 17 is a crown-armed pyridoimidazopyrazin (PIP) derivative, where the aromatic PIP system acts as the fluorophore and the crown ether receptor recognises the two input signals, alkaline earth metal cations and thiocyanate anions.[36] When calcium or barium thiocyanate was added there was a significant quenching of the fluorescence; however, when the corresponding perchlorates

were added there was no fluorescence change. Also, the fluorescence remained unchanged when sodium or potassium thiocyanates and perchlorates were added. Quenching observed with the thiocyanate anion and not with the perchlorate anion is explained by the PET from the thiocyanate anion to the PIP ring.[19,37]

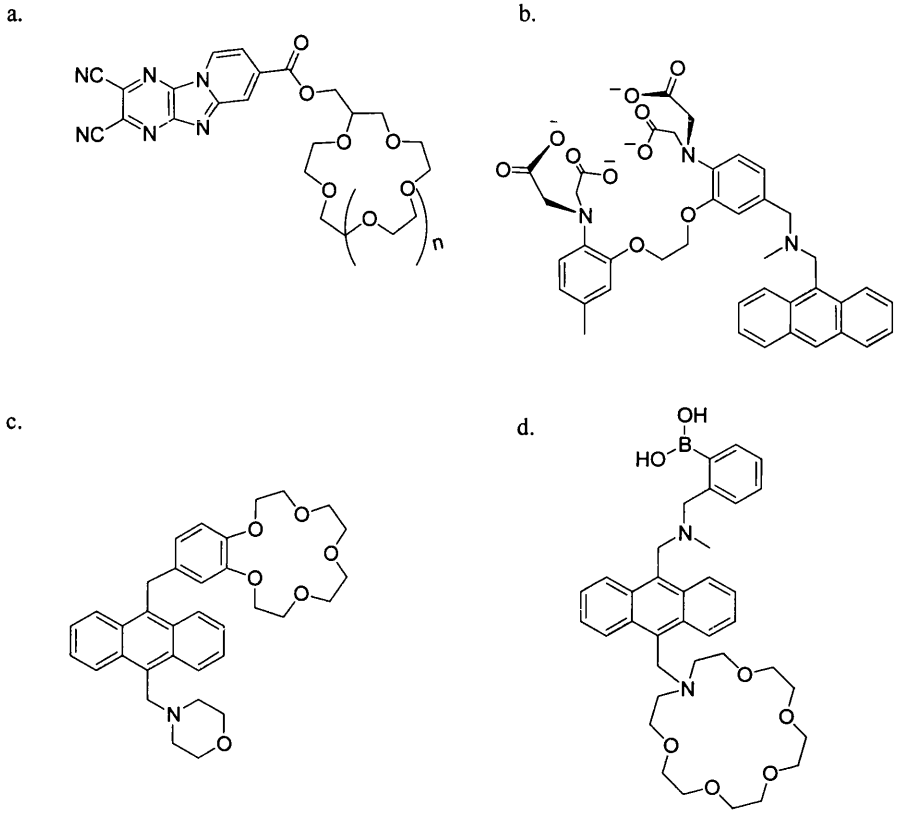

Figure 17. Examples of molecular AND logic gates.

De Silva and co-workers have designed an AND logic gate which binds to both Ca^{2+} and H^{+} to produce fluorescence (Figure 17b). This molecule and the AND logic gate in Figure 16 are based on the 'fluorophore-spacer$_1$-receptor$_1$-spacer$_2$-receptor$_2$' design shown in Figure 18.[38]

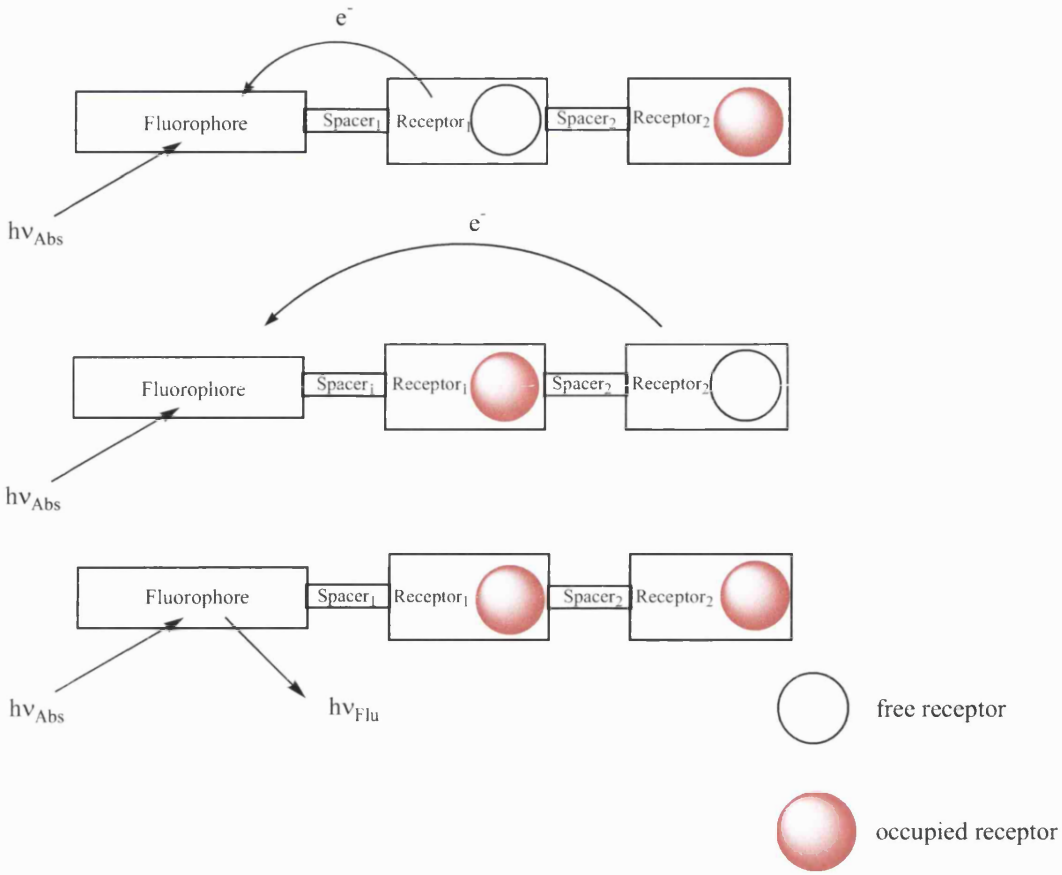

Figure 18. Design of an 'Off-On' AND logic gate fluorescent PET sensor; the 'fluorophore-spacer$_1$-receptor$_1$-spacer$_2$-receptor$_2$' design.

The AND logic gate in Figure 17c emits virtually no fluorescence unless both Na^+ and H^+ are present.[39] The fluorescence is quenched by PET in the molecule. When only H^+ is added the PET from the nitrogen lone-pair is stopped but the fluorescence is still quenched by PET from the crown ether of the sensor. Addition of Na^+ stops the PET from the crown ether, but there is still PET from the lone pair of the nitrogen. When both cations are added neither of the two PET actions can occur and the emission quantum yield ϕ_F increases from 0.0031 to 0.24. The sensor in Figure 17d is a PET sensor for D-glucosamine hydrochloride.[17,18] The sensor consists of monoaza-18-crown-6 ether as a binding site for the ammonium terminal of D-glucosamine hydrochloride, while a boronic acid serves as a binding

site for the diol part of the D-glucosamine hydrochloride. The nitrogen of the azacrown ether participates in PET with the anthracene, which is hindered by the binding of the ammonium ion. The boronic acid also participates in PET with the fluorophore, which stops upon diol binding. When both receptors are bound to their substrates the PET no longer occurs and the sensor will fluoresce. Hence, this sensor is an AND logic gate. This sensor and the previously described sensor in Figure 17c are both based on the 'receptor$_1$-spacer$_1$-fluorophore-spacer$_2$-receptor$_2$' format as illustrated in Figure 19.

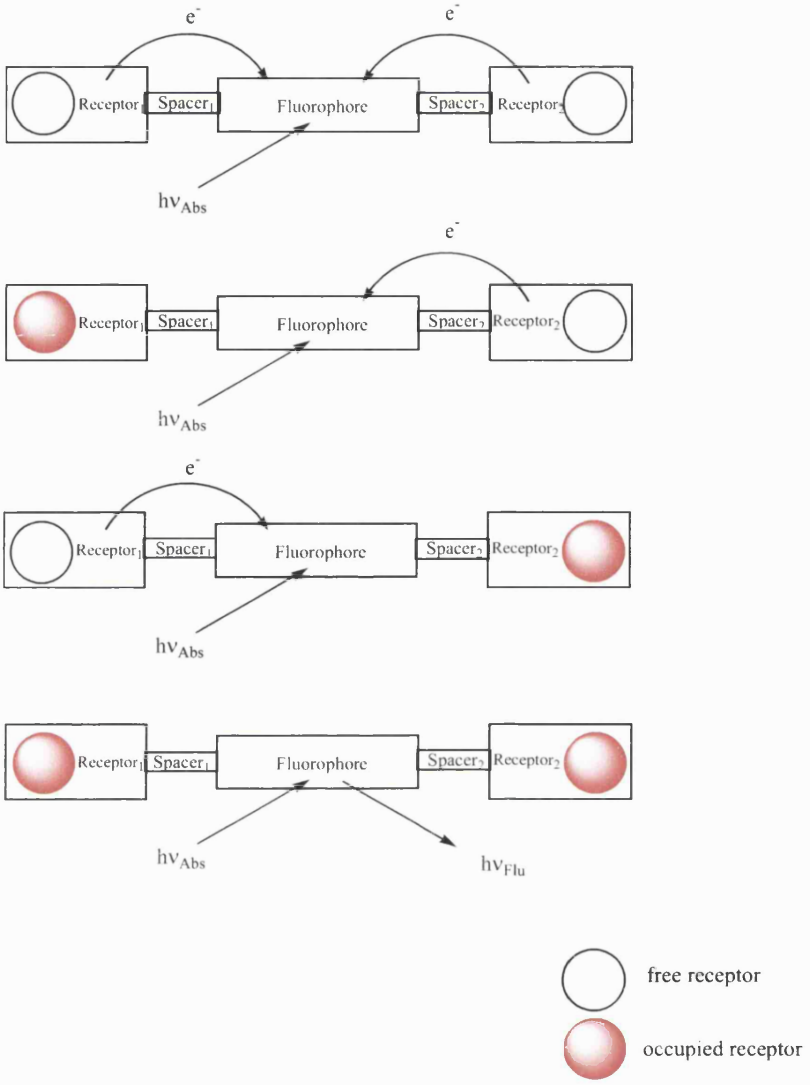

Figure 19. Design of fluorescent PET sensor displaying AND logic; the 'receptor$_1$-spacer$_1$-fluorophore-spacer$_2$-receptor$_2$' design.

Other types of AND logic operations have been designed, for example the self-assembly of DNA strands, where oligonucleotides represent the AND logic gate, input signals and output signals.[40] AND logic gates have even been used in the design of a chemically assembled electronic nanocomputer, which is based on rotaxanes.[31,32]

1.2 *Sensor systems for cations*

Many complex life processes depend on a few simple cations, e.g. sodium and potassium in membrane potential generation, calcium ions in intracellular signalling and protons in bioenergetics. A large number of fluorescent sensors for metal ions have been developed during the past decade and the chemistry of fluorescent systems is a wide area. The attention of this thesis is going to be focused on the fluorescent sensors designed for alkali and alkaline earth metals. For further reading on metal sensors the reader is directed to excellent reviews on fluorescent systems for transition metals[41,42] and electrochemical metal sensors.[43]

Crown systems

The discovery of crown ethers and their ability to form complexes with metal ions has been applied in many ways including the development of cation sensors.[44-48] In 1977, Sousa described the synthesis of naphthalene-crown ether probes in which the fluorophore π–system is insulated from the donor atoms by at least one methylene group (Figure 20).[49]

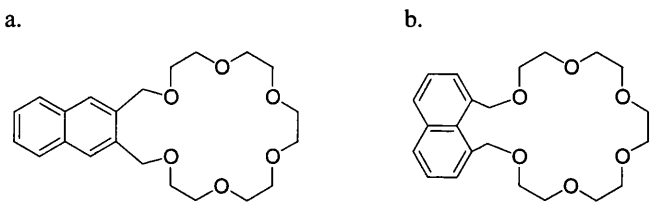

Figure 20. Sousa's metal sensors.[49]

These compounds demonstrated small but significant fluorescence changes upon binding of alkali metal salts. A number of sensing supramolecules contain anthracene as a fluorophore for its chemical stability and its strong and well characterised emission. De Silva and co workers developed an anthracene-based sensor for *s*-block metal ions (Figure 21a).[8,9]

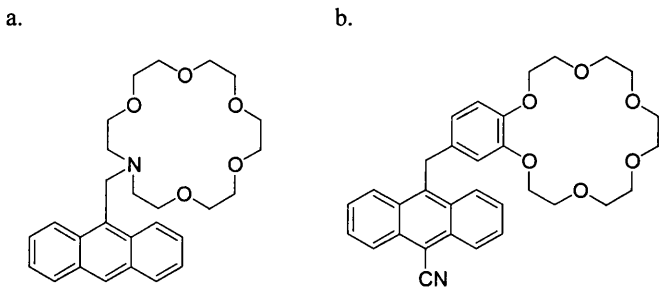

Figure 21. (a) De Silva's K^+ sensor and (b) the modified sensor.

The receptor is an 18-membered macrocycle containing five oxygen atoms and a nitrogen atom as donors (azacrown ether). This receptor unit is suitable for selective interaction with potassium ion. The fluorescence is quenched by PET from the amine lone-pair to the anthracene. Following metal coordination, the oxidation potential of the amine group is substantially lowered as the lone-pair is involved in the coordination and the electron-transfer process is prevented. As a consequence, fluorescence is restored. Addition of potassium enhances the fluorescence by a factor of 47. However, the sensor suffered from pH-dependent fluorescence. This problem was solved by designing a sensor which possessed no basic nitrogen centres (Figure 21b).[50,51] In methanol the fluorescence enhancement for potassium binding of this modified sensor was 3. Changing of the solvent to 2-propanol increased the enhancement factor to 45.

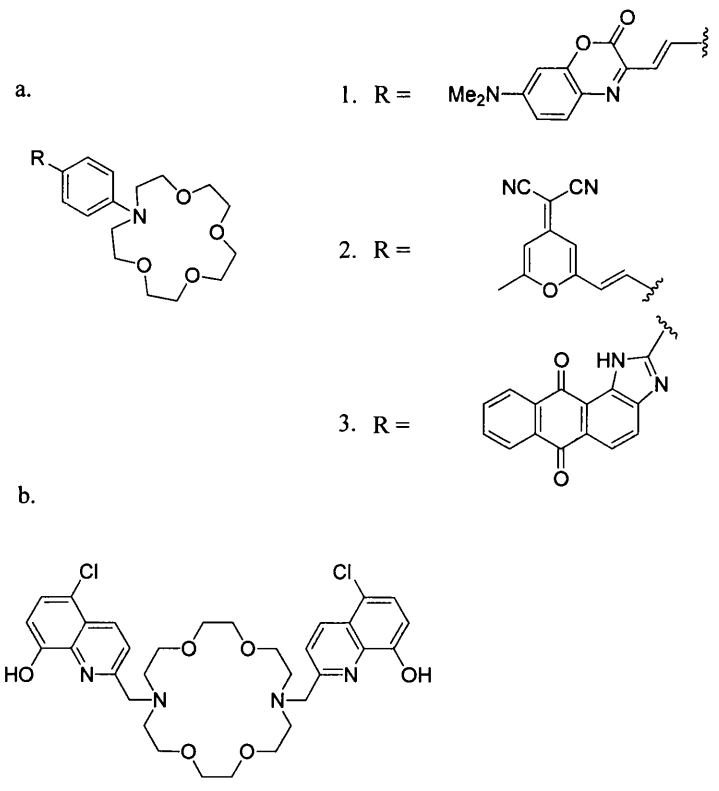

Figure 22. Azacrown ether appended sensors.

Azacrown ethers were also used as the receptor for metals in Valeur's fluorescent dyes (Figure 22a1 and a2).[52,53] The first sensor (Figure 22a1) displayed a clear colour change from red-orange to yellow on addition of alkaline earth metals in acetonitrile. The largest effect was observed for the Ca^{2+} complex. The fluorescence emission spectrum of the sensor undergoes a large hypsochromic shift from 642 nm to 574 nm upon complexation with calcium ion and enhancement of quantum yield and lifetime. Upon changing the terminal to 4-dicyanomethylene-2-methyl-4*H*-pyran (Figure 22a2), the sensor undergoes large changes in the absorption spectrum and fluorescence quantum yield. The emission spectrum is only slightly blue-shifted and the fluorescence lifetime is almost unchanged. Addition of metal salts quenches the fluorescence, which is more efficient with alkaline earth metal cations than with alkali metal cations. Also, alkaline earth metal perchlorates lead to stronger hypsochromic shifts than alkali metal perchlorates. Furthermore, the higher the charge density of the cation, the stronger is the observed effect. Therefore the best fluorescence quenching was obtained with Ca^{2+}. Nagamura and co-workers designed a sensor with an azacrown ether unit linked to a 2-phenylimidazoanthraquinone chromophore by a methylene spacer (Figure 22a3).[54,55] When metal ions were bound, electrostatic interaction between the lone pair electrons in the azacrown and alkali metal ions caused the fluorescence to increase. Binding of calcium and barium ions showed the largest enhancement in fluorescence. De Silva and co-workers have also designed a diazacrown unit complexed with europium(III), whose luminescence is switched on by binding of alkali metal ions.[56] Diazacrowns have also been used as recognition units for alkali metals. Bradshaw *et al.* designed the 8-hydroxyquinoline-containing sensor Figure 22b.[57-59] The sensor exhibits remarkable selectivity for K^+ and Ba^{2+} over other metal ions in methanol. The

group has subsequently developed more diazacrown appended sensors with fluorophores, chromophores and electrochemical ferrocene signalling units.[60]

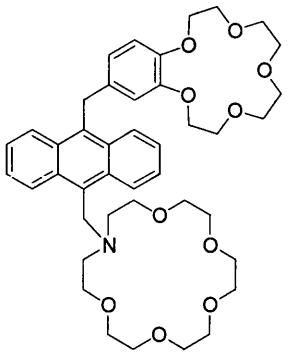

Figure 23. A ditopic cation sensor.

A combination of azacrown and benzo-15-crown-5 was used by Ji and co-workers and is shown in Figure 23.[61] Under basic conditions, the lone-pair electron on nitrogen in the azacrown ether quenches the fluorescence of the anthracene fluorophore by PET. When the potassium ion is added it forms a strong complex with the azacrown ether, which prevents PET and therefore causes enhancement of the fluorescence. Since the crown ether does not contribute to the PET under basic conditions, complexation of alkali metals by the crown ether does not affect the fluorescence. In acidic conditions, on the other hand, the nitrogen on the azacrown is protonated and the PET process now involves the benzo group of the benzocrown ether and anthrylmethyl ammonium. Addition of the sodium ion results in an increase of fluorescence. Since the nitrogen in the azacrown is protonated, no metal ions can complex with the azacrown ring because of electrostatic repulsion. The detection of both potassium and sodium ions can therefore be performed by the same sensor; in basic conditions the molecule works as a potassium sensor and in acidic conditions as a sodium sensor. Both ions cause an eight-fold fluorescence enhancement in their respective conditions.

Cryptands

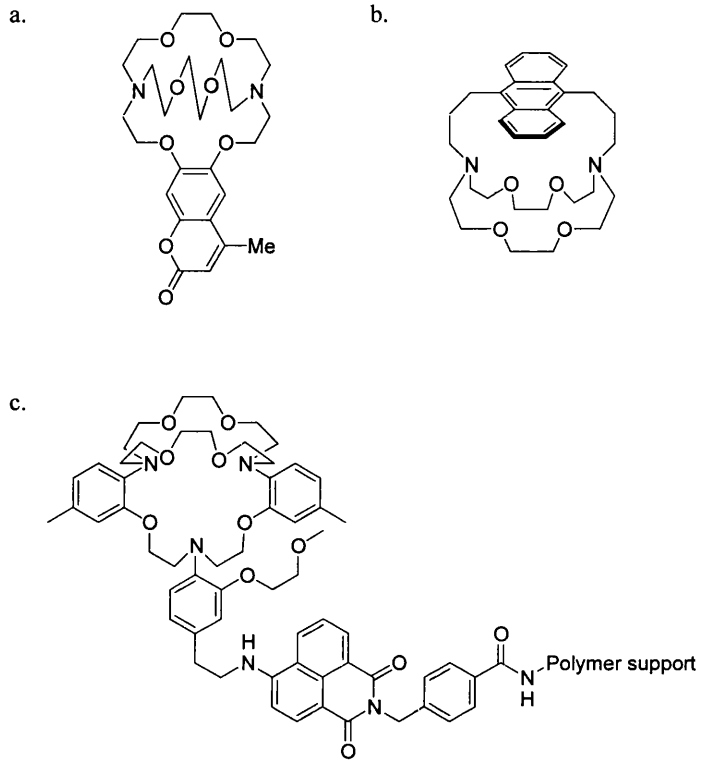

Figure 24. Cryptand appended cation sensors.

The favourable binding selectivity shown by cryptands toward alkali cations is exploited by the sensors in Figure 24.[62-64] These sensors show substantial fluorescence enhancements upon guest entry. The sensor in Figure 24a binds to potassium ions. In the absence of sodium cations potassium cations have a minimal effect on the fluorescence intensity. The presence of sodium ions increases the dissociation constant for potassium ions (1.9 mM). Compound in Figure 24b also binds Ag(I) because of cation-π interactions due to the antharacene lining the cryptand cavity, but no fluorescence was observed in that case. Sensor in Figure 24c is a fluorescent PET sensor and can bind potassium in

water.[65] The sensor has a good sensitivity and selectivity against sodium and other extracellular cation ions. There is no pH interference in the physiological pH range and so the sensor can be used for measurement of potassium in blood and serum.

Acyclic polyether systems

Although the complexation ability of acyclic polyether derivatives is not as strong compared with that of crown ethers[45], the conformation of these molecules changes drastically from a linear structure to a cyclic structure on complex formation with metal ions.

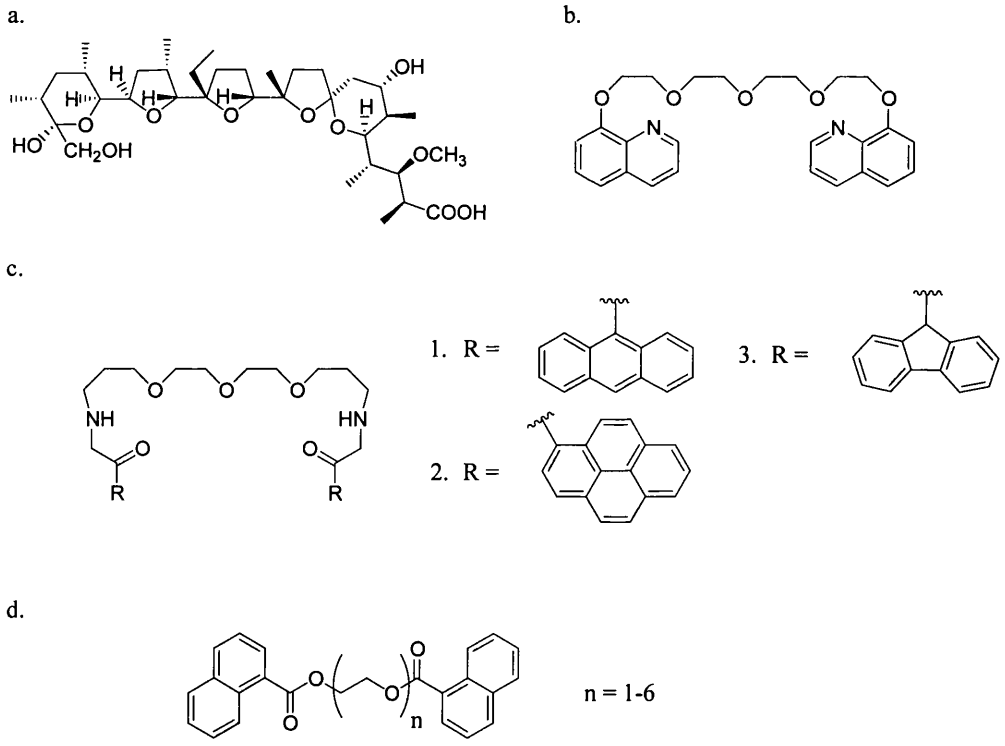

Figure 25. Examples of non-cyclic crown ethers. (a) naturally occurring non-cyclic ionophore monensin, (b), (c) and (d) artificial non-cyclic crown ethers

Monensin, Figure 25a, is a naturally occurring non-cyclic ion-carrier which is composed of three tetrahydrofuran units and two tetrahydropyran units with hydroxyl and carboxy units at its terminals.[66,67] In alkaline conditions monensin forms a pseudocyclic structure like a crown ether via an intramolecular head-to-tail hydrogen bond between the carboxylate anion and the hydroxyl group. It binds Na^+ strongly and passes through lipophilic membranes. The metal ion is released in acidic conditions when the carboxylate is protonated and the pseudo cyclic structure is broken. An early study on artificial non-cyclic crown ether derivatives was carried out by Vögtle *et al.*[68,69] They demonstrated that the oligo-oxyethylene compound, Figure 25b, with two quinoline units at its terminals, strongly bound K^+ by electrostatic interaction between the ion and oxygen atoms with the aid of π-π interactions between the terminal capped quinolines. The shape and peak of the fluorescence spectra of the sensor in Figure 25c1 is significally changed upon complexation with Ca^{2+}.[70] Three peaks around 400 nm change to a large and broad peak around 490 nm upon complexation. This phenomenon indicates that the structure of the ligand changes on complexation, and two antharacenes approach each other and then stack. The same spectral changes are observed in the presence of Sr^{2+} and Ba^{2+}. When the fluorophores were changed to pyrene (Figure 25c2) and fluorene (Figure 25c3) no spectral changes were observed on addition of metal salts. In the first case, this was because the pyrene units were already interacting strongly and the fluorescence spectrum was that of a dimer pyrene before complexation. The fluorene units, on the other hand, show little interaction with each other in the absence or presence of metal ions. Kawakami and co-workers investigated the effect of chain length on complexation of acyclic polyethers with alkali and alkaline earth metal ions in acetonitrile (Figure 25d).[71] Calcium and barium ions were the only metal cations to cause any fluorescence change in the

sensors and only with chain lengths of n = 4-6. The shorter polyether chains (n = 1-3) cannot form metal complexes. The most stable complexes were formed with calcium and barium cations with polyether chain length n = 5 and 6. The two chromophores can easily approach closely enough to interact when the oxygen atoms of the polyether chain of the sensor interact with a cation.

Other types of cation receptors

Tsien and de Silva have designed fluorescent sensors for calcium ions based on the cleft-like receptor for Ca^{2+}, which is lined with carboxylate groups, amine nitrogens and ether oxygens as shown in Figure 26a.[72-77] Tsien's FLUO-3 (Figure 26a1) and INDO-1 (Figure 26a2) detect intracellular calcium ions against other ions. FLUO-3 is capable of indicating changes in the Ca^{2+} concentration in fibroblasts and lymphocytes. Ion binding to INDO-1 leads to shifts in the fluorescence emission or excitation spectra. De Silva and co-workers used two different fluorophores, which differ in polarity, hydrophobicity and spectral properties. In both cases, the sensor response is highly selective for physiological levels of intracellular Ca^{2+} ($pCa^{2+} \sim 7$) against those of Mg^{2+} (pMg^{2+} 3) and H^+ (pH ~ 7). The fluorescence enhancement for Ca^{2+} is 5- and 26-fold more than for Mg^{2+} for the molecules in Figure 26a3 and a4 respectively. All four carboxylate units of the sensor are involved in the 1:1 binding of Ca^{2+}, whereas 1:1 binding of the smaller Mg^{2+} occurs preferentially at the two carboxylates furthest from the fluorophore leading to smaller fluorescence enhancement.

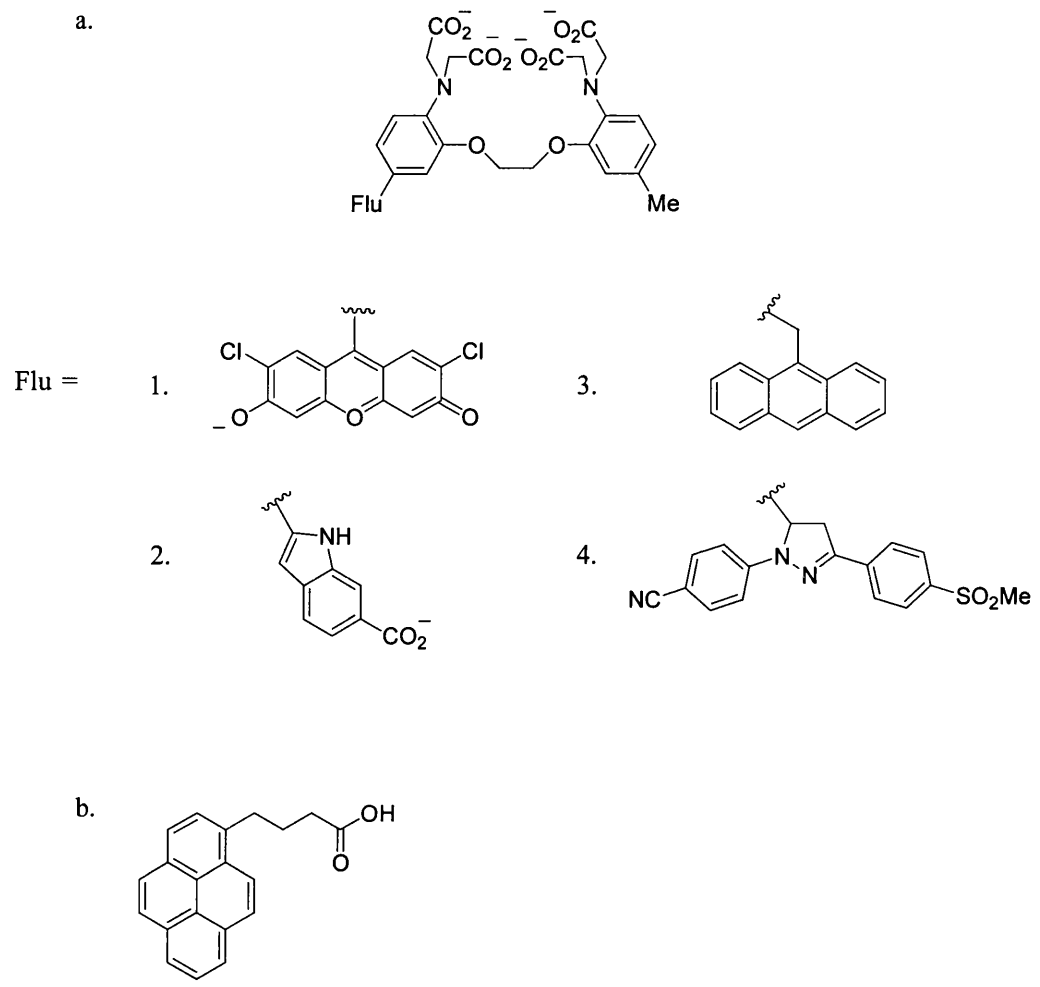

Figure 26. Calcium sensors.

The same principle was used by Prodi and co-workers with the 1-pyrenebutyric acid in Figure 26b by using the coordinating abilities of the carboxylate group.[78] Addition of base was used to deprotonate the carboxylic group and did not cause any change in the absorption or fluorescence spectra. This is expected because of the long distance between the pyrene moiety and the acidic function. Addition of metal ion on the other hand, caused strong changes in the spectra. Especially upon addition of Zn^{2+} and Ca^{2+} the absorption spectrum undergoes a broadening of the structured band of the pyrene up to a stoichiometric ratio of 1:2 (metal:ligand).

Addition of alkali metal ions does not cause any spectral change because they are not able to form a 1:2 complex. The 1:2 complex is required to form an excimer of the two pyrene fluorophores.

1.3 Sensor systems for anions

In the past few years a wide range of sensors have been developed that present varying degrees of affinity and selectivity toward anions such as fluoride, chloride, phosphate and carboxylates. These systems can be built by combinations of anion binding-units and signalling units that transform receptor-anion interaction into optical signals. These units can be fluorescent groups, where the output is a fluorescence change, or dyes, where the output is a colour change. Anion receptors can consist of protonated nitrogens, metal ions, hydrogen bonding sites and Lewis acid receptors.[79-85]

The design of anion receptors is particularly challenging. Anions are larger than isoelectronic cations[86] and therefore have a lower charge to radius ratio. This means that electrostatic binding interactions are less effective than they would be for the smaller cation.

Cation	*r* / Å	Anion	*r* / Å
Na^+	1.16	F^-	1.19
K^+	1.52	Cl^-	1.67
Rb^+	1.66	Br^-	1.82
Cs^+	1.81	I^-	2.06

Table 1. A comparison of the radii *r* of isoelectronic cations and anions in octahedral environments.[86]

Additionally anions may be sensitive to pH values, becoming protonated at low pH and so losing their negative charge. Thus, receptors must function within the pH

range of their target anion. Anions can also have a wide range of geometries and therefore a higher degree of design may be required to obtain suitable receptors.[87] Solvent effects also play a crucial role in controlling anion binding strength and selectivity. Electrostatic interactions generally dominate in anion solvation and hydroxylic solvents in particular can form strong hydrogen bonds with anions. A potential anion receptor must therefore compete with the solvent in which the anion recognition takes place. For example, a neutral receptor that binds anions solely through ion-dipole interactions may only complex anions in aprotic organic solvents, whereas a charged receptor has the capacity to bind highly solvated (hydrated) anions in protic solvent media.[88]

Hydrophobicity can also influence the selectivity of a receptor. The Hofmeister series,[89] which was first established through studies on the effect of salts on the solubility of proteins, orders anions by their hydrophobicity. Hydrophobic anions are generally bound more strongly in hydrophobic binding sites.

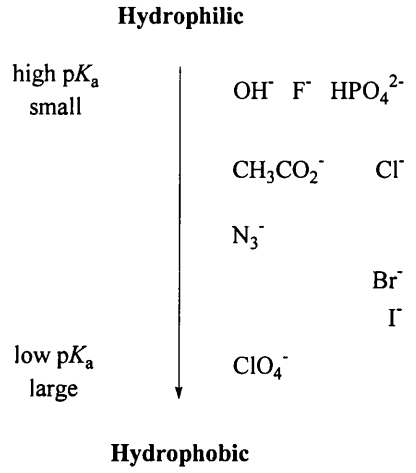

Figure 27. Hydrophilic/hydrophobic series of anions.

The (bis)thiourea in Figure 28a has been shown to form strong 1:1 binding complexes preferentially with $H_2PO_4^-$ in dimethyl sulfoxide through hydrogen bonding by its thiourea groups.[90]

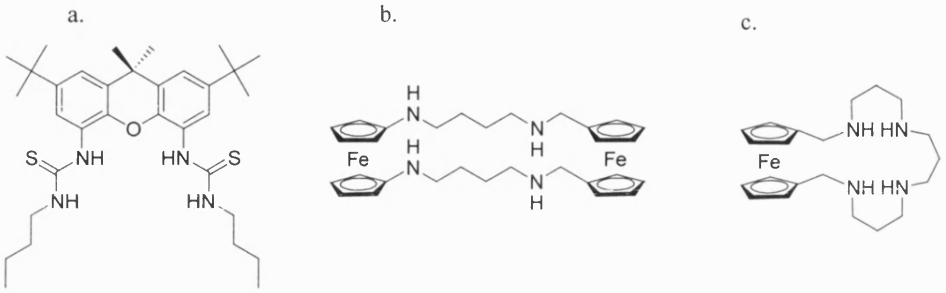

Figure 28. Selected electrochemical anion sensors.

The binding constant for the dihydrogenphosphate is 5.5×10^4 M^{-1}, which was measured using UV-VIS spectroscopy and ^1H NMR. Unfortunately, this system suffers from lack of sensitivity in that analyte concentrations must be at least 1mM to get a useful response. Sensors in Figure 28b and Figure 28c interact with anions initially through charge-pairing and hydrogen-bonding interactions from the ammonium/amine groups, they also interact by an electrostatic interaction when the ferrocene moieties are oxidized. The receptor in Figure 28b was found to selectively bind ATP over ADP and AMP at near neutral pH. The oxidation potential shifts by up to 100 mV on ATP binding.[91] Both sensors in Figure 28b and Figure 28c also produced pH-dependent cathodic shifts in the presence of sulphate (at pH 3-5) and phosphate (at pH 6-8). By adjusting the pH of the aqueous solution (THF-water, 7:3), sensor in Figure 28c was able the sense phosphate selectively even in the presence of other competing anions, such as nitrate, acetate or chloride.

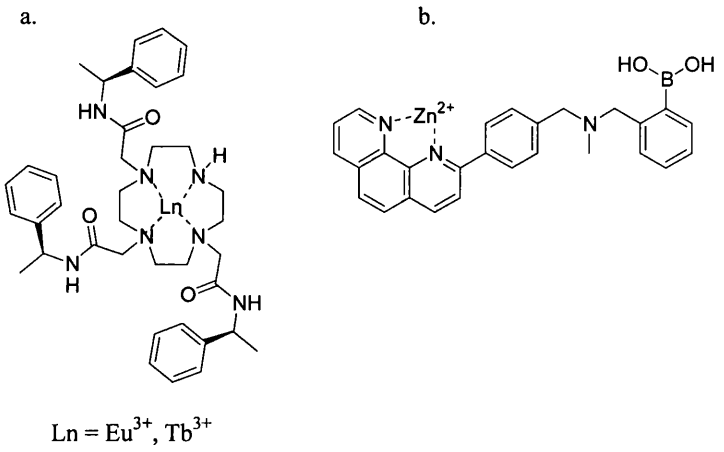

Ln = Eu^{3+}, Tb^{3+}

Figure 29. Selected metal-chelated anion sensors.

The Tb^{3+} and Eu^{3+} complexes of the sensor in Figure 29a were investigated with different anions.[92] Fluoride, acetate, bicarbonate or carbonate displaced metal-bound water molecules, resulting in increased lifetime or emission intensity of the lanthanide luminescence. HCO_3^- produced a large change in luminescence emission intensity at 620 nm for the Eu^{3+} complex. Such changes did not occur with $H_2PO_4^-$. The sensor in Figure 29b was used to sense uronic and sialic acids.[93] These acids are markers of specific biosynthesis processes and terminal recognition residues in glycoproteins and glycolipids, respectively.[94-96] The boronic acid moiety was incorporated to bind the sugar portion and the zinc chelate was intended to coordinate the carboxylate of the substrate. In the absence of zinc, the sensor in Figure 29b displayed little change in fluorescence upon introduction of the acids. Inclusion of the metal, forming a Zn(II) complex, however, enabled sensing of the uronic acids, presumably because of a cooperative interaction between the boronic acid and the zinc-chelating binding sites. Sugar complexation with the boronic acid moiety near pH 8 increased the B-N interaction, thereby decreasing the PET fluorescence quenching ability of the

amine. Thus, the fluorescence intensity increased in the presence of the acids. The sensor, however, was not selective for sialic acid over common monosaccharides.

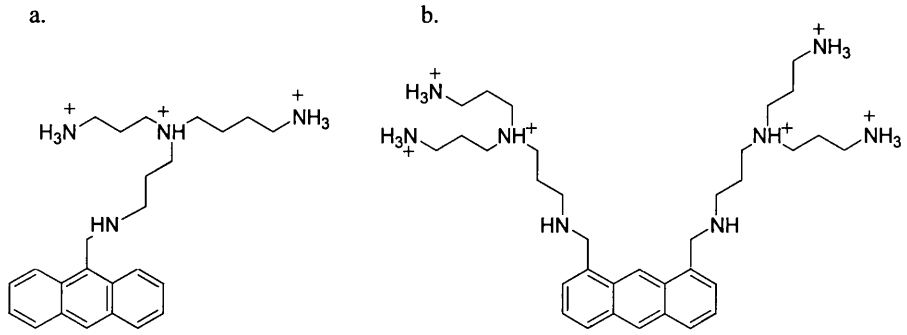

Figure 30. Sensors for phosphate.

Czarnik and co-workers developed a HPO_4^{2-} sensor in 1989 (Figure 30a). The fluorescence 'switching on' is due to hydrogen bonding between HPO_4^{2-} and the ammonium groups.[46] The binding constant for HPO_4^{2-} in aqueous solution at pH 6 was determined as logK = 0.83 with a fluorescence intensity increase of 145%. The stability constants were higher for ATP and citrate (logK = 4.2 and 2.3 respectively) but a smaller increase in the fluorescence intensity was observed (79% and 97% respectively). Five years later Czarnik published a PET chemosensor that displayed a thousandfold selectivity for pyrophosphate over phosphate ions (Figure 30b).[97] The sensor discriminates between phosphate and pyrophosphate ions on the basis of size. The pK_a of the phosphate sensor in Figure 30a was determined as 5.4, whereas the pK_a of the sensor in Figure 30b was measured as 6.7. This meant that the anion binding could be measured at pH 7 for sensor in Figure 30b (K_d = 2.9 μM with pyrophosphate) but not for sensor in Figure 30a.

Fluoride sensors

Fluoride is present in biological fluids and tissues, especially in bone and tooth. Typical levels in blood have been reported to be in the range 20-60 mg l^{-1} using a fluoride selective electrode.[98] Fluoride is of particular interest among the biologically important anions mostly because of its role in the prevention of dental caries.[99] It is also being explored extensively as a treatment for osteoporosis. Fluoride is easily absorbed but is excreted slowly from the body, which can result in chronic poisoning.[100] Overexposure to fluoride can lead to a variety of side effects, such as acute gastric and kidney disturbances, dental and skeletal fluorosis.[101] Monitoring the fluoride concentration of groundwater contamination from certain industrial plants and the fluoridation of water supplies is also of interest. Fluoride is also released during the hydrolysis of some chemical weapons such as sarin and determination of the fluoride concentration can be used to quantify the concentration of the nerve agent.[102,103]

Fluoride concentrations are currently determined using electrodes prepared from LaF_3.[104] While traditional methods of fluoride anion analysis such as ion selective electrodes and ^{19}F NMR spectroscopy remain important, there are alternative means of analysis, including chemosensors. Under certain circumstances, chemosensors would be of great advantage, for instance for the direct visualisation of intracellular fluoride.

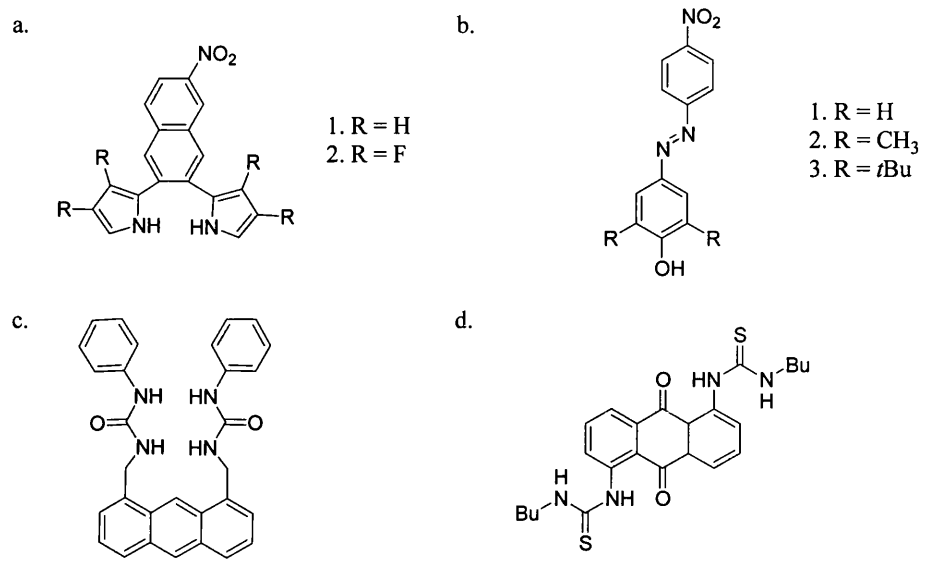

Figure 31. Examples of fluoride sensors; (a) colour sensor by Sessler, (b) azophenol colour sensor, (c) fluorescent PET sensor and (d) colour sensor by Martínez-Máñez

Fluoride sensors have been developed over recent years, especially fluoride sensors containing boron. Sessler and co-workers designed a fluorescent sensor for fluoride shown in Figure 31a1.[105] When the fluoride anion binds with the sensor (1:1) in dichloromethane, the fluorescence of the sensor is quenched. In addition the sensor undergoes a colour change from yellow to purple on fluoride binding. The changes are reversed upon addition of water probably due to competition between water and fluoride at the pyrrolic NH hydrogen bonding sites. The group developed this sensor further by fluorinating at four positions (Figure 31a2).[106] This enhanced the fluoride binding of the sensor. Recently this sensor was developed even further by using a fused dipyrrolylquinoxaline phenanthroline derivative and complexing this with ruthenium(II) and cobalt(III).[107] Hong *et al.* have developed colour sensors based on azophenol (Figure 31b).[108] All three sensors change colour from yellow to blue in chloroform upon addition of fluoride. However, the addition of protic polar solvents, like water, reverses the reaction.

This is presumably because protic solvents compete with fluoride at the phenolic OH hydrogen bond site.

Kim and Yoon have developed a fluorescent PET chemosensor 1,8-bisurea anthracene (Figure 31c).[109] The fluoride binds between the four amides by hydrogen bonding and quenches the fluorescence. The selectivity for fluoride ions was almost 120 fold compared to that of chloride ions in an acetonitrile-DMSO mixture (9:1, v/v). Martínez-Máñez and co-workers have developed a colour sensor (Figure 31d), that also uses hydrogen bonding like the sensor in Figure 31c.[110] This sensor has thiourea groups which are able to bind fluoride via hydrogen-bonding interactions and an anthraquinone group as a chromogenic signalling group. The colour changes were studied in acetonitrile with various anions (F^-, Cl^-, Br^-, I^-, NO_3^-, HSO_4^-, $H_2PO_4^-$, CN^-, SCN^-, acetate and benzoate). The most selective colour change was in the presence of fluoride from orange to brown.

Other fluorescent sensors for fluoride have used porphyrin[111] and trianthrylfluorosilane.[112]

Boronic acids and fluoride sensors

Boronic acids have been used to interact with fluoride. When boronic acid binds to certain anions (fluoride, hydroxide) the sp^2 hybridised trigonal boron atom becomes sp^3 hybridised.[113,114] The boron atom which is a 'hard acid' strongly interacts with the fluoride anion which is a 'hard base'. This specific boron-fluoride interaction has also been used to facilitate the transport of saccharide across a liquid membrane by stabilising the boronic acid-saccharide complex.[115]

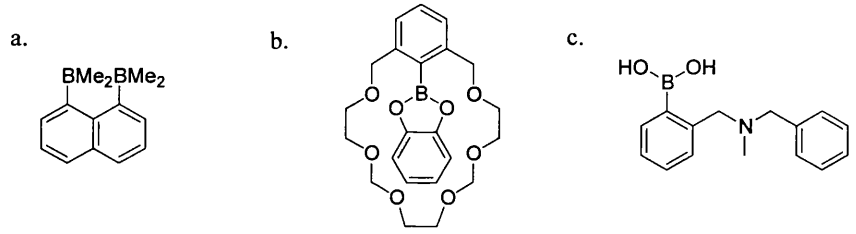

Figure 32. Selected examples of boron containing fluoride sensors.

Katz was the first to study boron-centred fluoride receptors.[116-118] The 1,8-naphthalenediylbis(dimethylborane) (Figure 32a) traps fluoride and hydroxide ions between the two electron-accepting boron atoms but does not complex with chloride. This relative instability is presumably a consequence of the larger ionic radius of the chloride anion, which gives a poor fit between the two boron binding sites, as well as the weak Lewis acidity of the molecule. In contrast the more strongly Lewis acidic $-BCl_2$ analog of the molecule is capable of binding chloride.[119]

Simultaneous complexation of cations and anions has been observed in the 21-membered ring boronate crown ether (Figure 32b). [120,121] This molecule is a

ditopic host for fluoride and metal ions. The potassium ion is bound by the crown ether, whilst the fluoride ion is held by a combination of orbital overlap with the Lewis-acid boron and electrostatic interactions with the potassium ion. The ligand fails to dissolve either potassium chloride or bromide as a consequence of the weaker nature of the boron-halide bonds.

James and Cooper developed a fluorescent sensor for fluoride using boronic acid (Figure 32c).[122] The system is based on the Lewis acid-base interaction between boron and fluoride. The system was specifically designed to increase the strength of fluoride bonding relative to phenylboronic acid by virtue of an additional hydrogen bonding site, which is available when the amine is protonated. The pK_a of the tertiary amine of this compound was determined from fluorescence pH titration and was found to be 5.5. At this pH the amine is half protonated and can participate in hydrogen bonding with fluoride.[6,12] Also, the sensor has a high fluorescence at this pH because the PET from the nitrogen is reduced on protonation. The fluorescence is decreased when fluoride is added in 50% (w/w) methanol-water buffer at pH 5.5.

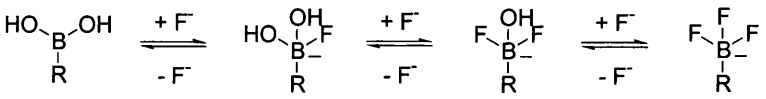

$$I_f = \frac{I_0 + I_\infty K_n[F^-]^n}{1 + K_n[F^-]^n} \qquad (1)$$

where $$K_n = \frac{[RB(OH)_{3-n}F_n]}{[RB(OH)_2][F^-]^n}$$

Scheme 2.

The experimental curve was fitted best using equation (1) and assuming the formation of monofluoro boronic acid derivative (n = 1) (Scheme 2).[123] The stability constant for fluoride was determined as 101 dm^3 mol^{-1}. Also the observed shifts from high to low frequency in the ^{11}B NMR are consistent with a shift from sp^2 to sp^3 boron on fluoride binding.[124]

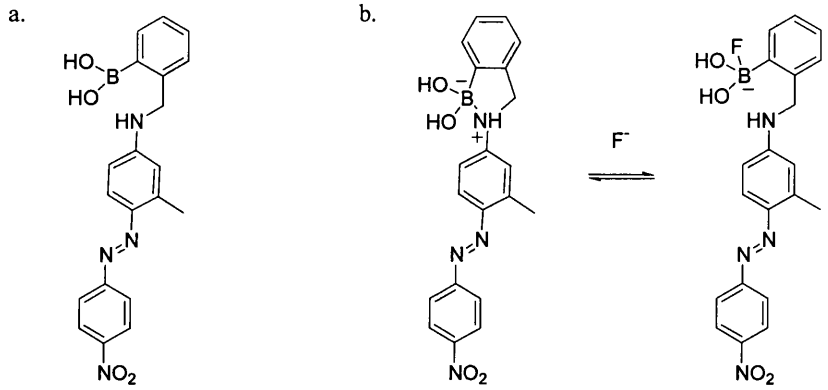

Figure 33. (a) A colorimetric fluoride sensor (b) binding of fluoride to the sensor.

A colorimetric fluoride sensor was developed by James and Ward.[125,126] When the azo dye molecule in Figure 33a is titrated with potassium fluoride in methanol the colour changes from orange to claret. The same colour change is observed for the pH titration of the compound. This colour change is associated with the formation of the tetrahedral boronate anion. Therefore, the addition of potassium fluoride to a solution of the sensor in methanol must also produce a tetrahedral boronate anion. The sensor exists in the form shown in Figure 33b. The B-N bond of the orange coloured species is broken by the addition of fluoride giving the claret coloured species. The stability constant for the fluoride was determined as 130 dm^3 mol^{-1} in methanol.

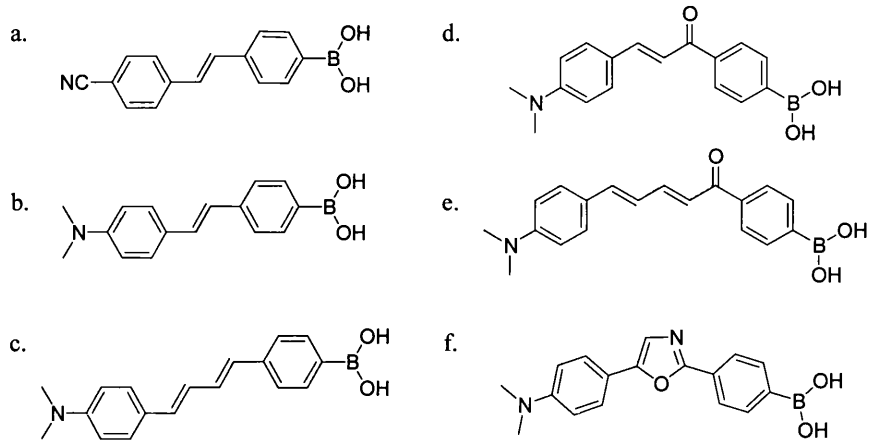

Figure 34. ICT sensors for fluoride.

DiCesare and Lakowicz have recently prepared a range of fluorescent sensors for fluoride (Figure 34).[127] All sensors use the ICT mechanism and combine the boronic acid group with electron donating (dimethylamino) or electron withdrawing (cyano) groups. The sensor in Figure 34a shows ICT when the anionic form of the boronic acid is induced. The sensors in Figure 34b, c and f show ICT for the neutral form of the boronic acid group because of the presence of the electron-donating *N,N*-dimethylamino group. The sensors in Figure 34d and e show ICT involving the *N,N*-dimethylamino group (donor) and the carbonyl (acceptor) group. All six sensors are fluorescent when fluoride is added but the sensor in Figure 34f had the largest binding constant for fluoride ($K = 6.6 \times 10^3$ dm^9 mol^{-3}) and biggest enhancement in fluorescence intensity ($I/I_0 = 14$) in water/methanol (2:1). Diphenyloxazole with electron donor and acceptor groups is known to be very sensitive and shows large spectral changes following perturbation of the ICT. The sensor shows a large Stokes shift and an emission at long wavelength.

Shinkai and co-workers have used ferroceneboronic acid in fluoride recognition.[128,129] The boronic acid, which is the fluoride binding site, is directly connected to a redox-active ferrocene moiety (Figure 35a). The measurements are carried out by cyclic voltammetry. The redox properties are remarkably changed upon addition of fluoride ions to a solution of ferroceneboronic acid in methanol-water. The sensor was further developed (Figure 35b) by adding an intramolecular tertiary amine. The sensor binds fluoride or saccharides at neutral pH.

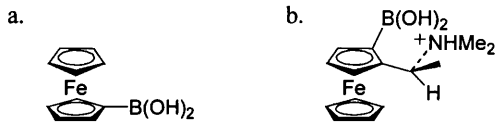

Figure 35. Electrochemical fluoride sensors.

1.4 Synthetic ditopic sensors

Ditopic receptors have two binding sites for two different guests. For example, AND logic gates can be ditopic receptors. There is an emerging interest in ditopic binding, where the host simultaneously binds both cationic and anionic guests. These heterotopic ligands can be designed to exhibit novel cooperative allosteric behaviour, where the binding of one charged guest can influence through electrostatic and conformational effects the subsequent coordination of the pairing ion. One example has already been discussed under fluoride sensors.[120,121] This receptor consists of a crown ether and a boronic ester and binds simultaneously to potassium and fluoride (Figure 32b). A similar ditopic receptor was designed by the same researchers, shown in Figure 36a.[130]

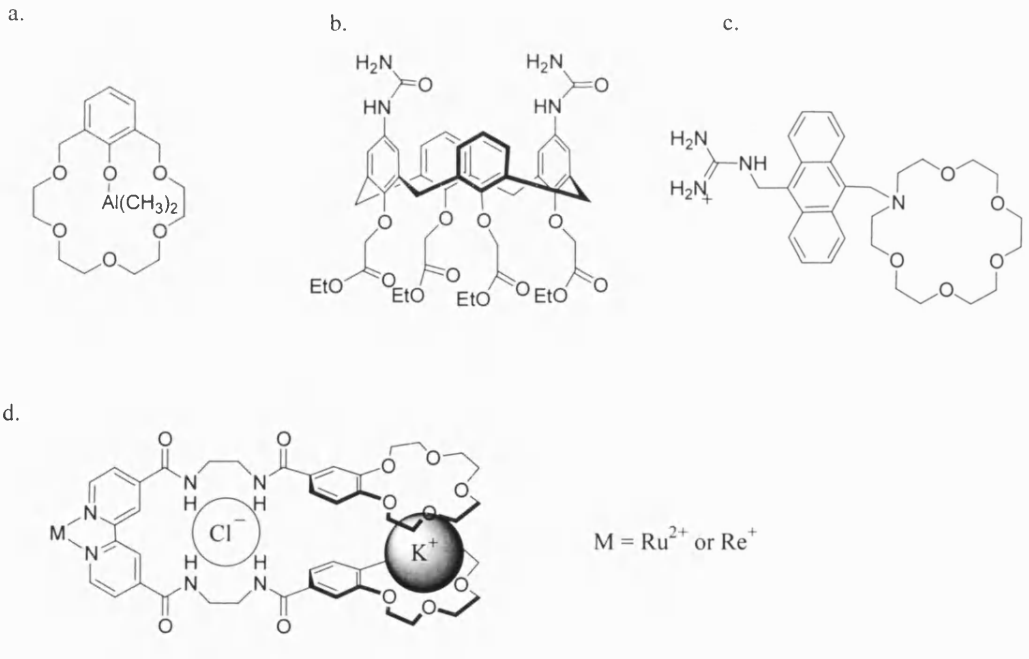

Figure 36. Selected examples of ditopic receptors.

This receptor forms a ditopic complex with LiCl, both in solution and solid-state. Reinhoudt and co-workers described a calix[4]arene scaffold with cation-binding ester groups on the lower rim and the anion-binding urea groups on the upper rim (Figure 36b).[131,132] In $CDCl_3$, the receptor adopts a pinched conformation due to intramolecular hydrogen bonding between the urea groups, thus preventing anion binding. However, when sodium ions are added cation complexation at the lower rim alters the calix conformation, thereby breaking the hydrogen bonds between the urea groups. As a result, chloride or bromide can bind to the upper rim. The binding is confirmed by ^1H NMR. The example in Figure 36c is a fluorescent PET sensor and is a sensor for γ-aminobutyric acid.[133] The monoaza-18-crown-6 ether binds to the ammonium terminal of γ-aminobutyric acid and the guanidinium unit binds to the carboxylate end. Beer and Dent have recently reported the synthesis of new heteroditopic ruthenium(II)- and rhenium(I)-bipyridyl-bisbenzocrown ether receptors, which complex potassium chloride ion pairs in a co-operative fashion (Figure 36d).[134] In the absence of potassium ion the receptors are selective of $H_2PO_4^-$ over Cl^-, whereas formation of the potassium-biscrown sandwich complex induces the reverse selectivity. This may be a consequence of favorable electrostatic attraction and conformational effects wherein the sandwich complex results in a pseudomacrocyclic preorganised structure suitable for chloride binding. Using a similar strategy, Reinhoudt and co-workers also constructed a receptor containing anion-binding Lewis-acidic UO_2^+ and amide moieties together with cation-binding crown ether groups.[135]

1.5 *Summary of introduction*

- A sensor is a device, which gives a signal upon guest binding.
- Fluorescence is emission of light from singlet excited states, in which the electron in the LUMO has the opposite spin as the remaining ground-state electron. Consequently, return to the ground-state is spin-allowed and occurs rapidly by emission of a photon. The emission rates of fluorescence are typically 10^8 s^{-1} and a typical fluorescence lifetime is near 10 ns.
- Photoinduced electron transfer (PET) is a deactivating process of the excited state that efficiently competes with fluorescence.
- Molecular logic gates rely on the binary 'yes-no' concept. One type of logic gates is the AND logic gate, which requires two inputs to provide an output.
- Crown ethers bind selectively to metal cations and are widely used in systems for cation sensors.
- Anion sensors can consist of protonated nitrogens, metal ions, hydrogen bonding sites and Lewis acid receptors.
- Boronic acids have been used as sensors for diols (saccharides) and fluoride.
- When boronic acids bind to fluoride anions the sp^2 hybridised trigonal boron atom becomes sp^3 hybridised. This can be observed in the shifts from high to low frequency in the ^{11}B NMR.

2 Results & Discussion

I did not fail 1000 times; the light bulb was developed in 1001 steps.

Thomas Alva Edison

2.1 *Introduction to the project*

The aim of the project was to synthesise a novel PET sensor with AND logic functionality. Previous work within the James group described a sensor (Figure 37b) for gluocosamine hydrochloride, which behaved like an AND logic gate.[17,18] As has been discussed in the introduction (see Figure 17d) this sensor consists of a fluorophore coupled with a boronic acid unit and an aza crown unit; both of which act as receptors. This sensor was designed as the basic AND logic gate model which was discussed in the introduction. The schematic representation of the sensor shows how the receptors are connected to each side of the fluorophore by spacer units (Figure 37a).

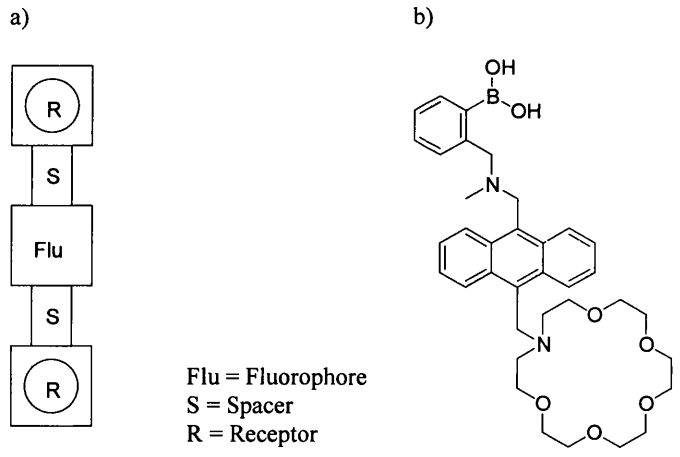

Figure 37. (a) Schematic representation of AND logic gate shown in (b).

Instead of the units being in a linear arrangement (Figure 37a), new sensors are designed with the fluorophore and the two receptors placed around a spacer as shown schematically in Figure 38a.

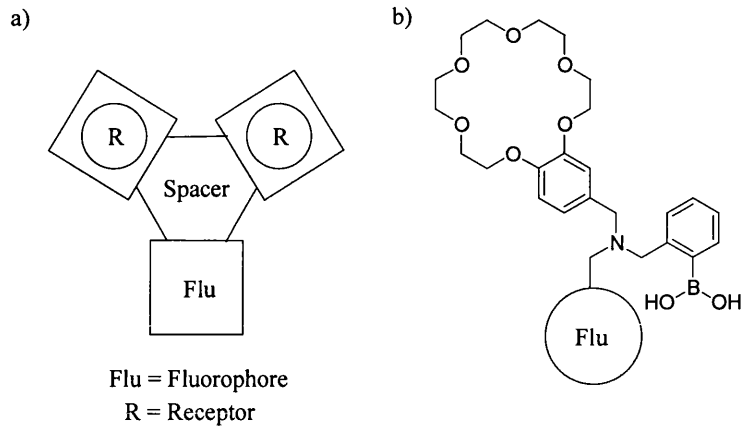

Figure 38. Schematic representation of target compounds.

The target compound contained a boronic acid unit as one of the receptors similar to the molecule in Figure 37b, but with a benzocrown ether in the place of the aza crown ether as the second receptor. As discussed in the introduction, the benzocrown ether is better than azo crown ether because it is pH independent. The benzocrown ether unit acts as a receptor for a suitable cation, such as ammonium, sodium or potassium. The boronic acid can act as a receptor for saccharides (diols) or fluoride as discussed in the introduction.

The fluorophores incorporated into the new sensors were pyrene and naphthalene. The use of different fluorophores allowed sensors with different optical properties to be obtained using similar synthetic routes. The size of the crown was varied between 15-crown-5 and 18-crown-6 to apply selectivity for cations. The sensors were divided into two series according to the fluorophore: the Pyrene series with pyrene as the fluorophore and the Naphthalene series with naphthalene as the fluorophore. These sensor molecules are illustrated in Figure 39.

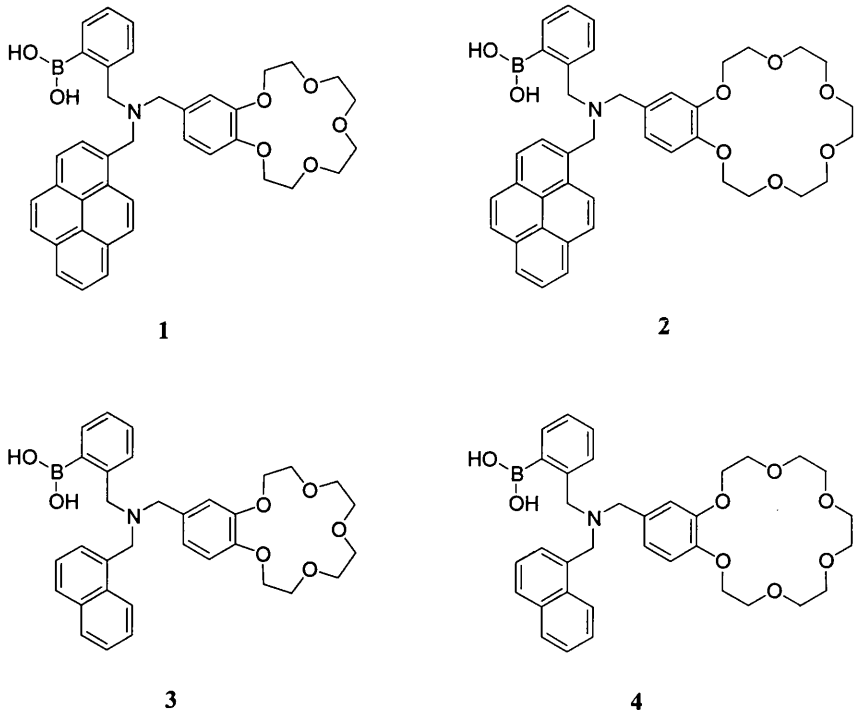

Figure 39. The Pyrene series sensors **1** and **2** and the Naphthalene series sensors **3** and **4**.

Reference molecules were needed for comparison with the sensors and so two types of model compounds were prepared for both series. The first set of reference molecules lacked the boronic acid unit and thus should not readily bind saccharides or fluoride ions. However, it still contained a crown ether unit to allow cation binding. These model compounds for the Pyrene series were the corresponding amines **5** and **6** (Figure 40).

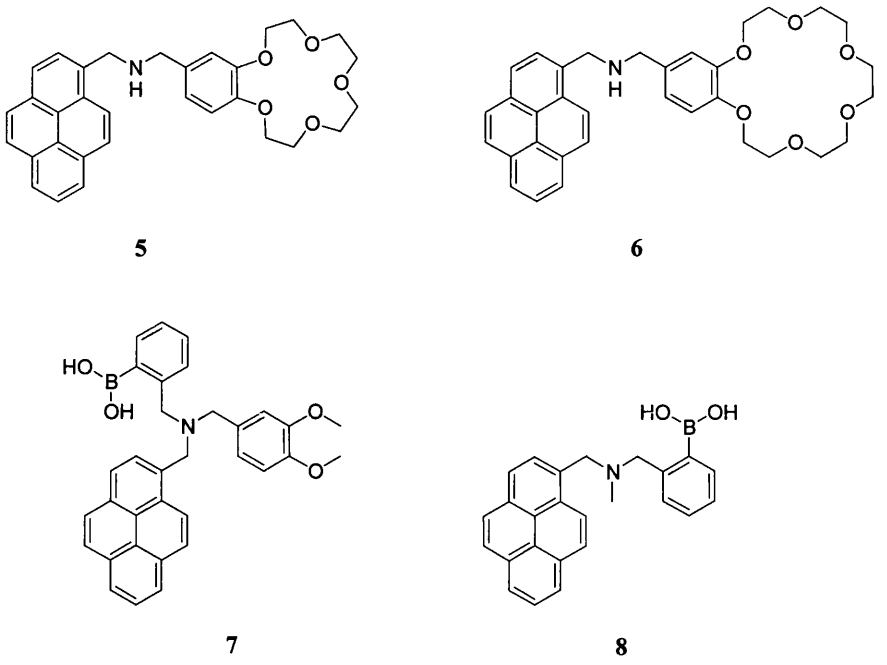

Figure 40. Pyrene series; model compounds.

The second set of model compounds contain a boronic acid unit and can thus bind saccharides and fluoride ions. However, in these molecules the crown ether unit has been replaced by a 3,4-dimethoxybenzyl group and so should not be able to bind cations. The model compound for the Pyrene series was the 3,4-dimethoxybenzyl compound **7** (Figure 40). The third set of model compounds also contain a boronic acid unit and lack a crown ether unit. In these model compounds (compound **8** for the Pyrene series in Figure 40) the crown ether unit has been replaced by a methyl group.

The same sets of model compounds were prepared for the Naphthalene series. The model compounds of the Naphthalene series are shown in Figure 41.

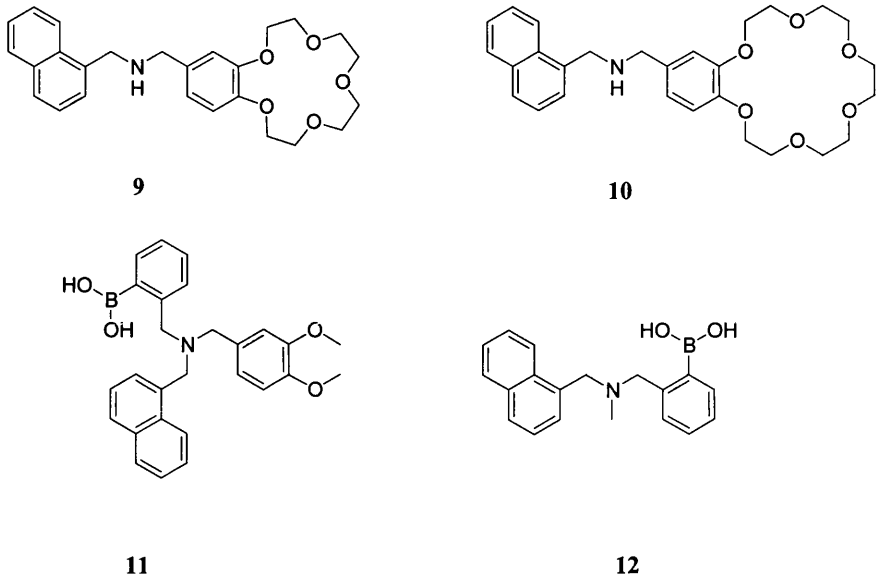

9 **10**

11 **12**

Figure 41. Model compounds of the Naphthalene series.

The first set of reference molecules with a crown ether but no boronic acid were compounds **9** and **10** for the Naphthalene series. The second set of model compounds containing a boronic acid unit and a 3,4-dimethoxybenzyl group was compound **11** for the Naphthalene series. The third set of model compounds containing a boronic acid unit and a methyl group replacing the crown ether was represented by compound **12** for the Naphthalene series (Figure 41).

The following section (2.2) describes the synthetic work undertaken in which the synthesis of the sensors of the pyrene series and the naphthalene series (**1-4**) and the model compounds for both series (**5-12**) are discussed in detail. The second part of this chapter (2.3) describes the analytical element of the project; the evaluation of the sensors and model compounds by fluorescence measurements and ^{11}B NMR.

2.2 *Synthesis of sensors*

The sensors were catalogued in two series according to the fluorophore moiety they incorporated: series 1 - the Pyrene series and series 2 - the Naphthalene series. The general synthesis of both series is shown in Scheme 3.

The reaction of the benzocrown ether aldehyde or 3,4-dimethoxybenzaldehyde with the required fluorophore component resulted in the formation of the respective imines which were then reduced by sodium borohydride to the corresponding amines. The boronic acid was subsequently added to these amines via the cyclic boronate ester **17** to give the four targeted sensors **1, 2, 3, 4** and the two model compounds **7** and **11.** The four sensors (**1, 2, 3** and **4**) were obtained in 80%, 61%, 60% and 53% yields, respectively.

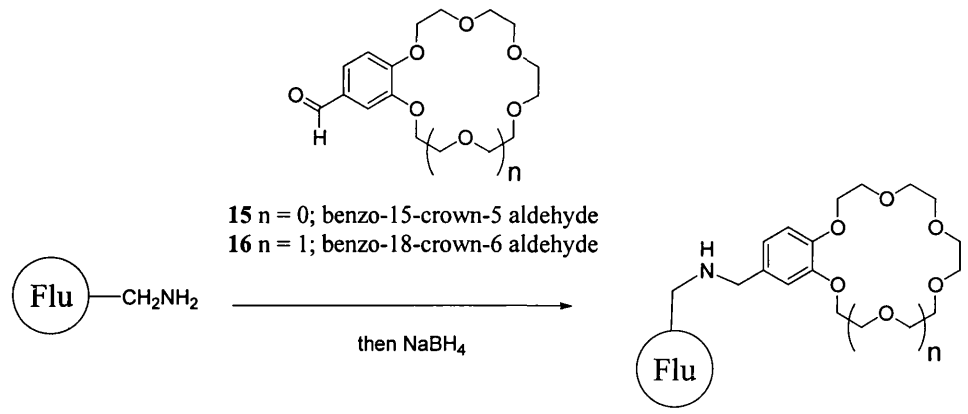

13 Flu = Pyrene
14 Flu = Naphthalene

5 Flu = Pyrene, n = 0
6 Flu = Pyrene, n = 1
9 Flu = Naphthalene, n = 0
10 Flu = Naphthalene, n = 1

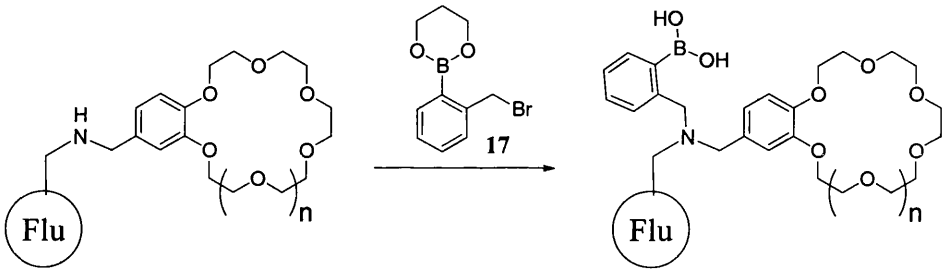

5 Flu = Pyrene, n = 0
6 Flu = Pyrene, n = 1
9 Flu = Naphthalene, n = 0
10 Flu = Naphthalene, n = 1

1 Flu = Pyrene, n = 0
2 Flu = Pyrene, n = 1
3 Flu = Naphthalene, n = 0
4 Flu = Naphthalene, n = 1

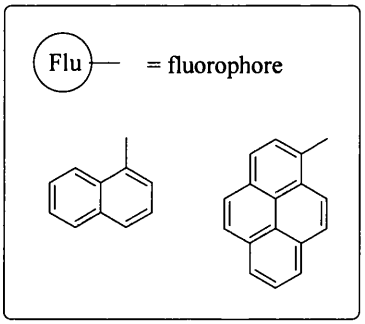

Scheme 3. Synthesis of fluorescent sensors series 1 and 2.

Formation of benzocrown ether unit

The first step in the synthesis of the sensor was the formylation of the of crown ether substrates, benzo-15-crown-5 **18** and benzo-18-crown-6 **19**, required for one of the receptor units in each sensor.

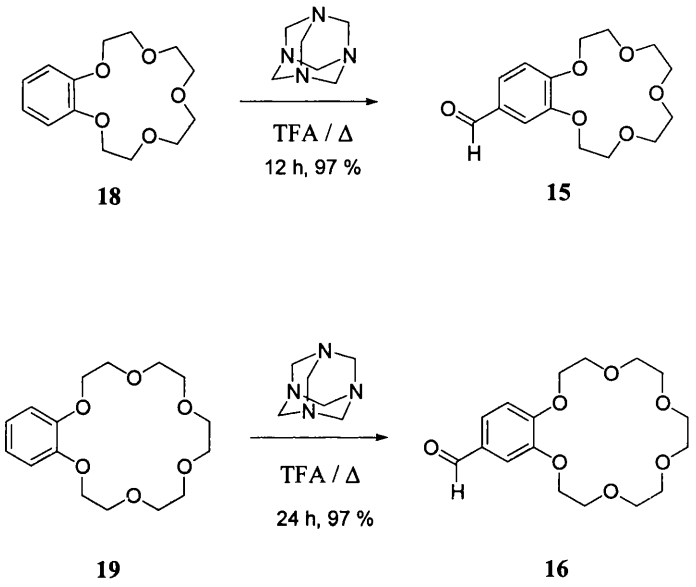

Scheme 4. Formylation of benzocrown ethers *via* the Duff reaction.

The procedure for the formylation of the benzocrown ether, the Duff reaction,[136] was carried out with hexamethylenetetramine as the formylating agent. The probable mechanism[137] for this reaction is depicted in Scheme 5. Hexamethylenetetramine undergoes decomposition under the reaction conditions to form four equivalents of the electrophile $[CH_2=NH_2]^+$ *in situ.* Electrophilic attack upon the aromatic ring provides the aminoalkylated product which then undergoes dehydrogenation promoted by more of the $[CH_2=NH_2]^+$ formed. Hydrolysis of the intermediate imine product then gives the aldehyde as shown in Scheme 5.

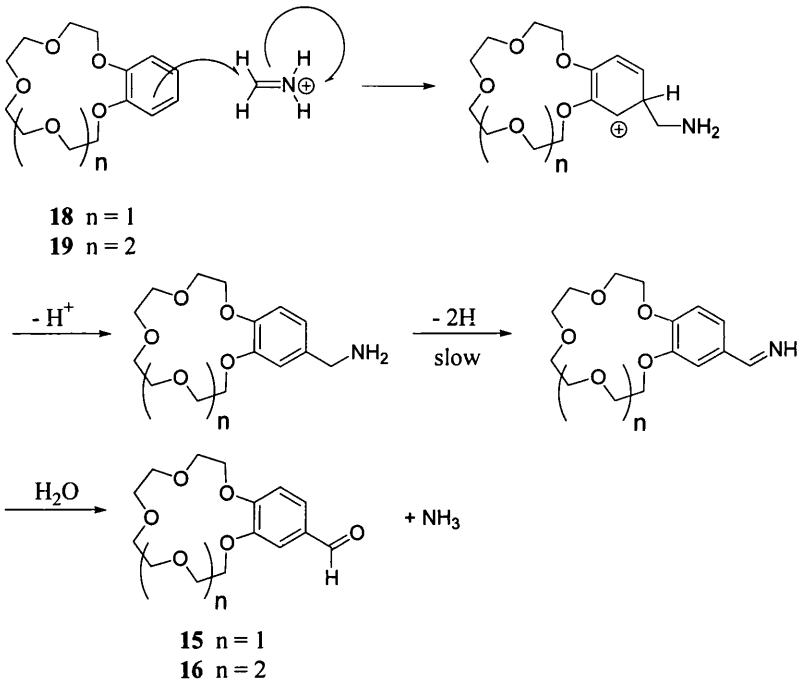

Scheme 5. Proposed mechanism of Duff reaction.

Both benzo-15-crown-5 **18** and benzo-18-crown-6 **19** were heated under reflux with hexamethylenetetramine in TFA under nitrogen. Benzo-15-crown-5 **18** was heated under reflux for 12 hours whereas the benzo-18-crown-6 **19** required a longer reaction time of 24 hours. Initial reaction conditions, which followed the literature procedure[138], used equimolar amounts of reagents, but this resulted in a very low yield (15% for compound **15**). The solvents used in the extraction and the purification were changed from benzene and heptane (as stated in the literature) to the less toxic chloroform and hexane, which may have affected the yield of the reaction. In the literature the yields for the reaction were around 80% for the formation of both benzo-15-crown-15 aldehyde **15** and benzo-18-crown-6 aldehyde **16**. By increasing the equivalents of hexamethylenetetramine to 3.5 equivalents the obtained yields increased significantly to 50% for the benzo-15-crown-5 aldehyde **15**. Both reactions were extracted with

chloroform but resulted in low yields because of the high water solubility of the product. Different organic solvents were examined, including the literature one (benzene), but chloroform seemed to be most effective. The benzo-18-crown-6 aldehyde **16** was more difficult to extract from the aqueous layer due to its high solubility. However, it was later discovered that adding chloroform directly to the reaction mixture without any addition of water prior to extraction aided the migration of the product into the organic layer. Two different methods of purifying the crude product were attempted. The first attempt of purification was to heat the crude product with hexane under reflux for 5 hours and then collect the hexane solution. Following the evaporation of the hexane the product crystallised as a white solid. This method gave a pure crystalline product but had to be repeated a number of times to obtain benzo-15-crown-5 aldehyde **15** in a good yield (70%). The yields were poorer for the benzo-18-crown-6 aldehyde **16**; an average of 50% was typical. Purification by chromatography upon silica proved a more efficient method. This afforded the product as a colourless oil which subsequently solidified as a cream coloured solid upon standing. This method gave significantly higher yields for the aldehydes; 97% yields being obtained for both substrates.

Amine sensors

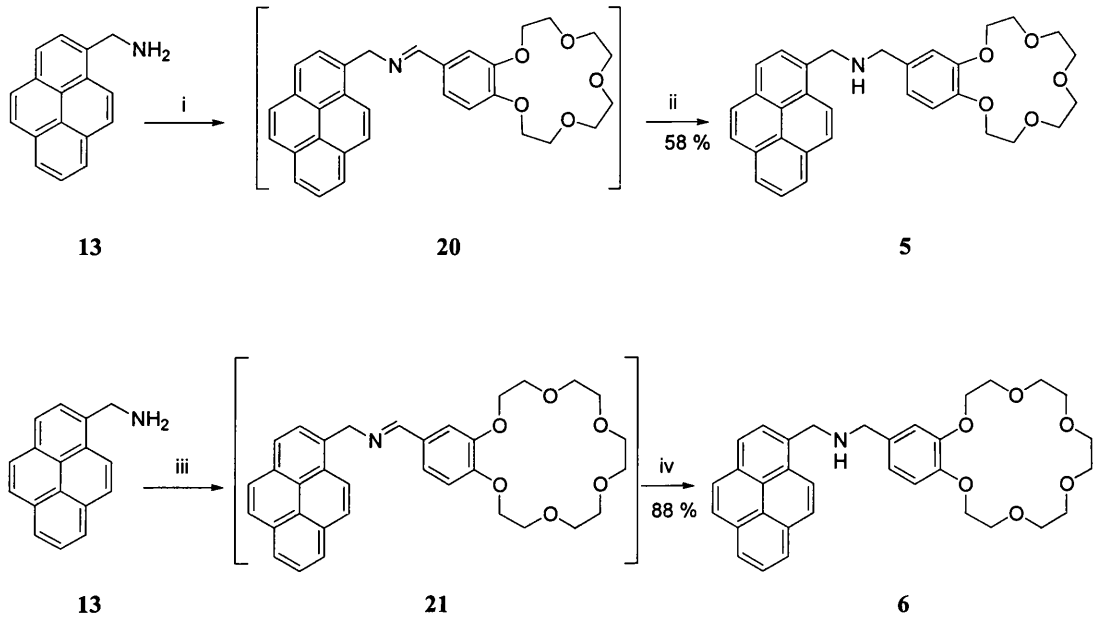

Scheme 6. Synthetic procedure for the amines in the Pyrene series: i) Benzo-15-crown-5 aldehyde **15** / MeOH:THF (1:1, v/v), rt, 5h; ii) $NaBH_4$ / MeOH:THF (1:1, v/v), rt, 5h; iii) Benzo-18-crown-6 aldehyde **16** / MeOH:THF (1:1, v/v), rt, 5h; iv) $NaBH_4$ / MeOH:THF (1:1, v/v), rt, 5h.

The pyrene amine was purchased as the hydrochloride salt and the reaction was first attempted using this salt directly. The starting material, 1-pyrenemethyleneamine hydrochloride and benzo-15-crown-5 aldehyde **15** were dissolved in a mixture of methanol and THF and stirred at room temperature. Sodium borohydride was added and stirred for a further 5 hours at room temperature. Despite evidence in the NMR that some of the imine product **20** had formed, the attempted purification failed. The hydrochloride was converted to the free amine by extracting with sodium bicarbonate. The formation of imine **20** was then performed with the pyrene amine **13** by stirring with benzo-15-crown-5 aldehyde **15** in a mixture of methanol and THF at room temperature. The imines **20** and **21** were not isolated but the characteristic imine peak at

8.2 ppm in a crude ^{1}H NMR confirmed that the imines had been formed. The imine was reduced as before with sodium borohydride in a mixture of methanol and THF at room temperature. Amine **5** was obtained in 58% yield after purification by Bio Beads S-X8 polystyrene (THF) gel chromatography. The reaction was performed in the same way for the benzo-18-crown-6 ether appended amine **6** and gave a good yield of 88%.

The amines of the Naphthalene series were synthesised from the commercially available naphthalene amine **14**. As with the Pyrene series, the imines **22** and **23** were not isolated but their formation was confirmed by the characteristic imine peak at 8.3 ppm in a crude ^{1}H NMR. Sodium borohydride reduction of imine **22** in methanol resulted in amine **9** with 91% yield without need for further purification. The reaction was performed by the same method to afford the benzo-18-crown-6 ether appended amine **10** in 66% yield.

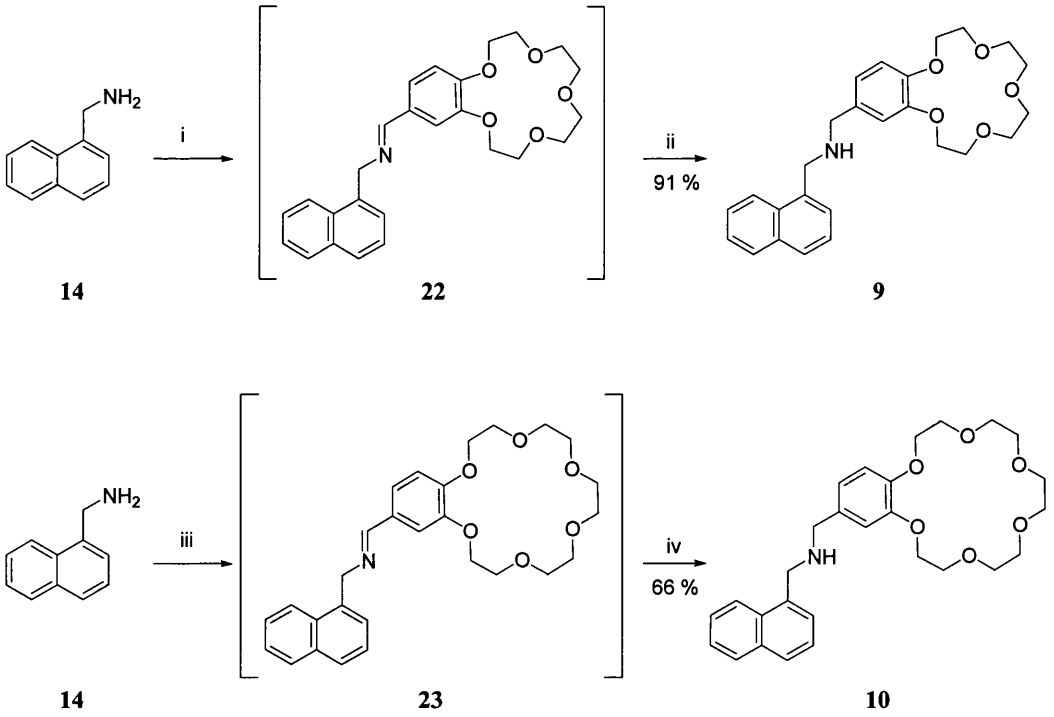

Scheme 7. Synthetic procedure of the amines in the Naphthalene series: i) Benzo-15-crown-5 aldehyde **15** / MeOH:THF (1:1, v/v), rt, 5h; ii) $NaBH_4$ / MeOH:THF (1:1, v/v), rt, 5h; iii) Benzo-18-crown-6 aldehyde **16** / MeOH:THF (1:1, v/v), rt, 5h; iv) $NaBH_4$ / MeOH:THF (1:1, v/v), rt, 5h.

These amines, **5** and **6** for the pyrene series and **9** and **10** for the Naphthalene series, were used as the model compounds containing the crown ether unit and lacking the boronic acid unit.

Boronic acid sensors

The reaction between cyclic boronate ester **17** and secondary amines is well documented in the literature[139] and was performed to obtain boronic acids **1**, **2**, **3** and **4**.

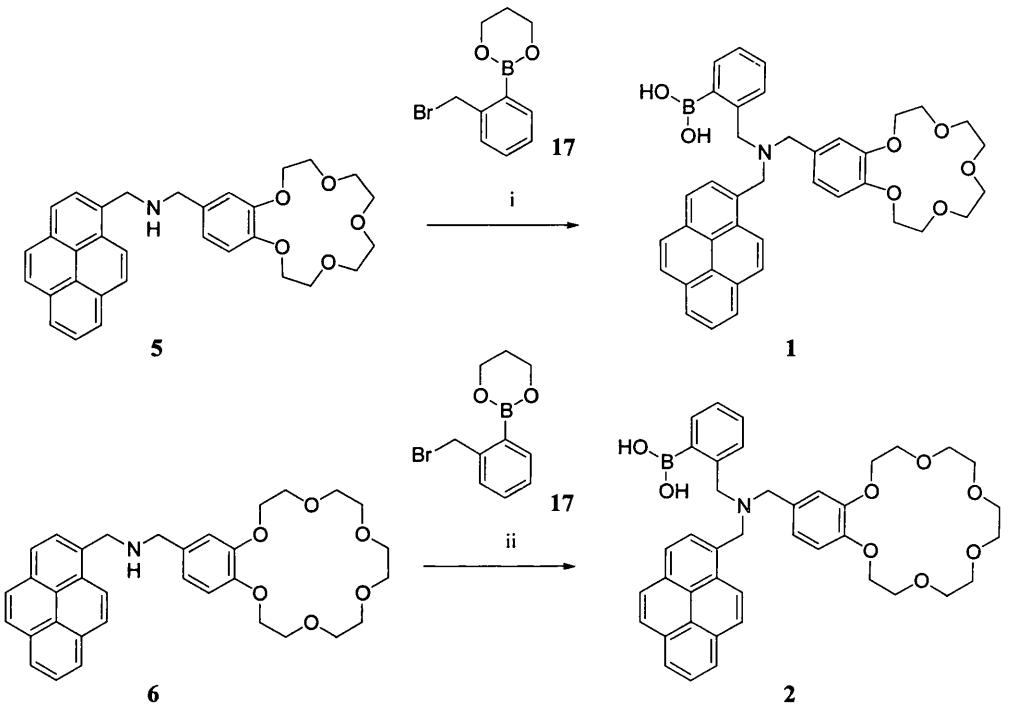

Scheme 8. Synthetic procedure for sensors **1** and **2**: i) Na_2CO_3 / MeCN:THF (1:1, v/v), reflux, 5h; ii) Na_2CO_3 / MeCN:THF (1:1, v/v), reflux, 5h.

The purified amine **5** was heated under reflux with the protected boronic acid **17** and sodium carbonate in a mixture of acetonitrile and tetrahydrofuran to form sensor **1**. Sodium carbonate was used to neutralise the hydrogen bromide that was formed by the S_N2 reaction of the boronic acid and the amine. Potassium carbonate was also used for this reaction but the NMR of the product was very complicated and purification was not possible. We believe that this was due to the potassium ion strongly binding with the 15-crown-5 forming a potassium sandwiched structure.[20] Purification was achieved by

trituration with chloroform and hexane. A sonic bath was used to prevent the formation of a gum-like solid. The synthetic procedure for the naphthalene sensors is shown below in Scheme 9.

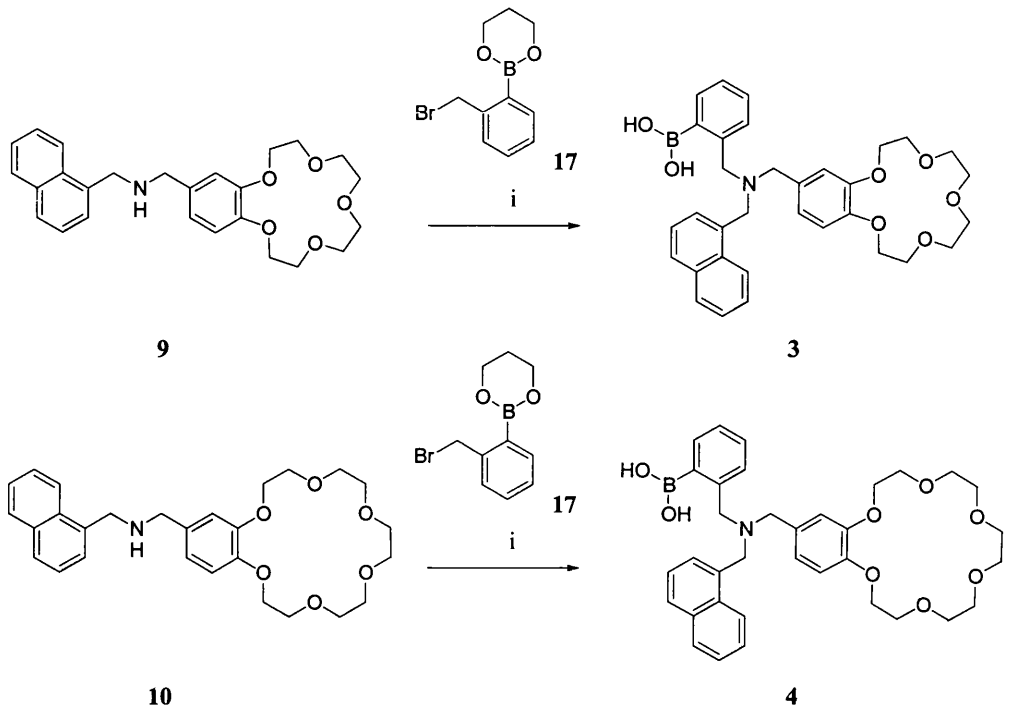

Scheme 9. Synthetic procedure of sensors **3** and **4**: i) Na_2CO_3 / MeCN:THF (1:1, v/v), reflux, 5h.

The purified amine **9** was heated under reflux with the protected boronic acid **17** and sodium carbonate in a mixture of acetonitrile and tetrahydrofuran. As before, sodium carbonate was used instead of potassium carbonate, for the same reasons as for the Pyrene series. Purification was carried out by precipitating from methanol using ice. This was performed by dissolving the crude product in a small amount of methanol and pouring the solution on ice. The product precipitated as a white solid. This procedure only worked for the naphthalene sensors and only when the reaction was done on a large scale. Therefore, trituration with chloroform and hexane was found to be the best

purification method. The yields for the naphthalene sensors **3** and **4** were obtained as 60% and 53% respectively.

2.3 Model compounds

Model compounds were prepared for comparison with the sensors. The first set of model compounds, which still contain the crown ether unit but lack the boronic acid, were synthesised as depicted in Scheme 6 for the Pyrene series and Scheme 7 for the Naphthalene series. The second set of model compounds, where the boronic acid exists but the crown ether unit has been replaced with a 3,4-dimethoxybenzyl group were synthesised in a similar manner to the sensor molecules as depicted in Scheme 10.

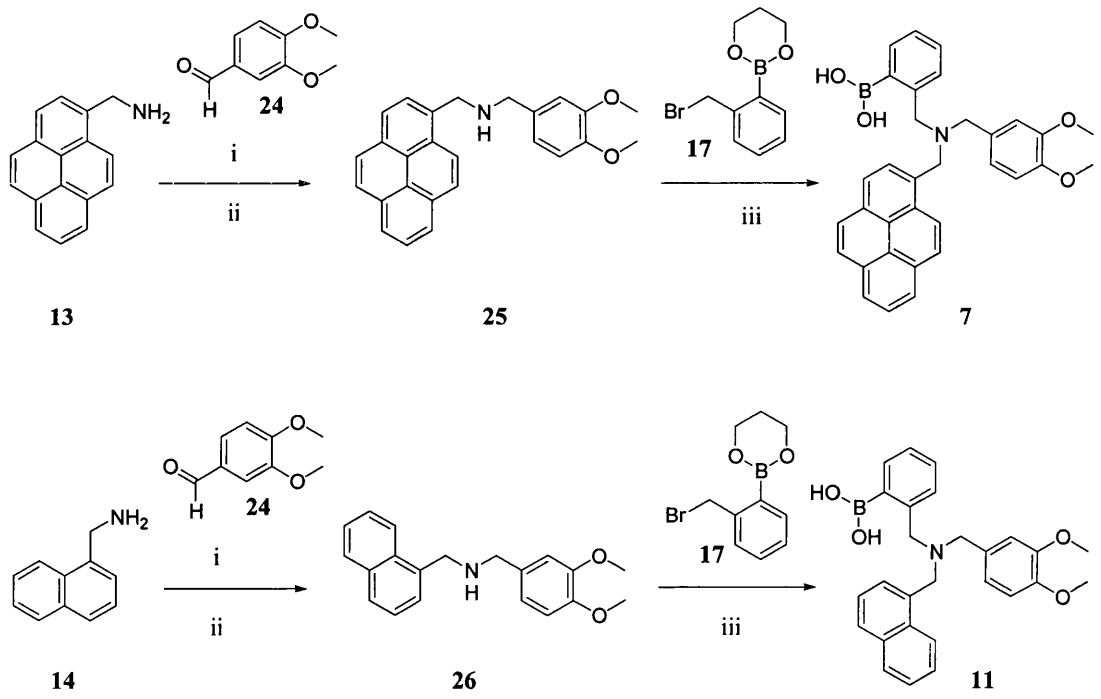

Scheme 10. Synthetic procedure for model compounds **7** and **11**: i) MeOH:THF (1:1, v/v), rt, 5h; ii) $NaBH_4$ / MeOH:THF (1:1, v/v), rt, 5h; iii) K_2CO_3 / MeCN:THF (1:1, v/v), reflux, 5h.

Reductive amination of the 3,4-dimethoxybenzaldehyde was performed using amine **13** or **14** by stirring at room temperature overnight. The formation of the intermediate imine was confirmed by crude ^1H NMR, the reaction mixture was then reduced *in situ*

to the amine by stirring with 5 equivalents of sodium borohydride. The pyrene amine **25** was purified by Bio Beads S-X8 polystyrene gel chromatography. Purification of the naphthalene amine **26** was not required. Treatment of the amines **25** and **26** with cyclic boronate ester **17** (1.2 equivalents) with sodium carbonate in a mixture of dry acetonitrile and dry THF (1:1) afforded the crude boronic acids **7** and **11.** As expected the reaction worked no differently with potassium carbonate and sodium carbonate. This was due to the dimethoxybenzyl group, which does not complex strongly with either sodium or potassium unlike the crown ether. Both boronic acids were purified by recrystallisation from a mixture of chloroform and hexane to yield white solids in 53% and 42% respectively. Crystals suitable for X-ray analysis were obtained. The crystal structure of one molecule of compound **11** is shown in Figure 42. In the structure compound **11** forms a dimer. The dimeric structure and data associated with the X-ray analysis are given in the Appendix 1-3. From the crystal structure it is evident that the boron (B1) is sp^2 hybridised. Therefore in the solid state no significant B-N interaction is observed.

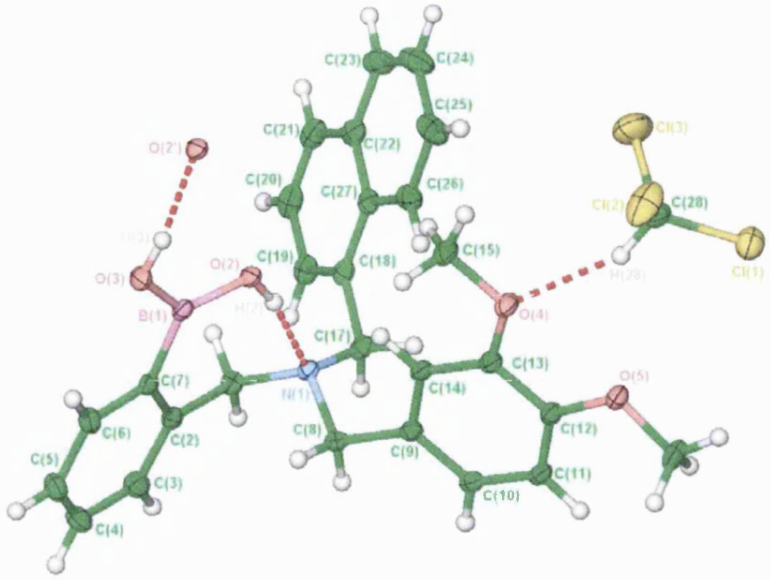

Figure 42. Crystal structure of compound **11**, showing the labelling scheme used. Thermal ellipsoids are represented at the 30% probability level.

The synthesis of the third set of model compounds, where the boronic acid remains but the crown ether unit has been replaced by a methyl group (**8** for the Pyrene series and **12** for the Naphthalene series) is depicted in Scheme 11.

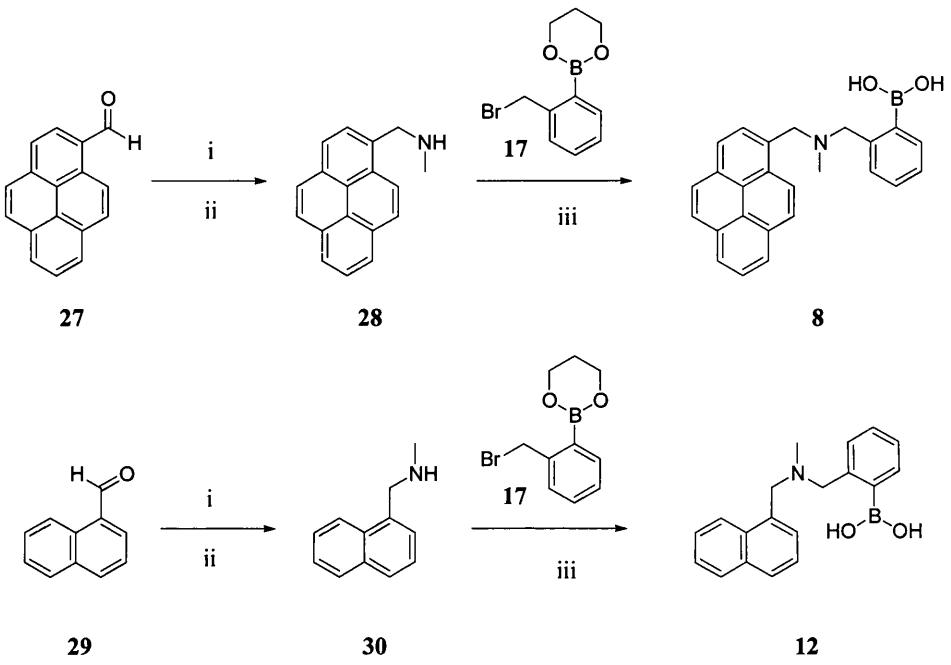

Scheme 11. Synthetic procedure for model compounds **8** and **12**: i) $MeNH_2$ / MeOH, rt, 5h; ii) Na_2BH_4 / MeOH, rt, 5h; iii) K_2CO_3 / MeCN:THF (1:1, v/v), reflux, 5h.

These model compounds were prepared by treating pyrene-1-carboxaldehyde or 1-naphthaldehyde with a solution of methylamine in methanol (3 equivalents) to give the corresponding intermediate imines. These imines were not isolated, as they were reduced *in situ* with sodium borohydride (5 equivalents) at room temperature. The amines **28** and **30** were afforded in yields of 57% and 78% respectively and no purification was necessary. The amines were then treated with 1.1 equivalents of cyclic boronate ester **17** with potassium carbonate in dry acetonitrile to afford the corresponding boronic acids **8** and **12** in 57% and 95% yield respectively.

2.4 Evaluation of sensors

Sensors **1** and **2** were designed to function as sensors for glucosamine hydrochloride, since they both had a crown ether unit and a boronic acid to bind ammonium and diol, respectively. In contrast to the glucosamine hydrochloride sensor designed earlier (Figure 37)[17,18], they do not possess a basic nitrogen. This would be a great advantage making the sensor pH-independent. The binding of glucosamine with sensors **1** and **2** was investigated in aqueous buffer but both compounds failed to give a fluorescence response. The binding with saccharides and metal ions was also investigated in aqueous buffer but this system also failed to give a detectable fluorescence response. The failure of these systems to work in aqueous solution prompted us to investigate the properties of **1** and **2** in chloroform, a non-coordinating solvent. When tetrabutylammonium fluoride was added to **1** and **2** in chloroform the fluorescence of the sensors was quenched. This result prompted us to investigate sensors **1** and **2** as ditopic receptors for metal cation and fluoride in methanol. The results follow below and as a pleasant bonus the sensors turned out to behave as AND logic gates as well.

In chloroform, titrations on eight sensors **1**, **2**, **3**, **4**, **7**, **8**, **11** and **12** and the four model compounds **5**, **6**, **9** and **10** were performed with tetrabutylammonium salts to evaluate the complexation of fluoride in chloroform.

In methanol, studies have been carried out with the four sensors **1-4** and the eight model compounds **5-12** with potassium salts or caesium salts in order to evaluate ditopic and AND logic functionality of the sensors.

Fluoride sensors - Interaction of sensors 1 and 2 with tetrabutylammonium salts

Titrations with tetrabutylammonium fluoride, chloride and bromide were performed in chloroform to measure the interaction between the fluoride and the boronic acid in chloroform.

The intensity of the fluorescence emission (I_F) of sensors **1**, **2**, **7** and **8** in chloroform was measured at different concentrations of tetrabutylammonium fluoride, tetrabutylammonium chloride and tetrabutylammonium bromide. When the sensors are titrated with tetrabutylammonium fluoride in chloroform, the fluorescence of the compounds decreases with added tetrabutylammonium fluoride. This fluorescence quenching is shown in Figure 43. The fluorescence of the model compounds **5** and **6** on the other hand is unchanged when tetrabutylammonium fluoride is added. Addition of the fluoride anion breaks the B-N bond of the molecule and hence quenches the fluorescence via the released nitrogen lone electron pair.

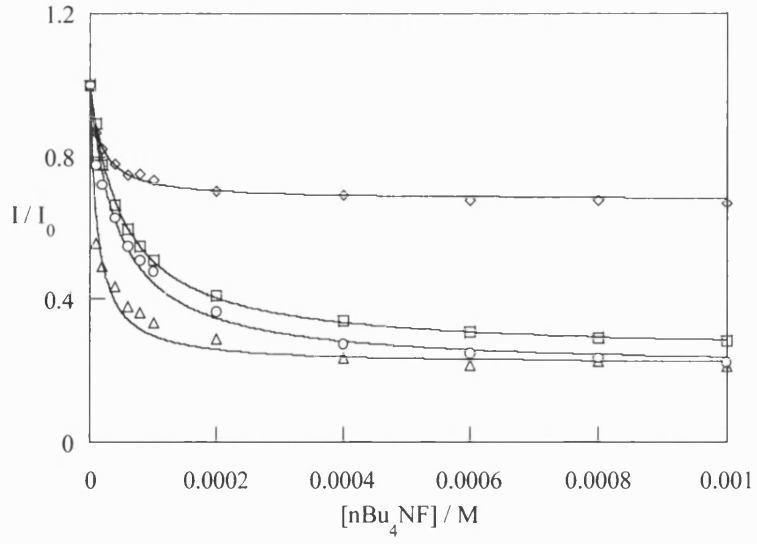

Figure 43. Relative fluorescence intensity *versus* nBu_4NF concentration profile of Pyrene sensors **1**, **2**, **7** and **8** (5×10^{-7} mol dm^{-3}) with (◊) sensor **1**, (Δ) sensor **2**, (□) sensor **7**, (○) sensor **8** in $CHCl_3$. λ_{ex} = 345 nm, λ_{ex} = 347 nm, λ_{ex} = 343 nm, λ_{ex} = 342 nm, respectively, λ_{em} =397 nm.

The fluorescence of sensor **1** is not quenched as much as the fluorescence of the other sensors. The two sensors with no crown ether unit, sensors **7** and **8**, are quenched most by the addition of tetrabutylammonium fluoride. When the compounds were titrated with tetrabutylammonium chloride and tetrabutylammonium bromide the fluorescence was not quenched. The graphs of the titrations of compounds **1**, **2**, **7** and **8** and also the model compounds **5** and **6** with all three tetrabutylammonium salts are given in Appendix 4-13.

The curves were analysed using equation (1) assuming the formation of a monofluoro boronate ($n = 1$).[123]

$$I_f = \frac{I_0 + I_\infty K_n[F^-]^n}{1 + K_n[F^-]^n} \qquad (1)$$

where $$K_n = \frac{[RB(OH)_{3-n}F_n]}{[RB(OH)_2][F^-]^n}$$

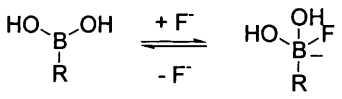

Scheme 12. Formation of monofluoro boronate.

The stability constants of the sensors **1**, **2**, **7** and **8** are shown in Table 2. The model compounds **5** and **6** do not bind fluoride due to the lack of boronic acid and hence do not have a stability constant.

Sensor	nBu_4NF K / dm^3mol^{-1}	r^2
1	$5.9 \times 10^4 \pm 3.5 \times 10^3$	0.996
2	$8.7 \times 10^4 \pm 8.4 \times 10^3$	0.997
7	$1.9 \times 10^4 \pm 3.4 \times 10^2$	1.000
8	$2.3 \times 10^4 \pm 1.4 \times 10^3$	0.995

Table 2. Stability constants of sensors **1**, **2**, **7** and **8** with nBu_4NF in chloroform.

The stability constants of the Pyrene sensor series are given in the graphical representation below (Figure 44).

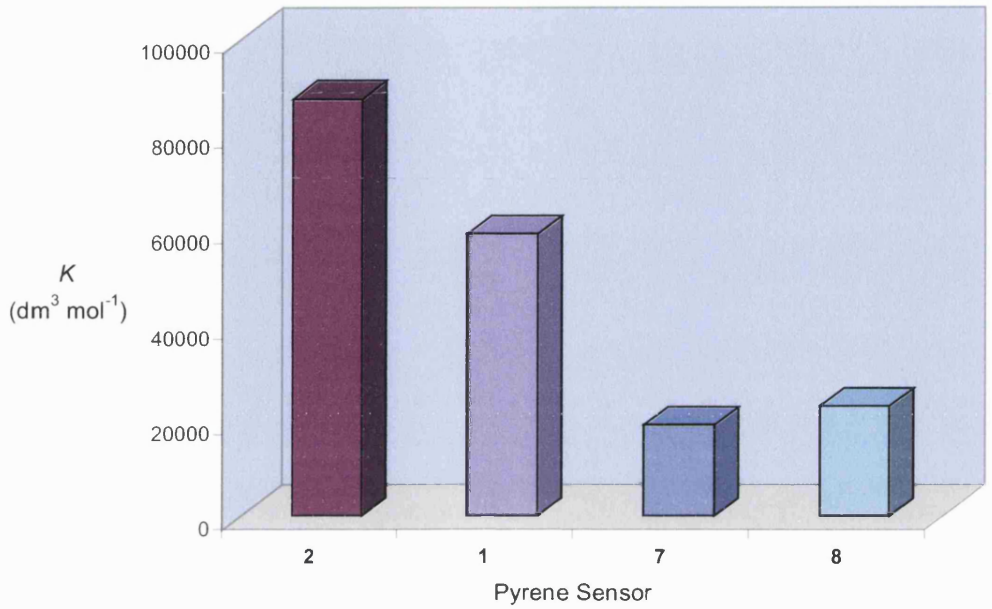

Figure 44. Graphical representation of the stability constants of the Pyrene series with tetrabutylammonium fluoride in chloroform.

The graph shows that the stability constants are highest for the sensors **1** and **2**. Both compounds contain a large benzocrown ether group, which makes the molecule sterically crowded, as a result this makes the B-N bond weaker. Since this B-N bond is weaker, it is easier to break and hence the binding constant of the fluoride anion is larger. For the other two pyrene sensors **7** and **8** this B-N bond is stronger and harder to break; hence the observed binding constants are smaller.

The titrations with the tetrabutylammonium salts in chloroform were also performed with the second series of sensors, the Naphthalene series. When compounds **3**, **4**, **11** and **12** are titrated with tetrabutylammonium fluoride in chloroform, the fluorescence of the naphthalene compounds also decreases with added tetrabutylammonium fluoride. This fluorescence quenching is shown in Figure 45. The fluorescence of the model compounds **9** and **10** on the other hand is unchanged, as expected, when tetrabutylammonium fluoride is added.

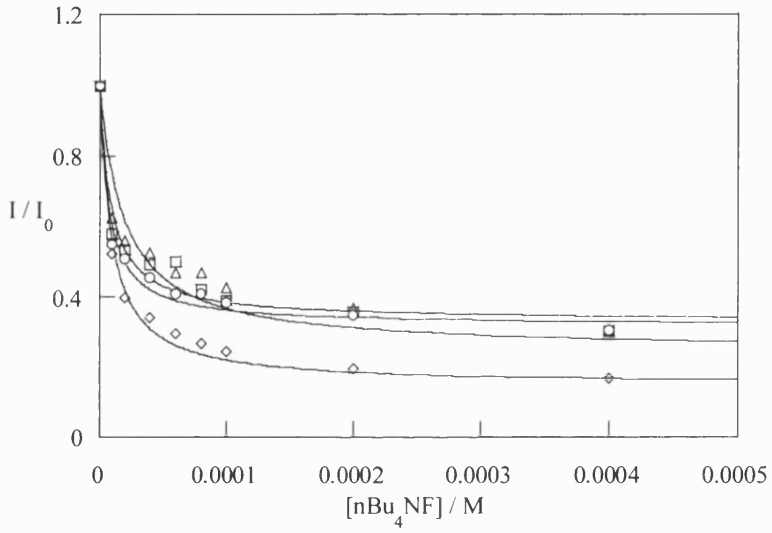

Figure 45. Relative fluorescence intensity *versus* nBu_4NF concentration profile of Naphthalene sensors **3**, **4**, **11** and **12** (5×10^{-7} mol dm^{-3}) with (◊) sensor **3**, (Δ) sensor **4**, (□) sensor **11**, (○) sensor **12** in $CHCl_3$. λ_{ex} = 288 nm, λ_{ex} = 288 nm, λ_{ex} = 270 nm, λ_{ex} = 288 nm, respectively, λ_{em} =335 nm.

In the Naphthalene series sensor **3** exhibits the greatest fluorescence quenching. The two sensors with no crown ether unit, sensors **11** and **12**, exhibit the smallest quenching effects when tetrabutylammonium fluoride is added but are still quenched considerably. When the compounds were titrated with tetrabutylammonium chloride and tetrabutylammonium bromide the fluorescence was not quenched. The graphs of the

titrations of compounds **3**, **4**, **11** and **12** and also the model compounds **9** and **10** with all three tetrabutylammonium salts can be found in Appendix 14-23.

The stability constants for the Naphthalene series are listed in Table 3.

Sensor	nBu_4NF K / dm^3mol^{-1}	r^2
3	$1.1 \times 10^5 \pm 7.4 \times 10^3$	0.995
4	$5.2 \times 10^4 \pm 7.0 \times 10^3$	0.975
11	$1.1 \times 10^5 \pm 1.6 \times 10^4$	0.979
12	$1.4 \times 10^5 \pm 1.6 \times 10^4$	0.988

Table 3. Stability constants of sensors **3**, **4**, **11** and **12** with nBu_4NF in chloroform.

Graphical representation of the stability constants of the Naphthalene series with tetrabutylammonium fluoride in chloroform is depicted in Figure 46. From the graph in Figure 46 it is apparent that the largest binding constants are observed for compounds **11** and **12** in contrast to the Pyrene series. Generally the values are much greater for the Naphthalene series than for the Pyrene series.

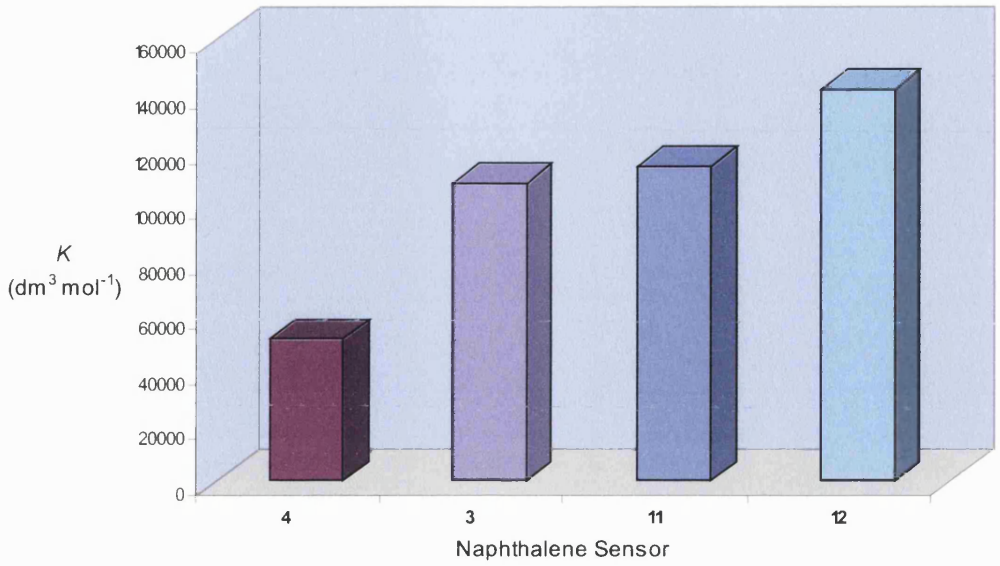

Figure 46. Graphical representation of the stability constants of the Naphthalene series with tetrabutylammonium fluoride in chloroform.

^{11}B NMR experiments were performed to confirm the presence of the fluoride adducts in chloroform for all compounds and are listed in Table 4. The changes in the hybridisation of boron are reflected in its chemical shift in the ^{11}B NMR spectrum.[140] When the boron atom is tetrahedral its chemical shift is upfield from that observed for a trigonal planar geometry, where the peaks corresponding to sp^3 and sp^2 occur at approximately 0 and 30 ppm respectively.

The Naphthalene series do not behave as we expected and we have been unable to explain the behaviour. The naphthalene fluorophore is excited in the same wavelength region as the benzene of the crown receptor, which may be one of the factors causing the confusing results. Therefore it is impossible to determine which of the π-systems is responding to the excitation.

Compound	^{11}B in $CDCl_3$ (ppm)	^{11}B with nBu_4NF in $CDCl_3$ (ppm)
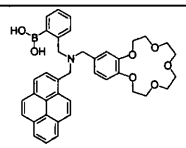 **1**	— [a]	— [a]
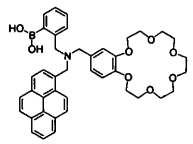 **2**	— [a]	4.3 (sp^3)
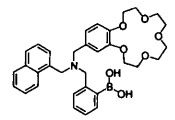 **3**	— [a]	5.8 (sp^3)
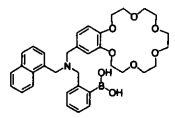 **4**	— [a]	0.40 (sp^3)
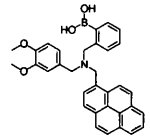 **7**	— [a]	4.6 (sp^3)
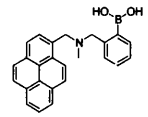 **8**	— [a]	4.4 (sp^3)
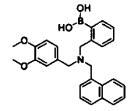 **11**	26.3 (sp^2)	4.9 (sp^3)
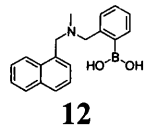 **12**	30.6 (sp^2)	4.9 (sp^3)

Table 4. Shift in signals in the ^{11}B NMR upon addition of nBu_4NF to solutions of sensors and model compounds in $CDCl_3$. [a]Measured but signal is not observed.

Even though the compounds did dissolve in chloroform, the ^{11}B peaks were broad for most of the compounds and could not be assigned. Sensor **11** shows a peak at 26.3 ppm

which corresponds to free boronic acid (sp^2). On addition of tetrabutylammonium fluoride the peak shifts to 4.9 ppm. The observed shifts from high to low field in the ^{11}B NMR are consistent with a change from sp^2 to sp^3 boron centre on fluoride binding.[141] The crystal structure of compound **11** (Appendix 1-3) also indicated that the compound has no B-N bond. However, previous spectroscopic studies have indicated a weak interaction between the boron and nitrogen.[125,126,142] Sensor **12** shows similar behaviour as sensor **11**. The ^{11}B peak shifts from 30.6 ppm to 4.9 ppm on addition of tetrabutylammonium fluoride. The corresponding pyrene sensor **7** did not show a definitive ^{11}B peak but on addition of tetrabutylammonium fluoride there was a sharp peak at 4.6 ppm confirming fluoride binding. Sensors **3**, **4**, **2** and **8** behaved similarly, not showing a definitive peak before addition of fluoride.

AND logic functionality - Interaction of sensors with potassium and caesium fluoride

Potassium fluoride consists of two ions that can bind with the sensors, the potassium ion with the crown ether unit and the fluoride ion with the boronic acid. The same applies to caesium fluoride. The binding of these reagents was compared with the chloride and bromide salts. The intensity of the fluorescence emission (I_F) of sensors **1** and **2** and model compound **7** was measured at different concentrations of potassium fluoride and caesium fluoride in methanol solution.

When the binding sites of the sensor are free, the PET process quenches the fluorescence (Scheme 13). When a substrate ion, e.g. potassium (Path A), is bound to one of the receptors this hinders PET from the bound receptor, however there is still a PET process from the second unbound receptor. Likewise, when only the second receptor is occupied by a guest, e.g. fluoride (Path B), the PET process is not turned off since the other receptor is still free. For PET to be turned off and fluorescence restored both receptors must be bound to the corresponding guests (potassium and fluoride); the PET is then turned off and the sensor is able to fluoresce (Path C and D).

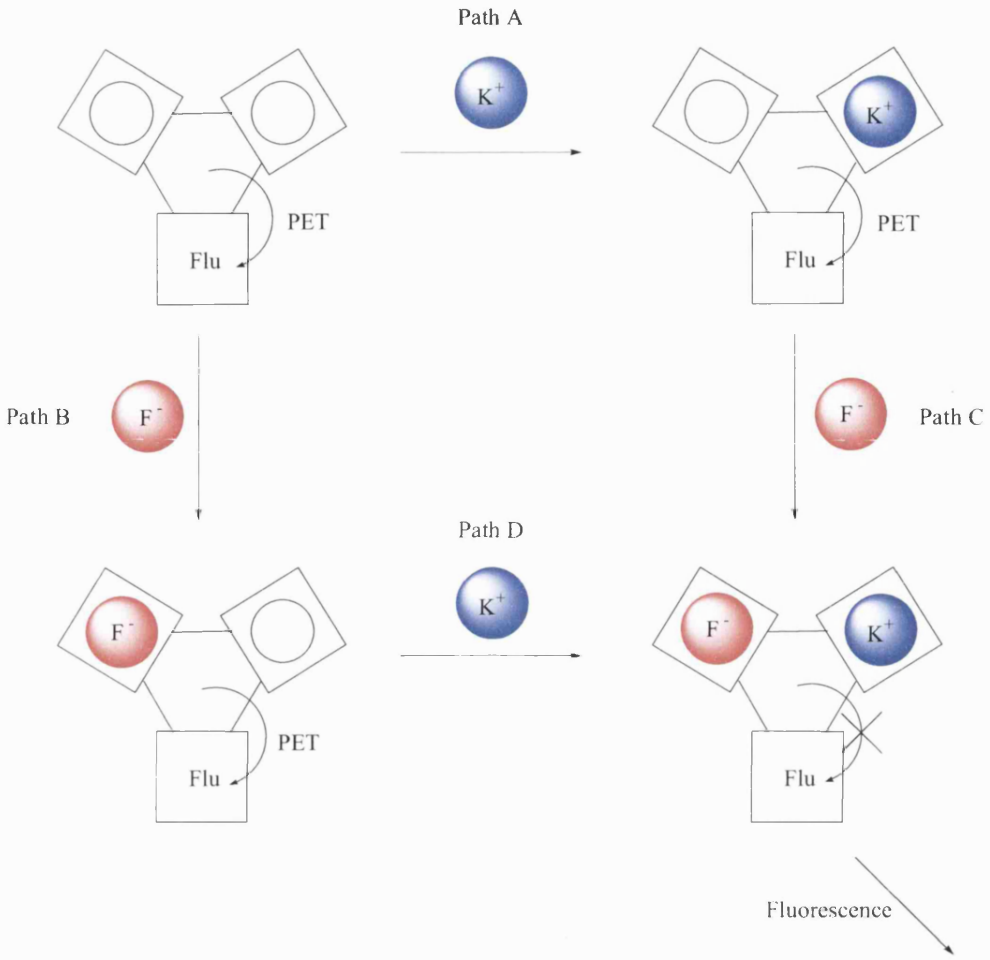

Scheme 13. Schematic explanation of PET involvement in an AND sensor with potassium fluoride.

The information in Scheme 13 can be summarised in terms of equations 2 and 3.[143]

$$\Delta G_{PET} = -E_{S.fluorophore} + E_{ox.fluorophore} - E_{red.receptor} + \Delta G_{ion\ pair} \quad (2)$$

$$E_{S.fluorophore} = E_{ox.fluorophore} - E_{red.fluorophore} \quad (3)$$

ΔG_{PET} is the thermodynamic driving force for PET, E_{ox} and E_{red} are the related oxidation and reduction potentials, E_S is the singlet energy and $\Delta G_{ion\ pair}$ is the attractive energy

between a contact radical ion pair created upon the occurrence of the PET process and assumed to be -0.1 eV.[144]

The titration curves of **1**, **2** and **7** with potassium fluoride and caesium fluoride (Figure 47-Figure 49 and Figure 51-Figure 53, respectively) were analysed using the following model. A model involving only two complexes was employed, the 1:1 cation (M) and sensor (S) complex (MS) and the ternary complex (MSF) with the cation and fluoride (F). This model defined two formation constants:

$$M + S \rightleftharpoons MS \qquad \beta(110) = \frac{[MS]}{[M][S]}$$

$$M + S + F \rightleftharpoons MSF \qquad \beta(111) = \frac{[MSF]}{[M][S][F]}$$

The model assumed that all fluorescence arose from three species; S, MS and MSF. The initial observed intensity and the analytical concentration of the sensor S defined an 'emissive constant' a(S). The magnitude of the 'emissive constant' for MS (a(MS)) was determined from the limiting value of the fluorescence enhancement factor (EF) observed on addition of MCl and MBr to the sensor S when MSF cannot be formed. Thus, a(MS) = a(S) × EF. The unknown constant a(KSF) was refined during the fitting process.

Curve fitting was performed using the DOS version of the program OPIUM[145] based on a linear response function for the total fluorescence intensity (OPIUM type 7 calibration function). The input datafile was structured according to the sample file INPANS. Alternative models with additional complexes, such as SF complexes did not give

refined values. Refining a(MS) and/or a(S) recovered values similar to the fixed input values and moreover did not alter the values of formation constants, but increased their uncertainties considerably. Values are reported as $\pm 3\sigma$ to give the 95% confidence limit as calculated by the program. The model fits exceeded $r^2 = 0.997$ in all cases. The output file was imported to Excel for subsequent plotting. The graphs obtained for the potassium fluoride titrations are illustrated in the figures below (Figure 47-Figure 49).

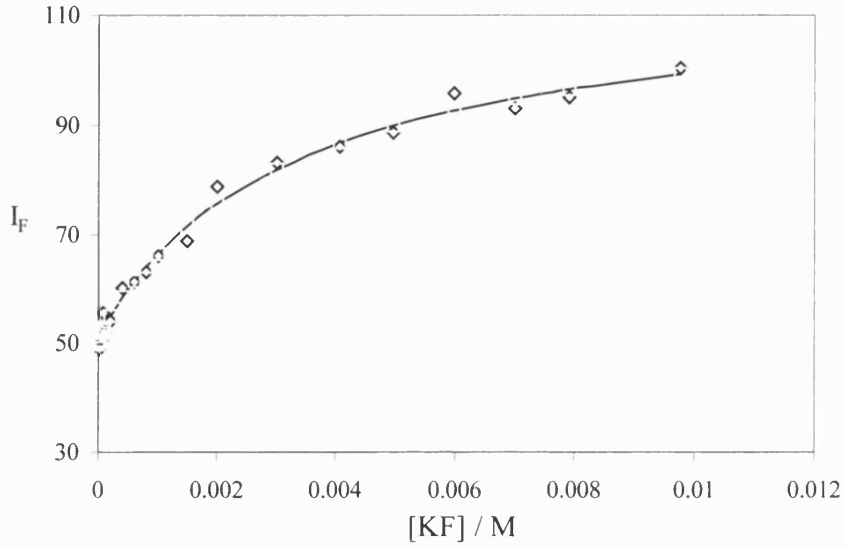

Figure 47. Fluorescence Intensity (I_F) of sensor **1** (5×10^{-7} M) *versus* KF (♦) at 25 °C in methanol; $\lambda_{ex} = 345$ nm, $\lambda_{em} = 397$ nm.

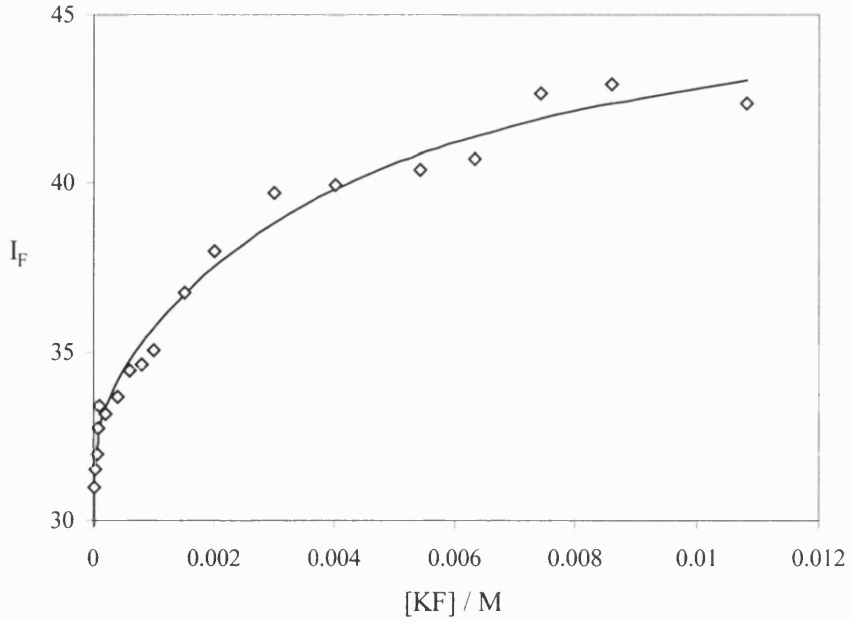

Figure 48. Fluorescence Intensity (I_F) of sensor **2** (5×10^{-7} M) *versus* KF (♦) at 25 °C in methanol; λ_{ex} = 347 nm, λ_{em} = 397 nm.

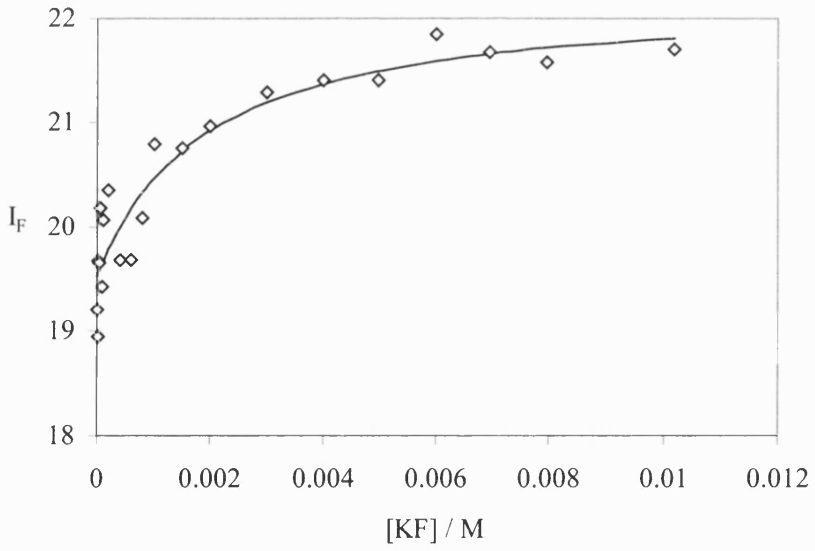

Figure 49. Fluorescence Intensity (I_F) of model compound **7** (5×10^{-7} M) *versus* KF (♦) at 25 °C in methanol; λ_{ex} = 343 nm, λ_{em} = 397 nm.

The enhancement of the fluorescence intensity (I_F) is much greater for sensor **1** than for sensor **2** when adding potassium fluoride. The fluorescence enhancement for model

compound **7** is poor when adding potassium fluoride. Model compound **7** can bind fluoride but cation binding is weak, resulting in a low precision in the curve fitting.

For comparison the intensity of fluorescence emission of these molecules was also measured with potassium chloride and potassium bromide in methanol. The relative fluorescence intensities were then plotted against the concentration of the added salt. The graph for sensor **1** with potassium salts is shown in Figure 50. The graphs for sensor **2** and model compounds **5-8** are found in the Appendix 24-31.

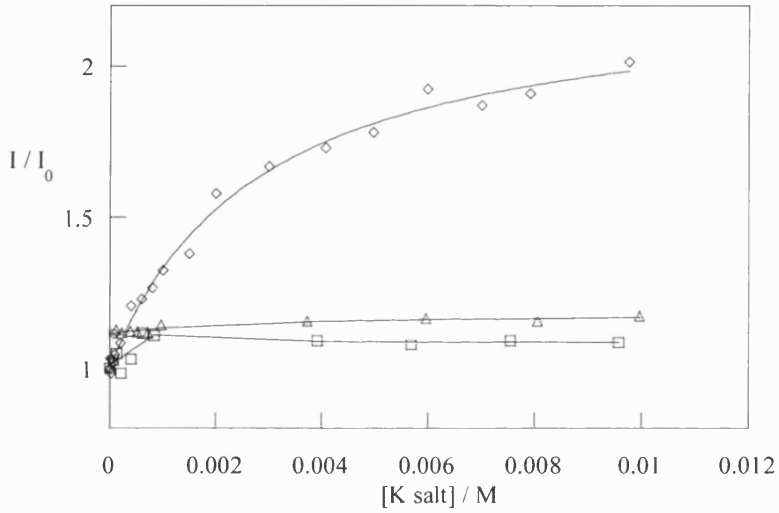

Figure 50. Relative Fluorescence Intensity of sensor **1** (5×10^{-7} M) *versus* KF (◊), KCl (Δ) and KBr (□) at 25 °C in methanol; $\lambda_{ex} = 343$ nm, $\lambda_{em} = 397$ nm.

The graphs of the caesium fluoride titrations with sensors **1** and **2** and model compound **7** with caesium fluoride are shown below (Figure 51-Figure 53).

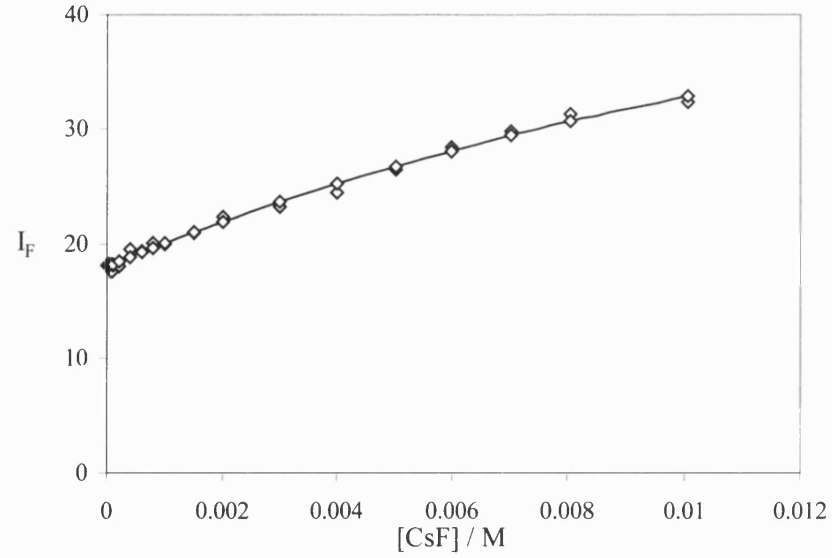

Figure 51. Fluorescence Intensity (I_F) of sensor **1** (5×10^{-7} M) *versus* CsF (♦) at 25 °C in methanol; λ_{ex} = 345 nm, λ_{em} = 397 nm.

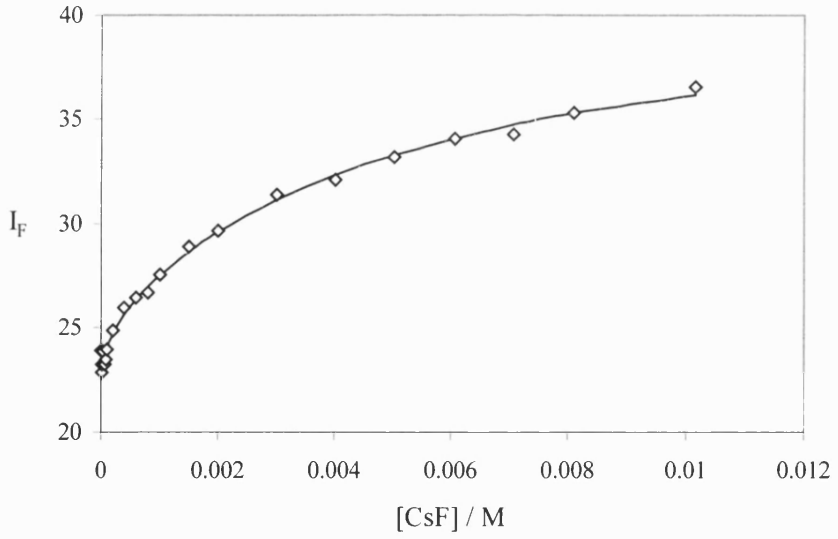

Figure 52. Fluorescence Intensity (I_F) of sensor **2** (5×10^{-7} M) *versus* CsF (♦) at 25 °C in methanol; λ_{ex} = 347 nm, λ_{em} = 397 nm.

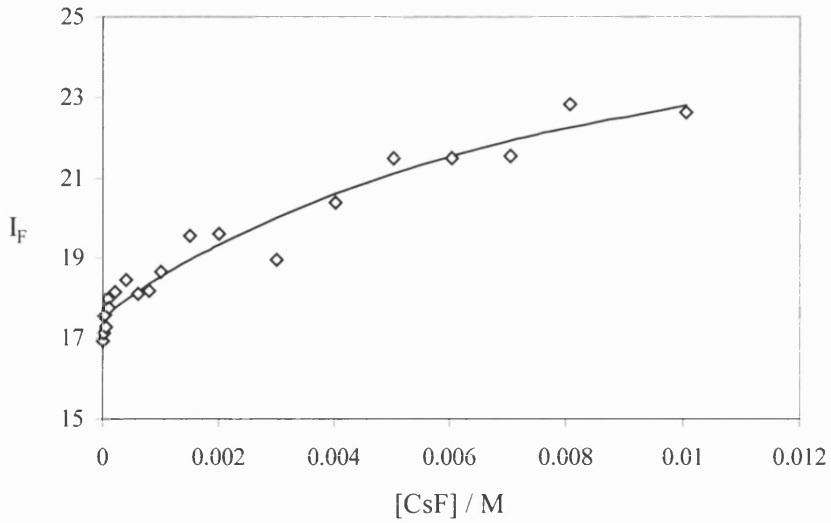

Figure 53. Fluorescence Intensity (I_F) of model compound **7** (5×10^{-7} M) *versus* CsF (♦) at 25 °C in methanol; λ_{ex} = 343 nm, λ_{em} = 397 nm.

Again, for comparison the intensity of fluorescence emission of these molecules was also measured with caesium chloride and caesium bromide in methanol. The relative fluorescence intensities were then plotted against the concentration of the added salt (Figure 54). The graphs for sensors (**1** and **2**) and model compounds (**5-8**) with caesium salts are given in the Appendix 32-39.

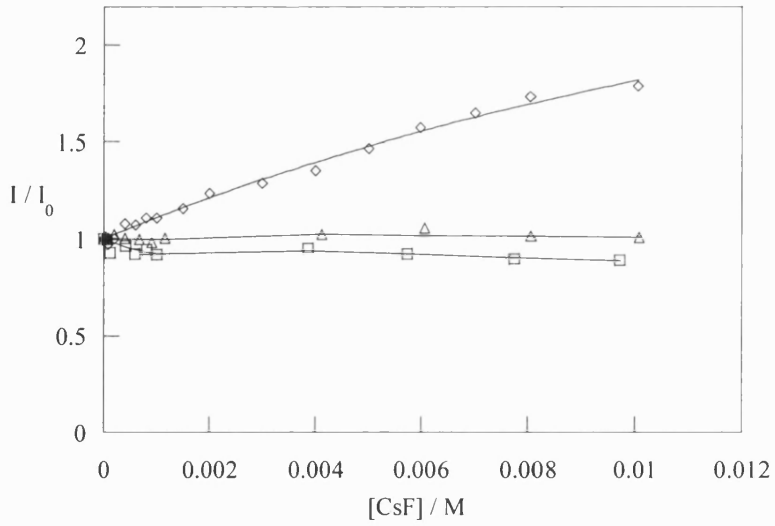

Figure 54. Relative Fluorescence Intensity of sensor **1** (5×10^{-7} M) *versus* CsF (◊), CsCl (Δ) and CsBr (□) at 25 °C in methanol; λ_{ex} = 343 nm, λ_{em} = 397 nm.

The stability constants *K* of the complexes formed between the sensors and potassium fluoride and caesium fluoride were analysed with the program OPIUM[145]. The models for the stability constants were

$$[K] + [Sensor] \rightleftharpoons [KSensor]$$

$$[K] + [Sensor] + [F] \rightleftharpoons [KSensorF]$$

and the same for CsF

$$[Cs] + [Sensor] \rightleftharpoons [CsSensor]$$

$$[Cs] + [Sensor] + [F] \rightleftharpoons [CsSensorF]$$

The system of the CsF with sensor **2** did not fit well because there was very little curvature in the data. This is related to the lack of an enhancement due to Cs binding. The two model systems, model compound **7** with KF and CsF, displayed fluoride binding but not cation binding. Unsurprisingly the precision was poor in both cases.

The stability constants of sensors **1** and **2** and model compound **7** are shown in Table 5.

Sensor	K^+ K /dm^{3}mol^{-1}	F^- K /dm^{3}mol^{-1}	KF K /dm^{3}mol^{-1}	Cs^+ K /dm^{3}mol^{-1}	F^- K /dm^{3}mol^{-1}	CsF K /dm^{3}mol^{-1}
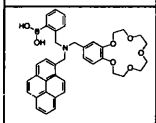 **1**	4.0 ± 0.5	2.5 ± 0.5	6.5 ± 0.4	4 ± 3	2 ± 3	6 ± 3
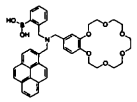 **2**	4.7 ± 0.2	2.4 ± 0.2	7.1 ± 0.2	3.6 ± 0.2	2.2 ± 0.2	5.8 ± 0.2
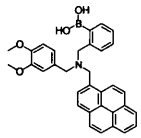 **7**	-[a]	2.7 ± 1.1	-[a]	-[a]	2.0 ± 1.2	-[a]

Table 5. Stability constants K for sensors **1** and **2**. [a]Does not form a stable complex with potassium or potassium fluoride.

From the graphical representation in Figure 55 it is clear that the stability constants are highest for the potassium fluoride complex with sensor **2**. The stability constant of sensor **1** is similar but lower. The stability constant with caesium fluoride is quite similar for both sensors.

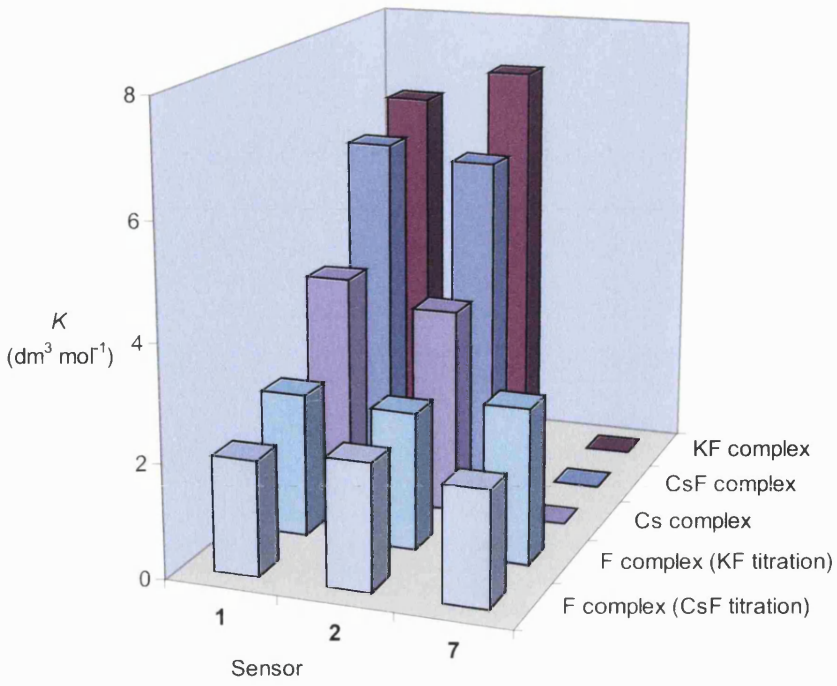

Figure 55. Stability Constants K (dm^3 mol^{-1}) of sensors **1** and **2**.

The fluorescence titrations with potassium and caesium fluoride, chloride and bromide were also performed with the Naphthalene series sensors **3** and **4** and reference compounds **9-12**. These fluorescence titrations were noisy and the fitting of the graphs did not work well. We believe that this is due to the overlapping of the excitation wavelengths of the naphthalene fluorophore and the benzene of the crown ether. During the fluorescence measurements it is not only the naphthalene that is excited but also the benzyl rings. The graphs of the naphthalene sensors **3** and **4** titrations with potassium salts and examples of the titrations are shown in the Appendix 40-46.

Because sodium salts do not dissolve well in methanol, which was used as solvent, the fluorescence titrations were very noisy and therefore the data points were erratic and unreliable. Examples of the graphs for these titrations are shown in the Appendix 47-48.

Enhancement factors (EF) for all sensors and model compounds of the Pyrene series were measured by adding 6 mM of potassium fluoride or caesium fluoride to a solution of 5×10^{-7} M sensor in methanol. Three sets of measurements were performed for each salt and sensor. The average values of the measurements are listed in Table 6.

Sensor	Added salt	EF
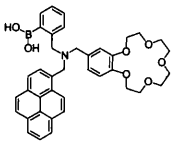 **1**	KF	1.77 ± 0.04
	CsF	1.39 ± 0.03
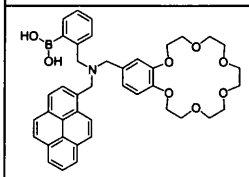 **2**	KF	1.60 ± 0.06
	CsF	1.55 ± 0.01
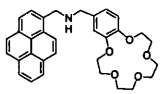 **5**	KF	0.88 ± 0.03
	CsF	0.99 ± 0.09
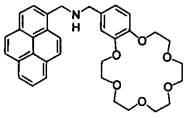 **6**	KF	0.93 ± 0.03
	CsF	0.98 ± 0.02
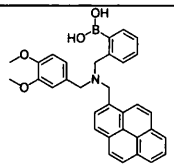 **7**	KF	1.07 ± 0.02
	CsF	1.14 ± 0.02
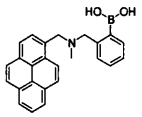 **8**	KF	1.13 ± 0.03
	CsF	1.23 ± 0.02

Table 6. Table of enhancement factors (EF) when adding 6 mM of potassium fluoride or caesium fluoride.

From these values it can be seen that addition of potassium fluoride or caesium fluoride to all of the model compounds (**5-12**) does not enhance the fluorescence. Addition of potassium salt to sensor **1** and sensor **2** enhances the fluorescence intensity considerably. Caesium fluoride also enhances the fluorescence but less for sensor **1** than sensor **2**. Model compounds **5**, **6**, **7** and **8** were not affected much by the addition of the salts.

Measurements were performed with sensors **1** and **2** to test the 'Off-On' action of the sensors. This is schematically explained in Scheme 14. When both potassium and fluoride are occupying respective receptors, the sensor emits fluorescence. Addition of 2.2.2-cryptand removes the potassium ion and switches the sensor off. Fluorescence is restored by addition of potassium, for example as potassium chloride.

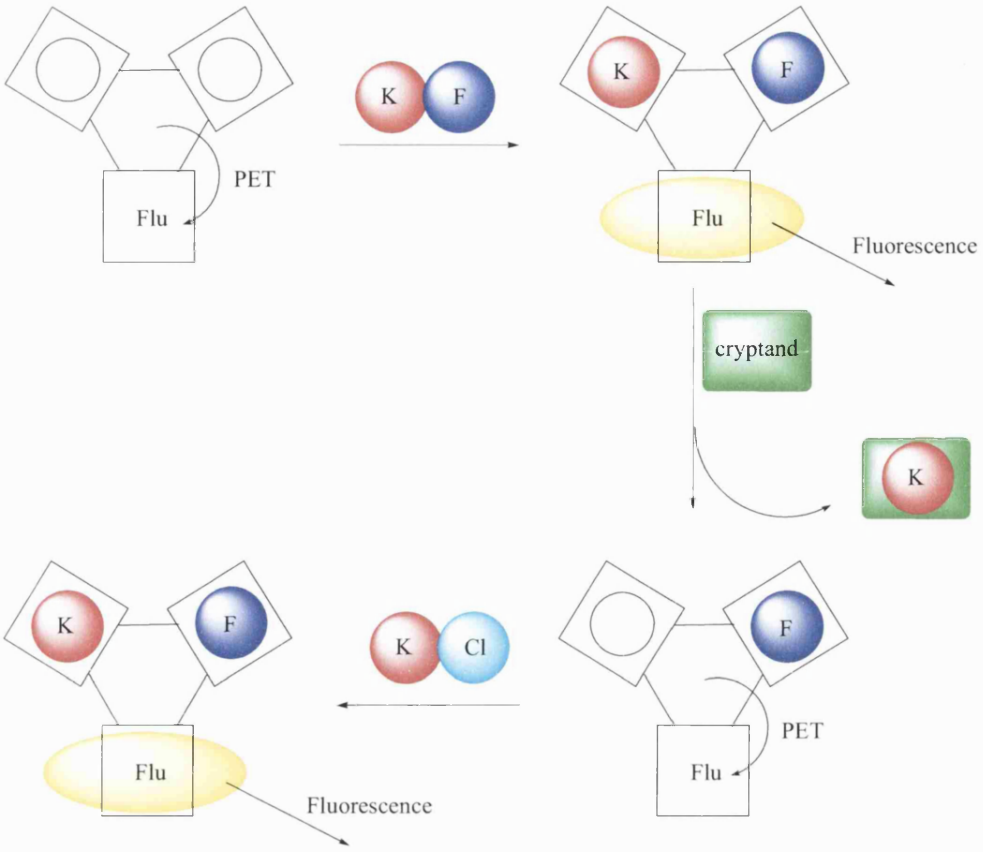

Scheme 14. Schematic explanation of the 'Off-On' action.

The measurements for the 'Off-On' action were repeated three times. Examples of these titrations are in the Appendix 49-51. When adding potassium fluoride to sensor **1** the intensity increases. This is read as the 'On' (1) action of the sensor. When 1 equivalent (6 mM) of 2.2.2-cryptand (Figure 56) is added the fluorescence is suppressed at initial intensity, switching off the sensor ('Off' (0) action).

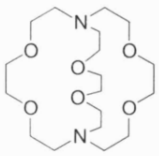

Figure 56. Structure of 2.2.2-Cryptand.

The 2.2.2-cryptand has a higher binding constant with potassium than 15-crown-5 (10.6 for 2.2.2-cryptand and 3.43 for 15-crown-5 in logarithmic units)[45] and removes the potassium from the crown ether of the sensor. Since the sensor needs both potassium and fluoride to be switched on, the sensor does not work without the potassium being bound to the crown ether. When potassium cation is added in the form of potassium chloride, the sensor is turned on again and the fluorescence goes up to the same level as with the first addition of potassium fluoride.

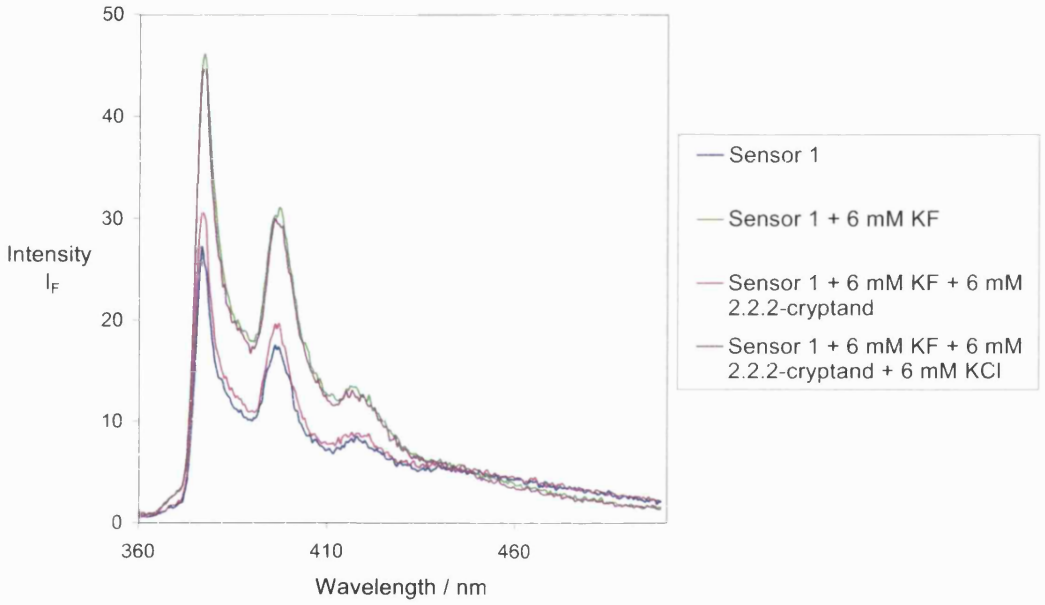

Figure 57. 'Off-On' action of sensor **1** with addition of potassium fluoride, 2.2.2-cryptand and potassium chloride.

The enhancement factors for the 'Off-On' action are listed in the table below (Table 7).

Sensor	Added salt	EF
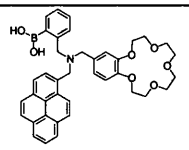 **1**	KF	1.76 ± 0.07
	2.2.2-Cryptand	1.07 ± 0.08
	KCl	1.64 ± 0.2
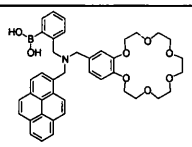 **2**	KF	1.61 ± 0.01
	2.2.2-Cryptand	1.01 ± 0.03
	KCl	1.56 ± 0.01

Table 7. Average enhancement factors for sensors **1** and **2** with added potassium fluoride, 2.2.2-cryptand and potassium chloride.

The experiment was repeated but instead of adding potassium chloride after switching the sensor off with 2.2.2-cryptand, caesium chloride was added. Again, the sensor was turned on, this time by the caesium ion binding to the crown ether. The fluorescence intensity did not reach the same level as with potassium fluoride but there is a clear 'On'-action when caesium fluoride is added. The lower level of intensity is due to the lower binding constant for caesium.

The average enhancement factors for sensor **1** during the 'Off-On' action when caesium chloride was used to switch the sensor on again are listed in the table below (Table 8).

Sensor	Added salt	EF
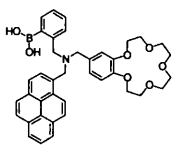 **1**	KF	1.76 ± 0.04
	2.2.2-Cryptand	1.02 ± 0.04
	CsCl	1.25 ± 0.02

Table 8. Average enhancement factors for sensor **1** with added potassium fluoride, 2.2.2-cryptand and caesium chloride.

^{11}B (96 MHz) NMR experiments were performed to compare the chemical shifts of the compounds both with and without fluoride. The results are shown in Table 9.

Compound	^{11}B without KF in CD_3OD	^{11}B with KF in CD_3OD
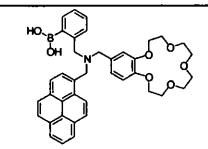 **1**	— [b]	— [b]
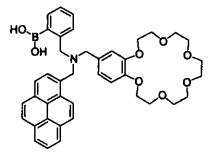 **2**	— [b]	— [b]
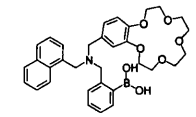 **3**	29.8 (sp^2)	5.4 (sp^3)
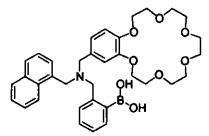 **4**	28.9 (sp^2) *(main peak)* 18.1 (sp^3) *(minor peak)*	5.1 (sp^3)
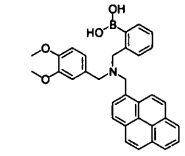 **7**	— [a]	— [a]
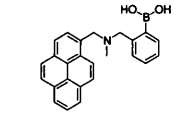 **8**	33.0 (sp^2) *(minor peak)* 11.0 (sp^3) *(main peak)*	8.9 (sp^3)
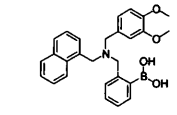 **11**	29.0 (sp^2) *(main peak)* 18.8 (sp^3) *(minor peak)*	6.5 (sp^3)
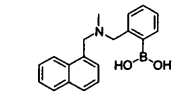 **12**	29.9 (sp^2) *(minor peak)* 9.0 (sp^3) *(main peak)*	8.8 (sp^3)

Table 9. Shift in signals in the ^{11}B NMR upon addition of KF to solutions of sensors and model compounds. [a]Compound not soluble in CD_3OD. [b]Measured but signal is not observed.

The changes in the hybridisation of boron are reflected in its chemical shift in the ^{11}B NMR.[140] When boron is tetrahedral its chemical shift is upfield from that trigonal planar geometry, where pure sp^3 and sp^2 are found at approximately 0 and 30 ppm respectively. From the measured ^{11}B NMR it can be seen that the boronic acid in sensors **11**, **3** and **4**, when dissolved in d_4-methanol, are predominantly sp^2 hybridised. There is a smaller peak, which shows that some of the molecules are sp^3 hybridised. When fluoride ion is added, the ^{11}B peak shifts by approximately 25 ppm and the boronic acid is completely sp^3 hybridised. The boronic acids in model compounds **12** and **8** already display mostly sp^3 hybridisation but there is still a small peak at about 30 ppm, which corresponds to some sp^2 hybridisation. After addition of fluoride there is only one peak around 8 ppm which means that the boronic acids are now completely sp^3 hybridised.

To ensure that protons from the solvent do not contribute to the behaviour of sensor **1** and to demonstrate that the boronic acid was completely fluorinated, the following experiment was performed. The fluorescence of a 5×10^{-7} M solution of sensor **1** in methanol was measured after adding 6 mM of potassium fluoride and 6 mM of sodium hydroxide. This was repeated three times. An example of the fluorescence graph is shown in Figure 58. Sodium hydroxide was used to demonstrate the effect of hydroxide ions because sodium ions have no effect on the fluorescence intensity of the sensor, but this was because sodium chloride was not soluble.

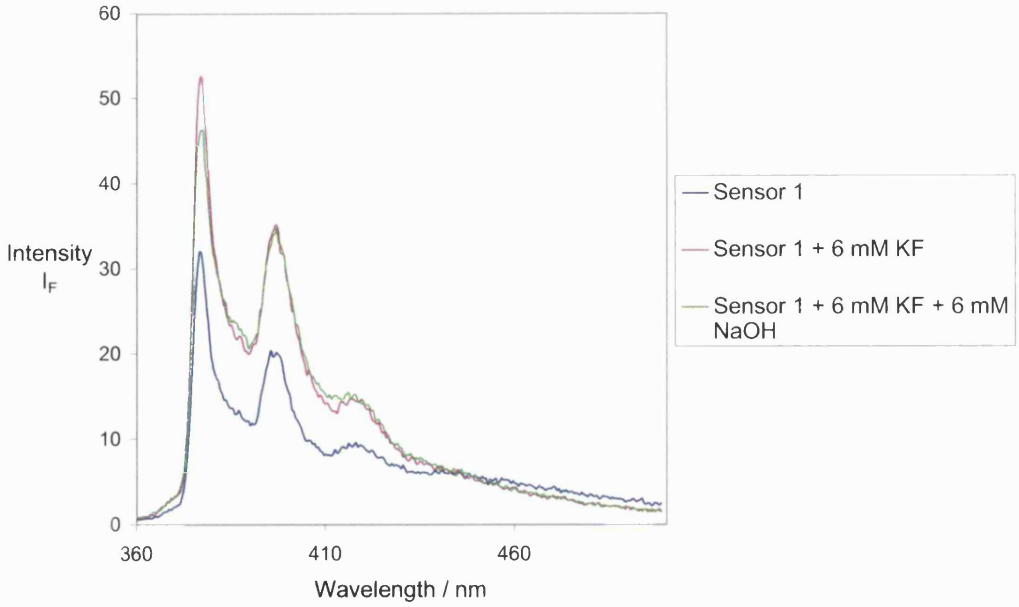

Figure 58. Fluorescence Intensity of sensor **1** with addition of potassium fluoride and sodium hydroxide.

The average values for the enhancement constants of each experiment are listed in Table 10.

Sensor	Added salt	EF
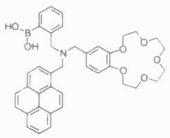 **1**	KF	1.78 ± 0.04
	KF + NaOH	1.69 ± 0.02

Table 10. Table of enhancement factors for sensor **1** with added potassium fluoride and sodium hydroxide.

From these values it is clear that addition of sodium hydroxide after the addition of potassium fluoride does not affect the fluorescence intensity. This means that the boronic acid is completely in the tetrahedral form after the addition of potassium fluoride; any free boronic acid would be converted to boronate on addition of sodium hydroxide, which would cause a change in the fluorescence. This is depicted in Scheme 15.

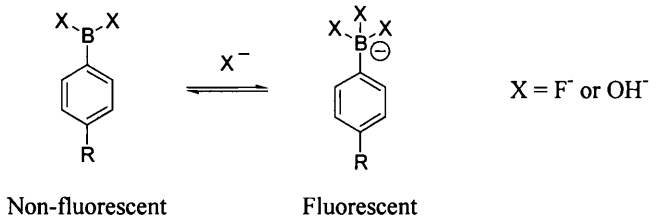

Scheme 15. Formation of the tetrahedral boronate anion with fluoride or hydroxide.

Also, the addition of sodium hydroxide, which is a strong base, would mop up any adventitious protons from the solvent. Since the addition of sodium hydroxide does not significantly affect the fluorescence, it is confirmed that the fluorescence is not caused by a change in pH, e.g. protonation by the solvent. This result further confirms that the observed change in the fluorescence is caused by binding of potassium fluoride.

2.5 *Summary of results and discussion*

- Two series of sensors and model compounds have been synthesized.
- Fluoride binding with the sensors in chloroform was investigated. It was found that fluoride binding to the boronic acid unit of the sensors caused fluorescence quenching. This fluorescence quenching is caused by the breaking of a very weak B-N bond in the sensor.
- Fluoride binding with benzocrown ether appended sensors is stronger, indicating that the B-N bond of sterically crowded molecules is weaker and therefore easier to break.
- The chemical shifts of ^{11}B NMR in $CDCl_3$ and CD_3OD were examined with and without the presence of fluoride. The boron peak shifted from around 30 ppm to 10 ppm indicating a change of hybridisation of the boron from sp^2 to sp^3 upon fluoride binding.
- The ditopic and AND logic gate functionality of the Pyrene series sensors with potassium and caesium salts was examined in methanol.
- Binding of potassium and caesium fluoride enhanced the fluorescence of sensors **1** and **2**, containing both binding units: benzocrown ether and boronic acid. Addition of chloride and bromide salts did not cause any change in the fluorescence intensity. The fluorescence of sensors lacking one of the binding units (model compounds **5-8**) did not change on addition of potassium and caesium salts.
- The 'Off-On' action of sensor **1** was examined. Addition of potassium fluoride 'switched on' the fluorescence of the sensor. The fluorescence was then 'switched off' by removing the potassium cation from the benzocrown ether

receptor of the sensor with 2.2.2-cryptand. The fluorescence was restored by the addition of the potassium cation as potassium chloride or the caesium cation as caesium chloride.

3 *Experimental*

Nu ska jag ut och öva mig på farligheter.

Astrid Lindgren, Ronja Rövardotter

3.1 General procedures

NMR spectroscopy: NMR spectra were recorded on a Bruker AC-300 or AM-300, a Varian Gemini 500, a Jeol 270-EX or a Jeol 400-EX spectrometer. All chemical shifts (δ) are described in parts per million relative to tetramethylsilane as the internal standard. The multiplicities of the spectroscopic data are presented in the following manner: s = singlet; d = doublet; t = triplet; m = multiplet; br = broad and the values of the coupling constants *J* are given in Hz. Due to quadrapolar relaxation, the aryl carbon atoms attached directly to the boronic acid boron atoms are not observed by ^{13}C NMR.

Infrared spectra: Infrared spectra were recorded on a Perkin-Elmer Paragon 1000 FT-IR spectrometer and a Perkin-Elmer 1600 Series FT-IR spectrometer. Samples were run either as a Nujol mull, as pressed KBr disks, solutions in chloroform or as neat samples. The frequencies (ν) as absorption maxima are given in wavenumbers (cm^{-1}) and s indicates a strong peak.

Mass spectrometry: Mass spectra and accurate mass were recorded at the EPSRC Mass Spectroscopy Centre, Swansea, at the University of Birmingham or at the University of Bath on a Kratos Profile or VG ProSpec for Electron Impact (E.I.), a VG ProSpec for Chemical Ionisation (C.I.), a VG ZabSpec for Fast Atom Bombardment (F.A.B.), a Micromass LCT for Electrospray Ionisation (E.I.) or a Micromass Autospec spectrometer with E.I., C.I., F.A.B. and Electrospray sources. Electrospray samples were prepared in a MeOH/H_2O 1:1 (v/v) solution and F.A.B. spectra were recorded

using *m*-nitrobenzyl alcohol or glycerol as a matrix. High Resolution Mass Spectra (HRMS) were obtained from all of the above instruments.

Elemental analyses were performed at the University of Birmingham and the University of Bath. Melting points were determined using a Gallenkamp melting point apparatus and are reported uncorrected.

Column Chromatography was performed using silica gel 60 (0.063-0.200 mm), supplied by Merck Ltd. and the column fractions were monitored by thin-layer chromatography (TLC). TLC was performed on pre-coated aluminium- or glass-backed silica gel (Silica Gel 60 F_{254}) plates supplied by Merck Ltd. Visualisation was achieved by UV light (254 nm).

Gel Chromatography was performed using Bio beads S-X8 supplied by BioRad and the column fractions monitored by TLC.

Fluorescence measurements were recorded on a Perkin Elmer LS 50 B Fluorimeter using quartz cuvettes with 10 mm path length.

Acetonitrile was dried by refluxing with calcium hydride. It was subsequently distilled and collected by dry syringe as required. Prior to use, tetrahydrofuran was distilled from sodium benzophenone ketyl under a nitrogen atmosphere. All other reagents and solvents were used as supplied by the Aldrich Chemical Co. Ltd., Lancaster Synthesis Ltd., Fisher Scientific Ltd., Acros Organics, Merck Ltd. and Frontier Scientific Europe Ltd.

3.2 Synthesis and characterisation

6,7,9,10,12,13,15,16-Octahydro-5,8,11,14,17-pentaoxa-benzocyclopentadecene-2-carbaldehyde (15)

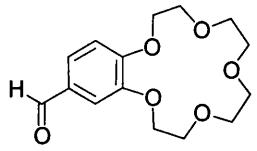

A mixture of hexamethylenetetramine (1.68 g, 12.0 mmol), trifluoroacetic acid (14.0 ml, 0.18 mol) and benzo-15-crown-5 (1.07 g, 4.0 mmol) was heated to 85-90°C under nitrogen overnight. Water (15 ml) was added and the mixture was extracted with chloroform (5 × 50ml). The combined organic extracts were dried with $MgSO_4$, filtered and concentrated under reduced pressure to give the crude product as a red oil.

Purification method 1: The product was extracted with hot hexane (60 ml) several times to give *aldehyde* **15** as a white solid (0.83 g, 70%).

Purification method 2: The product was purified by column chromatography on silica gel (20:1 chloroform/methanol) affording pure *aldehyde* **15** as a white solid (1.15 g, 97%); (Found: C, 60.7; H, 6.81. $C_{15}H_{20}O_6$ requires C, 60.80; H, 6.80%); mp 80-82°C (lit. 80-81.5 °C)[138]; ν_{max}(KBr disk)/cm^{-1} 1689s (C=O); δ_H(300 MHz; $CDCl_3$; Me_4Si) 3.75 (8H, s, 4×C*H*$_2$), 3.89-3.94 (4H, m, 2×C*H*$_2$), 4.16-4.20 (4H, m, 2×C*H*$_2$), 6.92 (1H, d, *J* 8.1 Hz, C*H*), 7.36 (1H, d, *J* 1.8 Hz, C*H*), 7.42 (1H, dd, *J* 1.8 Hz, 8.1 Hz, C*H*), 9.81

(1H, s, C*H*O); δ_C(75 MHz; $CDCl_3$) 68.67, 68.76, 69.16, 69.26, 70.27, 70.34, 71.20 (CH_2), 111.19, 111.92, 126.96 (Ar*C*H), 130.21, 149.40, 154.60 (Ar*C*), 190.92 (*C*HO); *m/z* (EI^+) 296 (43%, M^+) 164 (100%, $[M-C_6H_{12}O_3]^+$).

6,7,9,10,12,13,15,16,18,19-Decahydro-5,8,11,14,17,20-hexaoxa-benzocyclooctadecene-2-carbaldehyde (16)

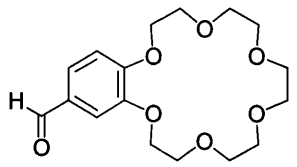

Benzo-18-crown-6 (2.92 g, 9.35 mmol) was added to a mixture of hexamethylenetetramine (4.60 g, 32.8 mmol) and trifluoroacetic acid (32 ml, 0.42 mol) and heated to reflux under nitrogen for 24 hours. Water (15 ml) was added and the water layer was extracted with chloroform (5 × 50ml). The combined organic extracts were dried with $MgSO_4$, filtered and concentrated under reduced pressure to give the crude product as a red oil.

Purification method 1: The product was extracted with hot hexane (60 ml) several times to give *aldehyde* **16** as a white solid (1.65 g, 52%).

Purification method 2: The product was purified by column chromatography on silica gel (19:2 chloroform/methanol) affording pure *aldehyde* **16** as a white solid (3.09 g, 97%); mp 66°C (lit. 61.3-62.8 °C)[138]; ν_{max}(KBr disk)/cm^{-1} 1684s (C=O); δ_H(300 MHz; $CDCl_3$; Me_4Si) 3.68-3.78 (12H, m, 6×CH_2), 3.91-3.96 (4H, m, 2×CH_2), 4.20-4.23 (4H,

m, 2×CH_2), 6.95 (1H, d, *J* 8.1, C*H*), 7.42-7.45 (2H, m, 2×C*H*), 9.83 (1H, s, C*H*O); δ_C(75 MHz; $CDCl_3$) 69.11, 69.18, 69.41, 69.53, 70.77, 70.81, 70.91, 70.99, 71.15, 71.17 (*C*H_2), 111.13, 112.08, 126.94 (Ar*C*H), 130.21, 149.24, 154.41 (Ar*C*), 190.86 (*C*HO); *m/z* (FAB$^+$) 341 (100%, $[M+H]^+$); (HRMS: Found 341.1599, $[M+H^+]$. $C_{17}H_{25}O_7$ requires 341.1600).

(3,4-Dimethoxy-benzyl)-naphthalen-1-ylmethyl-amine (26)

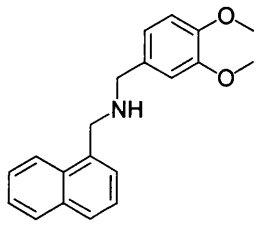

3,4-Dimethoxybenzaldehyde (1.37 g, 8.27 mmol) and 1-naphthalenemethylamine (1 g, 6.36 mmol) were dissolved in a mixture of methanol (15 ml) and THF (15 ml) and stirred at room temperature overnight. $NaBH_4$ (1.56 g, 41 mmol) was added and the reaction was stirred for a further 10 hours at room temperature. The solvent was removed under reduced pressure and the residue was dissolved in chloroform. The chloroform phase was washed with water (3 × 30 ml), dried with $MgSO_4$, filtered and concentrated *in vacuo* to yield *amine* **31** as an orange oil (1.62 g, 83%); $\nu_{max}(CHCl_3)/cm^{-1}$ 1513s (C–N); δ_H(400 MHz; $CDCl_3$; Me_4Si) 3.86 (2H, s, NCH_2-$C_6H_3(OMe)_2$), 3.88-3.89 (6H, m, 2×OCH_3), 4.23 (2H, s, Naph-CH_2N), 6.80-6.97 (3H, m, 3×$C_6H_3(OMe)_2$), 7.41-7.55 (4H, m, 4×NaphC*H*), 7.79 (1H, d, *J* 7.9, NaphC*H*), 7.86-7.89 (1H, m, NaphC*H*), 8.07-8.12 (1H, m, NaphC*H*); δ_C(75 MHz; $CDCl_3$) 51.09 (Naph-*C*H_2N), 53.92 (N*C*H_2-$C_6H_3(OMe)_2$), 56.57, 56.59 (O*C*H_3), 111.71, 112.22, 119.84, 124.51, 126.11, 126.39, 126.81, 127.04-, 128.61, 129.45 (Ar*C*H), 132.50, 134.59,

134.94, 136.12, 148.83, 149.65 (Ar*C*); *m/z* (ES^+) 308 (100%, $[M+H]^+$); (HRMS: Found 308.1649, $[M+H]^+$. $C_{20}H_{22}NO_2$ requires 308.1650).

(3,4-Dimethoxy-benzyl)-pyren-1-ylmethyl-amine (25)

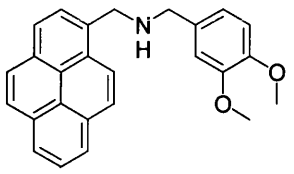

3,4-Dimethoxybenzaldehyde (900 mg, 5.42 mmol) and 1-pyrenemethyleneamine (964 mg, 4.17 mmol) were dissolved in a mixture of methanol (15 ml) and THF (15 ml) and stirred at room temperature overnight. $NaBH_4$ (1.0 g, 27.1 mmol) was added and the reaction was stirred for a further 10 hours at room temperature. The solvent was removed under reduced pressure and the residue was dissolved in chloroform. The chloroform phase was washed with water (3 × 30 ml), dried with $MgSO_4$, filtered and concentrated *in vacuo* to give the crude product. The product was purified by gel filtration (Bio beads S-X8 in THF) to yield *amine* **32** as a brown oil (1.22 g, 77%); $\nu_{max}(CHCl_3)/cm^{-1}$ 1514s (C–N); δ_H(300 MHz; $CDCl_3$; Me_4Si) 3.73 (2H, s, NCH_2-$C_6H_3(OMe)_2$), 3.77 (6H, s, 2×OCH_3), 4.33 (2H, s, Pyrene-CH_2N), 6.67-6.89 (3H, m, 3×$C_6H_3(OMe)_2$), 7.84-8.20 (9H, m, 9×PyreneC*H*); δ_C(75 MHz; $CDCl_3$) 51.19 (Pyrene-CH_2N), 53.75 (NCH_2-$C_6H_3(OMe)_2$), 56.35 (OCH_3), 56.78 (OCH_3), 111.33, 111.83, 120.78, 123.44, 123.83, 124.84, 125.25, 125.43, 125.65, 127.32, 127.75, 128.06, 128.72, 129.54, 131.11, 131.22, 131.69, 133.13, 133.98, 148.49, 149.41 (Ar); *m/z* (CI^+) 382 (30%, $[M+H]^+$), 215 (45%, $PyreneCH_2$), 151 (100%, M-$PyreneCH_2N$); (HRMS: Found 382.1809, $[M+H]^+$. $C_{26}H_{24}NO_2$ requires 382.1807).

Naphthalen-1-ylmethyl-(6, 7, 9, 10, 12, 13, 15, 16-octahydro-5, 8, 11, 14, 17-pentaoxa-benzocyclopentadecen-2-ylmethyl)-amine (9)

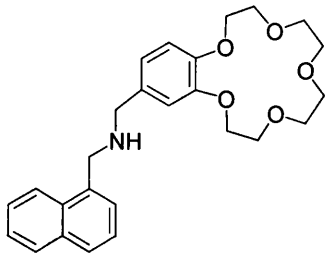

The procedure to form amine **31** was repeated with aldehyde **15** (1.37 g, 4.62 mmol) and 1-naphthalenemethylamine (558.7 mg, 3.55 mmol) to afford *amine* **9** (1.42 g, 91%) as a yellow oil; $\nu_{max}(CHCl_3)/cm^{-1}$ 1513s (C–N); δ_H(300 MHz; $CDCl_3$; Me_4Si) 3.64 (8H, s, 4×C*H*$_2$), 3.71 (2H, s, NC*H*$_2$-Benzocrown), 3.76-3.79 (4H, m, 2×C*H*$_2$), 3.99-4.02 (4H, m, 2×C*H*$_2$), 4.09 (2H, s, Naph-C*H*$_2$N), 6.69-6.82 (3H, m, 3×BenzocrownC*H*), 7.28-7.41 (4H, m, 4×NaphC*H*), 7.65 (1H, d, *J* 7.7, NaphC*H*), 7.72-7.76 (1H, m, NaphC*H*), 7.94-7.97 (1H, m, NaphC*H*); δ_C(75 MHz; $CDCl_3$) 51.08 (Naph-*C*H$_2$N), 53.77 (N*C*H$_2$-Benzocrown), 69.31, 69.55, 70.02, 70.05, 70.89, 70.92, 71.44 (*C*H$_2$), 114.34, 114.41, 121.34, 124.29, 125.79, 126.03, 126.41, 126.60, 126.68, 128.24 (Ar*C*H), 129.10, 132.24, 133.95, 134.28, 148.52, 149.58 (Ar*C*); *m/z* (ES^+) 438 (20%, $[M+H]^+$), 460 (95%, $[M+Na]^+$), 321 (100%, $[(M\text{-}NaphCH_2)+Na]^+$); (HRMS: Found 438.2296, $[M+H]^+$. $C_{26}H_{32}NO_5$ requires 438.2280).

(6,7,9,10,12,13,15,16-Octahydro-5,8,11,14,17-pentaoxa-benzocyclopentadecen-2-ylmethyl)-pyren-1-ylmethyl-amine (5)

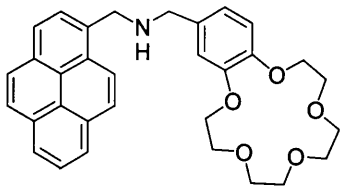

The procedure to form amine **32** was repeated with aldehyde **15** (1.07 g, 3.60 mmol) and 1-pyrenemethylamine (1 g, 4.32 mmol) to afford *amine* **5** as a yellow oil (1.07 g, 58%); $\nu_{max}(CHCl_3)/cm^{-1}$ 1513s (C–N); δ_H(300 MHz; $CDCl_3$; Me_4Si) 3.61 (8H, s, 4×C*H*$_2$), 3.71-3.76 (6H, m, C*H*$_2$-Benzocrown and 4×C*H*$_2$), 3.94-3.98 (4H, m, 2×C*H*$_2$), 4.27 (2H, s, Pyrene-C*H*$_2$N), 6.66-6.79 (3H, m, 3×BenzocrownC*H*), 7.81-8.02 (9H, m, 9×PyreneC*H*); δ_C(75 MHz; $CDCl_3$) 49.10 (Pyrene-*C*H$_2$N), 51.58 (N*C*H$_2$-Benzocrown), 67.19, 67.44, 67.83, 67.88, 68.72, 68.76, 69.29, 69.31 (*C*H$_2$), 112.27, 112.31, 119.18, 121.52, 122.87, 123.06, 123.20, 123.28, 124.09, 125.26, 125.32, 125.68, 125.74, 127.33, 128.84, 129.04, 129.50, 131.87, 132.10, 146.37, 147.45 (Ar); *m/z* (EI^+) 511 (10%, M^+), 230 (30%, [PyreneCH$_2$N]), 215 (100%, [PyreneCH$_2$]); (HRMS: Found 512.2433, $[M+H]^+$. $C_{32}H_{34}NO_5$ requires 512.2437).

(6,7,9,10,12,13,15,16,18,19-Decahydro-5,8,11,14,17,20-hexaoxa-benzocyclooctadecen-2-ylmethyl)-naphthalen-1-ylmethyl-amine (10)

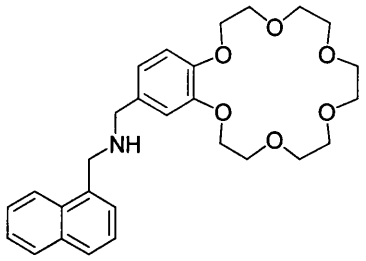

The procedure to form amine **31** was repeated with aldehyde **16** (2.08 g, 6.12 mmol) and 1-naphthalenemethylamine (740 mg, 4.71 mmol) to give *amine* **10** as a yellow oil (1.50 g, 66 %); $\nu_{max}(CHCl_3)/cm^{-1}$ 1514s (C–N); δ_H(300 MHz; $CDCl_3$; Me_4Si) 3.68-3.79 (12H, m, 6×CH_2), 3.83 (2H, s, NCH_2-Benzocrown), 3.90-3.93 (4H, m, 2×CH_2), 4.13-4.17 (4H, m, 2×CH_2), 4.21 (2H, s, Naph-CH_2N), 6.81-6.93 (3H, m, 3×BenzocrownC*H*), 7.41-7.52 (4H, m, 4×NaphC*H*), 7.76 (1H, d, *J* 7.7, NaphC*H*), 7.84-7.87 (1H, m, NaphC*H*), 8.05-8.08 (1H, m, NaphC*H*); δ_C(75 MHz; $CDCl_3$) 51.07 (Naph-*C*H_2N), 53.72 (N*C*H_2-Benzocrown), 69.42, 69.61, 69.86, 70.06, 70.09, 71.14, 71.22 (*C*H_2), 114.33, 114.51, 120.27, 125.76, 126.01, 126.45, 126.59, 126.68, 128.17, 129.08 (Ar*C*H), 132.22, 133.94, 134.26, 136.20, 148.33, 149.38 (Ar*C*); *m/z* (ES^+) 504 (100 %, $[M+Na]^+$), 482 (40 %, $[M+H]^+$); (HRMS: Found 482.2551 $[M+H]^+$. $C_{28}H_{36}NO_6$ requires 482.2543).

(6,7,9,10,12,13,15,16,18,19-Decahydro-5,8,11,14,17,20-hexaoxa-benzocyclooctadecen-2-ylmethyl)-pyren-1-ylmethyl-amine (6)

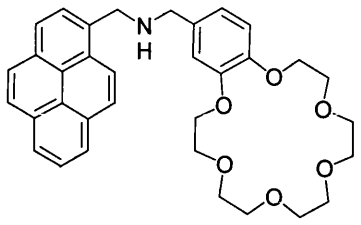

The procedure to form amine **32** was repeated with aldehyde **16** (482 mg, 1.42 mmol) and 1-pyrenemethylamine (393 mg, 1.70 mmol) to yield *amine* **6** as a yellow oil (693 mg, 88%); $\nu_{max}(CHCl_3)/cm^{-1}$ 1514s (C–N); δ_H(300 MHz; CD_3OD; Me_4Si) 3.58-3.67 (12H, m, 6×C*H*$_2$), 3.74-3.82 (6H, m, NC*H*$_2$-Benzocrown and 2×C*H*$_2$), 4.00-4.03 (4H, m, 2×C*H*$_2$), 4.34 (2H, s, Pyrene-C*H*$_2$N), 6.67-6.90 (3H, m, 3×BenzocrownC*H*), 7.85-8.16 (9H, m, 9×PyreneC*H*); δ_C(75 MHz; $CDCl_3$; Me_4Si) 44.63 (Pyrene-*C*H$_2$N), 53.05 (N*C*H$_2$-Benzocrown), 69.29, 69.34, 69.96, 71.04, 71.06, 71.10, 71.19 (*C*H$_2$), 103.41, 112.38, 113.59, 120.04, 123.08, 125.33, 125.40, 125.51, 126.11, 126.30, 127.42, 127.84, 128.13, 128.67, 130.93, 131.19, 131.57, 131.72, 136.86, 149.11, 149.29 (Ar); *m/z* (CI^+) 556 (10%, $[M+H]^+$), 217 (100%, [PyreneCH$_2$]), 44.2 (90%, [CH$_2$NHCH$_2$]); (HRMS: Found 556.2704, $[M+H]^+$. $C_{34}H_{38}NO_6$ requires 556.2699).

2-o-Tolyl-[1,3,2] dioxaborinane (31)

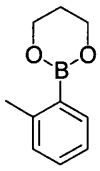

1,3-Propanediol (5.30 ml, 73.55 mmol) was added to a stirred solution of *o*-tolylboronic acid (5 g, 36.78 mmol) in benzene (30 ml). The mixture was heated and stirred under Dean and Stark conditions for 1 hour. After cooling, the reaction mixture was washed with water (3 × 20 ml), dried with $MgSO_4$, and filtered. The solvent was removed under reduced pressure to give *dioxaborinane* **33** as a yellow oil (5.8 g, 90%). $\nu_{max}(CHCl_3)/cm^{-1}$ 1393s (B–O), 1006s (B–C); δ_H(300 MHz; CD_3Cl_3; Me_4Si) 2.09-2.16 (2H, m, $OCH_2CH_2CH_2O$), 2.76 (3H, s, CH_3), 4.28 (4H, t, *J* 5.4, $OCH_2CH_2CH_2O$), 7.36 (1H, t, *J* 7.5 ArCH), 7.45-7.55 (2H, m, ArCH), 7.98 (1H, d, *J* 7.5, ArCH); δ_C(75 MHz; $CDCl_3$) 23.01 (CH_3), 27.93 ($OCH_2CH_2CH_2O$), 62.40 ($OCH_2CH_2CH_2O$), 125.20, 130.56, 135.44 (ArCH), 144.53 (ArC); *m/z* (FAB^+) 176 (100%, M^+); (HRMS: Found 176.1009, M^+. $C_{10}H_{13}{}^{11}BO_2$ requires 176.1009).

2-(2-Bromomethyl-phenyl)-[1,3,2]dioxaborinane (17)

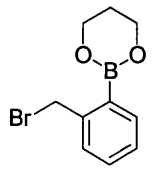

To a stirred solution of 2-o-tolyl-[1,3,2] dioxaborinane **33** (5.60 g, 31.81 mmol) in benzene (80 ml) was added *N*-bromosuccinimide (5.66 g, 31.81 mmol) and AIBN (0.30 g). The mixture was heated and stirred under reflux for 2 hours. After cooling on an ice-water-bath, the precipitate was removed by filtration. The filtrate solvent was removed under reduced pressure and the crude product was purified by flash column chromatography on silica gel (EtOAc:n-hexane, gradient elution) to yield *bromodioxaborinane* **18** as a brown oil (7.74 g, 95%). $\nu_{max}(CHCl_3)/cm^{-1}$ 1393s (B–O), 1006s (B–C); δ_H(300 MHz; $CDCl_3$; Me_4Si) 1.99-2.08 (2H, m, $OCH_2CH_2CH_2O$), 4.19 (4H, t, *J* 5.4, $OCH_2CH_2CH_2O$), 5.02 (2H, s, $ArCH_2Br$), 7.33-7.47 (3H, m, ArCH), 7.92 (1H, d, *J* 7.2, ArCH); δ_C(75 MHz; $CDCl_3$) 27.88 ($OCH_2CH_2CH_2O$), 35.25 ($ArCH_2Br$), 62.62 ($OCH_2CH_2CH_2O$), 128.07, 130.75, 130.95, 135.97 (ArCH), 143.97 (ArC); *m/z* (FAB^+) 255 (10 %, $[M+H]^+$), 175 (100 %, $[M-Br]^+$); (HRMS: Found 256.0093, M^+. $C_{10}H_{12}{}^{11}B^{81}BrO_2$ requires 256.0093).

Methyl-naphthalen-1-ylmethyl-amine (30)

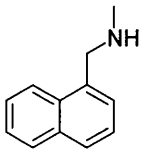

To a solution of 1-naphthalen-carboxaldehyde (3 ml, 22.1 mmol) in methanol (15 ml) was added methylamine (30 ml of a 2.0 M solution in methanol, 60.0 mmol). The reaction was stirred at room temperature overnight. $NaBH_4$ (4.18 g, 110.4 mmol) was added and the reaction was stirred for a further 5 hours at room temperature. The methanol was removed under reduced pressure and dichloromethane was added (30 ml). The organic layer was washed with water (3 × 30 ml), dried with $MgSO_4$ and filtered. The solvent was removed under reduced pressure to give the *amine* **30** as an orange oil (2.95 g, 78%). $\nu_{max}(CHCl_3)/cm^{-1}$ 1509s (C–N); δ_H(300 MHz; $CDCl_3$; Me_4Si) 1.39 (1H, br s, N*H*), 2.55 (3H, s, CH_3), 4.17 (2H, s, NCH_2), 7.47-7.61 (4H, m, 4×NaphC*H*), 7.62-7.84 (1H, m, NaphC*H*), 7.92 (1H, d, *J* 9.3, NaphC*H*), 8.18 (1H, d, *J* 8.4, NaphC*H*); δ_C(75 MHz; $CDCl_3$) 37.03 (*C*H_3), 54.18 (*C*H_2), 124.22, 126.45, 126.57, 126.70, 126.95, 128.21, 129.20 (Naph*C*H), 132.36, 134.39, 136.33 (Naph*C*); *m/z* (FAB^+) 172 (100 %, $[M+H]^+$); (HRMS: Found 172.1126, $[M+H]^+$. $C_{12}H_{14}N$ requires 172.1226).

2-[(Methyl-naphthalen-1-ylmethyl-amino)-methyl]-boronic acid (12)

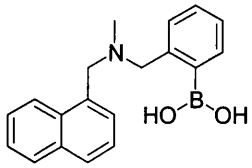

Methyl-naphthalen-1-ylmethyl-amine **30** (1.18 g, 6.89 mmol), 2-(2-bromomethyl-phenyl)-[1,3,2] dioxaborinane **18** (2.28 mg, 8.96 mmol) and Na_2CO_3 (1.46 g, 13.78 mmol) were mixed in dry acetonitrile (15 ml) and dry THF (15 ml). The mixture was heated under reflux for 5 hours under nitrogen atmosphere. After cooling, the solvent was removed under reduced pressure and the residue was dissolved in chloroform. The chloroform phase was washed with water (30 ml), 0.5 M HCl (30 ml) and water (30 ml). The organic phase was dried over $MgSO_4$ and filtered after which the product was concentrated *in vacuo* to give the *boronic acid* **12** as an orange solid (2.00 g, 95%); mp 110 °C; $\nu_{max}(CHCl_3)/cm^{-1}$ 1383s (B–O), 1003s (B–C); δ_H(300 MHz; CD_3OD; Me_4Si) 1.99 (3H, s, C*H*$_3$), 3.56 (2H, s, NC*H*$_2$-$C_6H_4(OH)_2$), 3.86 (2H, s, Naph-C*H*$_2$N), 7.00 (1H, d, *J* 7.2, $C_6H_4(OH)_2$), 7.17-7.31 (6H, m, 3×$C_6H_4(OH)_2$ and 3×NaphC*H*), 7.56-7.82 (4H, m, 4×NaphC*H*); δ_C(75 MHz; CD_3OD, Me_3Si) 42.09 (*C*H$_3$), 57.26 (NC*H*$_2$-$C_6H_4(OH)_2$), 65.10 (Naph-C*H*$_2$N), 125.42, 126.73, 126.97, 127.49, 127.87, 128.38, 129.09, 129.54, 129.81, 129.98, 130.35 (Ar*C*H), 130.66, 130.97, 134.11, 135.63 (Ar*C*); *m/z* (ES^+) 306 (100%, M^+); (HRMS: Found 306.1663, $[M+H]^+$. $C_{19}H_{21}{}^{11}BNO_2$ requires 306.1665).

Methyl-pyren-1-ylmethyl-amine (28)

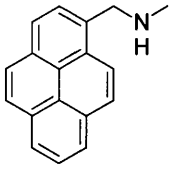

Methylamine (10 ml of a 2.0 M solution in methanol, 20.0 mmol) was added to a solution of pyrene-1-carboxaldehyde (1.00 g, 4.38 mmol) in methanol. The reaction was stirred at room temperature overnight. $NaBH_4$ (828 mg, 21.9 mmol) was added and the reaction was stirred for a further 5 hours at room temperature. The methanol was removed under reduced pressure and dichloromethane was added (30 ml). The organic layer was washed with water (3 × 30 ml), dried with $MgSO_4$ and filtered. The solvent was removed under reduced pressure to give the *amine* **28** as a yellow oil (523 mg, 57%). $\nu_{max}(CHCl_3)/cm^{-1}$ 1509s (C–N); δ_H(300 MHz; $CDCl_3$; Me_4Si) 1.70 (1H, br s, N*H*), 2.38 (3H, s, CH_3), 4.19 (2H, s, NCH_2), 7.70-8.12 (9H, m, 9×PyreneC*H*); δ_C(75 MHz; $CDCl_3$) 36.98 (*C*H_3), 54.25 (*C*H_2), 123.50, 125.05, 125.29, 125.43, 125.50, 126.28, 127.40, 127.48, 127.87, 128.04, 129.46, 131.07, 131.24, 131.71, 134.00 (Ar); *m/z* (FAB^+) 245 (50%, M^+), 215 (100%, $[M\text{-}NHCH_3]^+$; (HRMS: Found 245.1205, M^+. $C_{18}H_{15}N$ requires 245.1205);

2[(Methyl-pyren-1-ylmethyl-amino)-methyl] phenyl boronic acid (8)

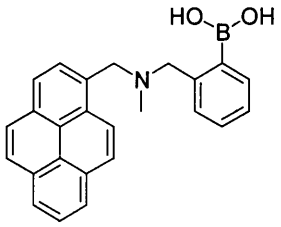

Methyl-pyren-1-ylmethyl-amine **28** (597 mg, 2.44 mmol), 2-(2-bromomethyl-phenyl)-[1,3,2] dioxaborinane **18** (680 mg, 3.17 mmol) and Na_2CO_3 (517 mg, 4.88 mmol) were mixed in dry acetonitrile (15 ml) and dry THF (15 ml). The mixture was heated under reflux for 5 hours under nitrogen atmosphere. After cooling the solvent was removed under reduced pressure and the residue was dissolved in chloroform. The chloroform phase was washed with water (30 ml), 0.5 M HCl (30 ml) and water (30 ml). The organic phase was dried over $MgSO_4$, filtered and concentrated *in vacuo* to give the crude product as a brown oil. Recrystallisation from chloroform/hexane afforded the *boronic acid* **8** as a pale yellow solid (523 mg, 57%); mp 164 °C (dec.); $\nu_{max}(CHCl_3)/cm^{-1}$ 1383s (B–O), 1003s (B–C); δ_H(300 MHz; CD_3OD; Me_4Si) 2.30 (3H, s, C*H*$_3$), 4.08 (2H, s, NC*H*$_2$-$C_6H_4(OH)_2$), 4.55 (2H, s, Pyrene-C*H*$_2$N), 7.17 (1H, d, *J* 7.2, $C_6H_4(OH)_2$), 7.23-7.36 (2H, m, 2×$C_6H_4(OH)_2$), 7.68 (1H, d, *J* 6.3, $C_6H_4(OH)_2$), 7.94-8.16 (9H, m, 9×PyreneC*H*); δ_C(75 MHz; CD_3OD, Me_3Si) 42.21 (*C*H$_3$), 55.69 (NCH$_2$-$C_6H_4(OH)_2$), 60.79 (Pyrene-*C*H$_2$N), 114.98, 123.98, 124.90, 125.21, 125.81, 126.42, 126.69, 127.12, 127.47, 127.93, 129.05, 130.23, 130.92, 131.34, 131.49, 131.64, 132.06, 132.38, 142.04, 142.43 (Ar); *m/z* (ES^+) 380 (100%, M^+); (HRMS: Found 380.1827, $[M+H]^+$. $C_{25}H_{23}{}^{11}BNO_2$ requires 380.1822).

2-{[(3,4-Dimethoxy-benzyl)-naphthalen-1-ylmethyl-amino]-methyl}-phenyl boronic acid (11)

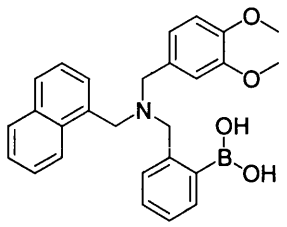

(3,4-Dimethoxy-benzyl)-naphthalen-1-ylmethyl-amine **31** (200 mg, 0.65 mmol), 2-(2-bromomethyl-phenyl)-[1,3,2] dioxaborinane **18** (249 mg, 0.98 mmol) and K_2CO_3 (269 mg, 1.95 mmol) were mixed in dry acetonitrile (20 ml). The mixture was heated under reflux for 5 hours. After cooling the solvent was removed under reduced pressure and the residue was dissolved in chloroform. The chloroform phase was washed with water (3 × 30 ml), dried with $MgSO_4$. After filtration, the filtrate was concentrated *in vacuo* to give the crude product as a yellow oil. Recrystallisation from methanol-water afforded the *boronic acid* **11** as a white solid (121 mg, 42%); mp 86-90 °C; $\nu_{max}(CHCl_3)/cm^{-1}$ 1371s (B–O), 1003s (B–C);1028s δ_H(300 MHz; $CDCl_3$; Me_4Si) 3.54 (2H, s, NCH_2-$C_6H_4(OH)_2$), 3.71 (2H, s, NCH_2-$C_6H_3(OMe)_2$), 3.79 (6H, s, 2×OCH_3), 3.96 (2H, s, Naph-CH_2N), 6.70-6.77 (3H, m, 3×$C_6H_3(OMe)_2$), 7.13-7.45 (8H, m, 7×NaphC*H* and 1×$C_6H_4(OH)_2$), 7.65-7.77 (2H, m, 2×$C_6H_4(OH)_2$), 7.84-7.90 (1H, m, $C_6H_4(OH)_2$); δ_C(75 MHz; $CDCl_3$) 55.80 (Naph-CH_2N), 56.71 (OCH_3), 56.77 (OCH_3), 59.09 (NCH_2-$C_6H_4B(OH)_2$), 62.97 (NCH_2-$C_6H_3(OMe)_2$), 111.68, 113.68, 123.33, 124.60, 126.11, 126.63, 127.15, 128.42, 129.59, 129.85, 131.30, 132.41, 133.24, 134.66, 137.59, 149.43, 149.84 (Ar); *m/z* (ES^+) 442 (100%, $[M+H]^+$); (HRMS: Found 442.2185, $[M+H]^+$. $C_{27}H_{29}{}^{11}BNO_4$ requires 442.2189).

2-{[(3,4-Dimethoxy-benzyl)-pyren-1-ylmethyl-amino]-methyl}-phenyl boronic acid (7)

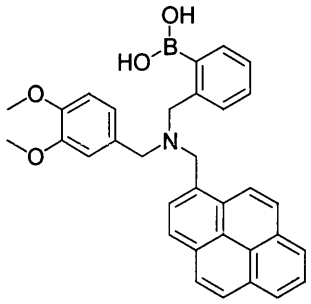

(3,4-Dimethoxy-benzyl)-pyren-1-ylmethyl-amine **32** (1.08 g, 2.82 mmol), 2-(2-bromomethyl-phenyl)-[1,3,2] dioxaborinane **18** (787 mg, 3.66 mmol) and Na_2CO_3 (597 mg, 5.64 mmol) were mixed in dry acetonitrile (15 ml) and dry THF (15 ml). The mixture was heated under reflux for 5 hours under nitrogen atmosphere. After cooling the solvent was removed under reduced pressure and the residue was dissolved in chloroform. The chloroform phase was washed with water (30 ml), 0.5 M HCl (30 ml) and water (30 ml). The organic phase was dried over $MgSO_4$ and filtered after which the product was concentrated in vacuo to give the crude product as a brown oil. Recrystallisation from chloroform/hexane afforded the boronic acid **7** as a pale yellow solid (767 mg, 53%); mp 142 °C (dec.); $\nu_{max}(CHCl_3)/cm^{-1}$ 1373s (B–O), 1028s (B–C); δ_H(300 MHz; $CDCl_3$; Me_4Si) 3.47 (2H, s, NCH_2-$C_6H_4(OH)_2$), 3.65 (2H, s, NCH_2-$C_6H_3(OMe)_2$), 3.69-3.75 (6H, m, 2×OCH_3), 4.11 (2H, s, Pyrene-CH_2N), 6.64-6.76 (3H, m, 3×$C_6H_3(OMe)_2$), 7.14-7.34 (4H, m, 4×$C_6H_4(OH)_2$), 7.68-8.07 (9H, m, 9×PyreneCH); δ_C(75 MHz; $CDCl_3$) 53.64 (NCH_2-$C_6H_4(OH)_2$), 54.08 (OCH_3), 54.14 (OCH_3), 56.60 (NCH_2-$C_6H_4B(OH)_2$), 60.46 (Pyrene-CH_2N), 109.02, 110.97, 120.64, 121.43, 122.89, 122.99, 123.45, 123.53, 124.19, 125.68, 125.78, 125.83, 126.06, 126.09, 127.14, 127.37, 128.36, 128.67, 128.98, 129.35, 129.54, 129.74, 135.06, 140.00, 146.78, 147.26

(Ar); m/z (ES^+) 516 (100%, M^+), 151 (90%, $[CH_2C_6H_3(OCH_3)_2]$); (HRMS: Found 516.2340, $[M+H]^+$. $C_{33}H_{31}{}^{11}BNO_4$ requires 516.2346).

2-{[(Naphthalen-1-ylmethyl-(6,7,9,10,12,13,15,16-octahydro-5,8,11,14,17-pentaoxa-benzocyclopentadecen-2-ylmethyl)-amino]-methyl}-phenyl boronic acid (3)

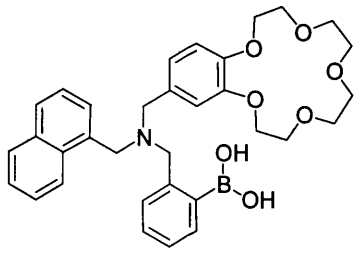

The above procedure was repeated with amine **9** (1.60 g, 3.65 mmol) in place of (3,4-dimethoxy-benzyl)-pyren-1-ylmethyl-amine **32** (all other reagents were used in the same molar ratios), to afford *boronic acid* **3** (1.25 g, 60%) as a white solid: mp 92 °C; $\nu_{max}(CHCl_3)/cm^{-1}$ 1372s (B–O); δ_H(300 MHz; $CDCl_3$; Me_4Si) 3.58 (2H, s, NCH_2-$C_6H_4(OH)_2$), 3.69-3.81 (8H, m, 4×CH_2), 3.89-3.92 (4H, m, 2×CH_2), 4.01-4.06 (6H, m, 3×CH_2), 4.12-4.15 (2H, m, CH_2), 6.76-6.80 (3H, m, 3×BenzocrownC*H*), 7.29-7.53 (8H, m, 1×$C_6H_4(OH)_2$ and 7×NaphC*H*), 7.77-7.85 (2H, m, 2×$C_6H_4(OH)_2$), 7.94-7.97 (1H, m, $C_6H_4(OH)_2$); δ_C(75 MHz; $CDCl_3$; Me_4Si) 55.20 (NCH_2-$C_6H_4B(OH)_2$), 58.52 (Naph-CH_2N), 62.47 (NCH_2-Benzocrown), 69.02, 69.44, 69.81, 69.99, 70.86, 70.92, 71.35, 71.48 (CH_2), 114.02, 115.61, 123.27, 124.14, 125.62, 126.07, 126.64, 127.80, 128.93, 129.06, 129.25, 129.60, 130.70, 131.81 (ArCH), 132.41, 132.76, 134.15, 137.08, 142.06, 148.92, 149.54 (ArC); *m/z* (ES^+) 572 (100%, $[M+H]^+$); (HRMS: Found 572.2820, $[M+H]^+$. $C_{33}H_{39}{}^{11}BNO_7$ requires 572.2819).

2-{[(6,7,9,10,12,13,15,16-Octahydro-5,8,11,14,17-pentaoxa-benzocyclopentadecen-2-ylmethyl)-pyren-1-ylmethyl-amino]-methyl}-phenyl boronic acid (1)

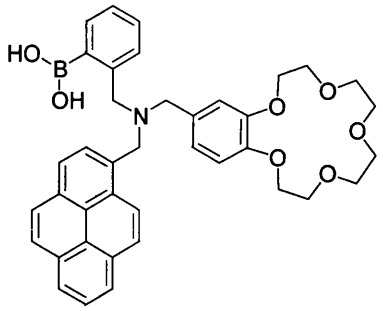

The previous procedure was repeated with amine **5** (300 mg, 0.59 mmol) in place of amine **9** (all other reagents were used in the same mole ratios), to afford *boronic acid* **1** (303 g, 80%) as a light yellow solid: mp 122 °C (dec.); $\nu_{max}(CHCl_3)/cm^{-1}$ 1371s (B–O), 1140s (B–C); δ_H(400 MHz; $CDCl_3$; Me_4Si) 3.53-3.76 (12H, m, 6×C*H*$_2$), 3.88 (4H, s, 2×C*H*$_2$), 4.00 (2H, s, NC*H*$_2$-$C_6H_4(OH)_2$), 4.07 (2H, s, NC*H*$_2$-Benzocrown), 4.25 (2H, s, Pyrene-C*H*$_2$N), 6.74-6.78 (3H, m, 3×BenzocrownC*H*), 7.31-7.41 (4H, m, 4×$C_6H_4(OH)_2$) 7.92-8.18 (9H, m, 9×PyreneC*H*); δ_C(100 MHz; $CDCl_3$; Me_4Si) 55.19 (N*C*H$_2$-$C_6H_4B(OH)_2$), 58.13 (Pyrene-*C*H$_2$N), 61.98 (N*C*H$_2$-Benzocrown), 68.48, 68.94, 69.24, 69.49, 70.34, 70.43, 70.84, 70.99 (*C*H$_2$), 113.45, 114.90, 122.63, 122.91, 124.42, 124.46, 124.64, 124.96, 125.03, 125.70, 127.18, 127.28, 127.67, 128.88, 129.81, 130.15, 130.47, 130.82, 131.00, 131.27, 133.81, 136.51, 141.30, 148.25, 148.87 (Ar); *m/z* (ES^+) 646 (100 %, $[M+H]^+$); (HRMS: Found 646.2973, $[M+H]^+$. $C_{39}H_{41}{}^{11}BNO_7$ requires 646.2976).

2-{[(6,7,9,10,12,13,15,16,18,19-Decahydro-5,8,11,14,17,20-hexaoxa-benzocyclooctadecen-2-ylmethyl)-naphthalen-1-ylmethyl-amino]-methyl}-phenyl boronic acid (4)

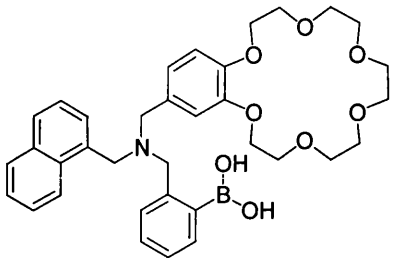

The above procedure was repeated with amine **10** (1.03 g, 2.13 mmol) in place of amine **5** (all other reagents were used in the same mole ratios), to afford *boronic acid* **4** (686 mg, 53%) as a cream coloured solid: mp 95 °C; $\nu_{max}(CHCl_3)/cm^{-1}$ 1370s (B–O), 1132s (B–C); δ_H(300 MHz; $CDCl_3$; Me_4Si) 3.58 (2H, s, NCH_2-$C_6H_4(OH)_2$), 3.70-3.81 (12H, m, 6×CH_2), 3.90-3.93 (4H, m, 2×CH_2), 4.01-4.07 (6H, m, 2×CH_2 and NCH_2-Benzocrown), 4.13-4.16 (2H, m, Naph-CH_2N), 6.78-6.80 (3H, m, 3×BenzocrownC*H*), 7.29-7.54 (8H, m, 7×NaphC*H* and 1×$C_6H_4(OH)_2$), 7.78-7.85 (2H, m, 2×$C_6H(OH)_{24}$), 7.97-7.99 (1H, m, $C_6H_4(OH)_2$); δ_C(75 MHz; $CDCl_3$; Me_4Si) 55.25 (NCH_2-$C_6H_4B(OH)_2$), 58.50 (Naph-CH_2N), 62.48 (NCH_2-Benzocrown), 69.10, 69.38, 69.88, 69.98, 71.01, 71.07, 71.12, 71.21 (CH_2), 113.85, 115.58, 123.24, 124.18, 125.60, 126.07, 126.42, 126.60, 127.80, 128.92, 129.05, 129.24, 129.60, 130.67 (Ar*C*H), 132.46, 132.77, 134.16, 137.05, 142.07, 148.67, 149.22 (Ar*C*); *m/z* (ES^+) 616 (100%, $[M+H]^+$), 482 (10%, $[M\text{-}CH_2C_6H_4B(OH)_2]^+$); (HRMS: Found 616.3083, $[M+H]^+$. $C_{35}H_{43}{}^{11}BNO_8$ requires 616.3081).

2-{[(6,7,9,10,12,13,15,16,18,19-Decahydro-5,8,11,14,17,20-hexaoxa-benzocyclooctadecen-2-ylmethyl)-pyren-1-ylmethyl-amino]-methyl}-phenyl boronic acid (2)

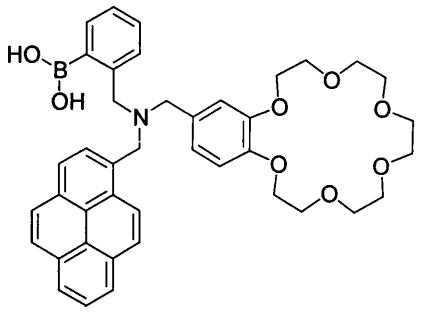

The above procedure was repeated with amine **6** (1.32 g, 2.37 mmol) in place of amine **10** (all other reagents were used in the same mole ratios), to afford *boronic acid* **2** (1.00 g, 61%) as a cream coloured solid: mp 133 °C (dec.); $\nu_{max}(CHCl_3)/cm^{-1}$ 1370s (B–O), 1130s (B–C); δ_H(300 MHz; $CDCl_3$; Me_4Si) 3.54 (2H, s, NCH_2-$C_6H_4(OH)_2$), 3.68-3.75 (16H, m, 8×CH_2), 3.86-3.89 (4H, m, 2×CH_2), 3.99-4.07 (2H, m, NCH_2-Benzocrown), 4.23 (2H, s, Pyrene-CH_2N), 6.69-6.71 (3H, m, 3×BenzocrownC*H*), 7.30-7.42 (4H, m, 4×$C_6H_4(OH)_2$), 7.91-8.17 (9H, m, 9×PyreneC*H*); δ_C(75 MHz; $CHCl_3$; Me_4Si) 55.65 (NCH_2-$C_6H_4B(OH)_2$), 58.50 (Pyrene-CH_2N), 62.45 (NCH_2-Benzocrown), 68.97, 69.25, 69.81, 69.95, 70.97, 70.05, 71.19 (CH_2), 113.67, 123.60, 124.97, 125.06, 125.26, 125.54, 125.62, 126.30, 127.78, 127.86, 128.14, 129.44, 130.42, 130.74, 131.07, 131.41, 131.62, 131.88, 137.00 (Ar); *m/z* (ES^+) 690 (100%, $[M+H]^+$), 556 (40%, $[M-CH_2C_6H_4B(OH)_2]^+$); (HRMS: Found 690.3235, $[M+H]^+$. $C_{41}H_{45}{}^{11}BNO_8$ requires 690.3238).

*Note: All boronic acid compounds (**1-4** and **7**, **8**, **11** and **12**) were submitted for elemental analysis. However, the compounds gave much lower CHN compositions than expected. Boronic acids have long been known to give poor correlations between calculated and found compositions.*[146]

3.3 Evaluation of sensor molecules

Fluoride sensors - Interaction with tetrabutylammonium salts

The sensor molecules were evaluated by the use of fluorescence spectroscopy. The fluorescence spectra of compounds **1-12** (5×10^{-7} M) in chloroform were recorded as increasing amounts of tetrabutylammonium salt (nBu_4NF, nBu_4NCl, nBu_4NBr), was added to the solution.

AND logic gates - Interaction with metal salts

The sensor molecules were evaluated by the use of fluorescence spectroscopy. The fluorescence spectra of compounds **1-12** (5×10^{-7} M) in HPLC methanol were recorded as increasing amounts of potassium salt (KF, KCl, KBr) or caesium salt (CsF, CsCl, CsBr), was added to the solution.

Enhancement Factors

The fluorescence enhancement of compounds **1-12** (5×10^{-7} M) in HPLC methanol was recorded as 6 mM of potassium salt (KF, KCl, KBr) or caesium salt (CsF, CsCl, CsBr) was added to the solution.

'Off-On' action

The fluorescence enhancement of compounds **1** and **2** (5×10^{-7} M) in HPLC methanol was recorded as 6 mM of potassium fluoride, 6 mM of 2.2.2-cryptand and then finally potassium chloride were added sequentially to the solution.

The same experiment was repeated by adding 6 mM of potassium fluoride, 6 mM of 2.2.2-cryptand and then caesium chloride instead of potassium fluoride to the solution.

Hydroxide check

The fluorescence enhancement of compound **1** (5×10^{-7} M) in HPLC methanol was recorded as 6 mM of potassium fluoride and 6 mM of sodium hydroxide were added to the solution.

4 Conclusions

Har du nån ångmaskin som vi kan explodera eller nånting annat som smäller bra?
Smälla ska det göra och roligt vill jag ha, annars är jag inte med.

Astrid Lindgren, Karlsson på taket smyger igen

The results show that it is possible to synthesise boronic acid appended sensors using relatively simple, clean and mild reaction conditions.

All molecules in the two series, naphthalene and pyrene, displayed a weak B-N interaction in chloroform. On addition of tetrabutylammonium chloride or bromide no change in fluorescence intensity was observed. When the sensors were titrated against tetrabutylammonium fluoride in chloroform, the fluorescence of the compounds decreased. The strongest fluorescence quenching with tetrabutylammonium fluoride was observed for the two sensors with no crown ether unit, sensors **7** and **8**. The fluorescence of the model compounds **5** and **6** on the other hand was unchanged when tetrabutylammonium fluoride was added. The stability constants are highest for the sensors **1** and **2**. Both compounds contain a large benzocrown ether group which makes the molecule crowded and makes the B-N interaction weaker. Since the B-N interaction is weak, it is easier to disrupt and hence the binding constant of the fluoride anion is larger.

The AND logic character of the sensors was evaluated by fluorescence titration in methanol with potassium fluoride and caesium fluoride. The fluorescence of sensors **1** and **2**, which both have two receptor units, a benzocrown ether unit for cation binding (benzo-15-crown-5 and benzo-18-crown-6, respectively) and a boronic acid unit for fluoride binding, was considerably increased by addition of potassium and caesium fluoride. Addition of the corresponding chloride and bromide salts did not cause any change in the fluorescence spectra. Fluorescence titrations with model compounds, lacking either the cation binding crown ether unit (compounds **7** and **8**) or the fluoride binding boronic acid unit (compounds **5** and **6**), with the potassium and caesium salts

did not cause any change in the fluorescence spectra. Therefore a conclusion can be drawn that sensors **1** and **2** behave as AND logic gates (i.e. two chemical inputs are needed to activate fluorescence recovery).

The sensors can be switched on for potassium or caesium and fluoride and off by removing the cation using a 2.2.2-cryptand, since the sensor cannot give an output signal with only one occupied receptor. Addition of more cation switches the sensor on again.

With appropriate modifications of the fluorophore and Lewis acid-binding site, fluoride selectivity could be fine tuned to any desired fluoride concentration range. It is therefore conceivable that this work could lead to the development of fluorescent fluoride sensors with AND logic characteristics for a variety of industrial and medicinal applications.

5 References

1. Bryan, A. J.; de Silva, A. P.; de Silva, S. A.; Rupasinghe, R. A. D. D.; Sandanayake, K. R. A. S. *Biosensors* 1989, **4**, 169.

2. Nassau, K. *The Physics and Chemistry of Colour*, 1st ed. John Wiley & Sons, 1983.

3. Czarnik, A. W. *Acc. Chem. Res.* 1994, **27**, 302.

4. Kavarnos, G. J. *Fundamentals of Photoinduced Electron Transfer* VCH Publishers, Inc.: New York, 1993.

5. de Silva, A. P.; Gunaratne, H. Q. N.; Gunnlaugsson, T.; McCoy, C. P.; Maxwell, P. R. S.; Rademacher, J. T.; Rice, T. E. *Pure Appl. Chem.* 1996, **68**, 1443.

6. James, T. D.; Sandanayake, K. R. A. S.; Shinkai, S. *Angew. Chem. Int. Ed. Engl.* 1996, **35**, 1911.

7. Czarnik, A. W. Fluorescent Chemosensors of Ion and Molecule Recognition. In *Abstracts of Papers of the American Chemical Society*; American Chemical Society: Washington, 1993; Vol. 206; pp. 203.

8. de Silva, A. P.; Rupasinghe, R. A. D. D. *Chem. Commun.* 1985, 1669.

9. Bissell, R. A.; de Silva, A. P.; Gunaratne, H. Q. N.; Lynch, P. L. M.; Maguire, G. E. M.; Sandanayake, K. R. A. S. *Chem. Soc. Rev.* 1992, **21**, 187.

10. de Silva, A. P.; Fox, D. B.; Moody, T. S.; Weir, S. M. *Trends Biotechnol.* 2001, **19**, 29.

11. de Silva, A. P.; Gunaratne, H. Q. N.; Lynch, P. L. M. *J. Chem. Soc., Perkin Trans. 2* 1995, **4**, 685.

12. de Silva, A. P.; Gunaratne, H. Q. N.; Gunnlaugsson, T.; Huxley, A. J. M.; McCoy, C. P.; Rademacher, J. T.; Rice, T. E. *Chem. Rev.* 1997, **97**, 1515.

13. Michaelis, A.; Becker, P. *Ber. Dtsch. Chem. Ges.* 1882, **15**, 180.

14. Kuivila, H. G.; Keough, A. H.; Soboczenski, E. J. *J. Org. Chem.* 1954, **19**, 780.

15. Lorand, J. P.; Edwards, J. D. *J. Org. Chem.* 1959, **24**, 769.

16. Wulff, G. *Pure Appl. Chem.* 1982, **54**, 2093.

17. Cooper, C. R.; James, T. D. *Chem. Commun.* 1997, 1419.

18. Cooper, C. R.; James, T. D. *J. Chem. Soc., Perkin Trans. 1* 2000, 963.

19. James, T. D.; Sandanayake, K. R. A. S.; Shinkai, S. *J. Chem. Soc., Chem. Commun.* 1994, 477.

20. James, T. D.; Shinkai, S. *J. Chem. Soc., Chem. Commun.* 1995, 1483.

21. James, T. D.; Linnane, P.; Shinkai, S. *Chem. Commun.* 1996, 281.

22. James, T. D.; Shinmori, H.; Shinkai, S. *Chem. Commun.* 1997, 71.

23. Linnane, P.; James, T. D.; Imazu, S.; Shinkai, S. *Tetrahedron Lett.* 1995, **36**, 8833.

24. Passafiume, J. F. *Digital Logic Design: Tutorials and Laboratory Exercises* Harper & Row: New York; London, 1985.

25. Aviram, A. *J. Am. Chem. Soc.* 1988, **110**, 5687.

26. Tour, J. M.; Kozaki, M.; Seminario, J. M. *J. Am. Chem. Soc.* 1998, **120**, 8486.

27. Baytekin, H. T.; Akkaya, E. U. *Org. Lett.* 2000, **2**, 1725.

28. Credi, A.; Balzani, V.; J., L. S.; Stoddart, J. F. *J. Am. Chem. Soc.* 1997, **119**, 2679.

29. de Silva, A. P.; Dixon, I. M.; Gunaratne, H. Q. N.; Gunnlaugsson, T.; Maxwell, P. R. S.; Rice, T. E. *J. Am. Chem. Soc.* 1999, **121**, 1393.

30. Gunnlaugsson, T.; Mac Donail, D. A.; Parker, D. *Chem. Commun.* 2000, 93.

31. Heath, J. R. *Pure Appl. Chem.* 2000, **72**, 11.

32. Pease, A. R.; Stoddart, J. F. *Struct. Bond.* 2001, **99**, 189.

33. Wild, U. P.; Bernet, S.; Kohler, B.; Renn, A. *Pure Appl. Chem.* 1992, **64**, 1335.

34. de Silva, A. P.; Gunaratne, H. Q. N.; Sandanayake, K. R. A. S. *Tetrahedron Lett.* 1990, **31**, 5193.

35. de Silva, A. P.; Gunaratne, H. Q. N.; McCoy, C. P. *Nature* 1993, **364**, 42.

36. Iwata, S.; Tanaka, K. *J. Chem. Soc., Chem. Commun.* 1995, 1491.

37. Bissell, R. A.; de Silva, A. P.; Gunaratne, H. Q. N.; Lynch, P. L. M.; Maguire, G. E. M.; McCoy, C. P.; Sandanayake, K. R. A. S. *Top. Curr. Chem.* 1993, **168**, 223.

38. de Silva, A. P.; McClenaghan, N. D. *J. Am. Chem. Soc.* 2000, **122**, 3965.

39. de Silva, A. P.; Gunaratne, H. Q. N.; McCoy, C. P. *J. Am. Chem. Soc.* 1997, **119**, 7891.

40. Wasiewicz, P.; Malinowski, A.; Nowak, R.; Mulawka, J. J.; Borsuk, P.; Weglenski, P.; Plucienniczak, A. *Future Generation Computer Systems* 2001, **17**, 361.

41. Prodi, L.; Bolletta, F.; Montalti, M.; Zaccheroni, N. *Coord. Chem. Rev.* 2000, **205**, 59.

42. Fabbrizzi, L.; Licchelli, M.; Pallavicini, P.; Perotti, A. *Angew. Chem. Int. Ed. Engl.* 1994, **33**, 1975.

43. Beer, P. D.; Gale, P. A.; Chen, G. Z. *J. Chem. Soc. Dalton Trans.* 1999, 1897.

44. Cram, D. J. *Science* 1988, **240**, 760.

45. Gokel, G. W. *Crown Ethers and Cryptands*, Stoddart, J. F. Ed.; Royal Society of Chemistry: Cambridge, 1991.

46. Huston, M. E.; Akkaya, E. U.; Czarnik, A. W. *J. Am. Chem. Soc.* 1989, **111**, 8735.

47. Pedersen, C. J. *J. Am. Chem. Soc.* 1967, **89**, 7017.

48. Pedersen, C. J. *Science* 1988, **241**, 536.

49. Sousa, L. R.; Larson, J. M. *J. Am. Chem. Soc.* 1977, **99**, 307.

50. de Silva, A. P.; Sandanayake, K. R. A. S. *J. Chem. Soc., Chem. Commun.* 1989, 1183.

51. de Silva, A. P.; Sandanayake, K. R. A. S. *Tetrahedron Lett.* 1991, **32**, 421.

52. Bourson, J.; Valeur, B. *J. Phys. Chem.* 1989, **93**, 3871.

53. Fery-Forgues, S.; Le Bris, M.-T.; Guette, J.-P.; Valeur, B. *J. Phys. Chem.* 1988, **92**, 6233.

54. Yoshida, K.; Mori, T.; Watanabe, S.; Kawai, H.; Nagamura, T. *J. Chem. Soc., Perkin Trans. 2* 1999, 393.

55. Kawai, H.; Nagamura, T.; Mori, T.; Yoshida, K. *J. Phys. Chem. A* 1999, **103**, 660.

56. de Silva, A. P.; Gunaratne, H. Q. N.; Rice, T. E.; Stewart, S. *Chem. Commun.* 1997, 1891.

57. Bordunov, A. V.; Bradshaw, J. S.; Xian Xin, Z.; Dalley, N. K.; Kou, X.; Izatt, R. M. *Inorg. Chem.* 1996, **35**, 7229.

58. Bradshaw, J. S.; Izatt, R. M. *Acc. Chem. Res.* 1997, **30**, 338.

59. Zhang, X. X.; Bordunov, A. V.; Bradshaw, J. S.; Dalley, N. K.; Kou, X.; Izatt, R. M. *J. Am. Chem. Soc.* 1995, **117**, 11507.

60. Su, N.; Bradshaw, J. S.; Zhang, X. X.; Savage, P. B.; Krakowiak, K. E.; Izatt, R. M. *J. Heterocyclic Chem.* 1999, **36**, 771.

61. Xu, X.; Xu, H.; Ji, H. F. *Chem. Commun.* 2001, 2092.

62. Konopelski, J. P.; Kotzyba-Hibert, F.; Lehn, J.-M.; Desvergne, J.-P.; Fages, F.; Castellan, A.; Bouas-Laurent, H. *J. Chem. Soc., Chem. Commun.* 1985, 433.

63. Fages, F.; Desvergne, J.-P.; Bouas-Laurent, H.; Marsau, P.; Lehn, J.-M.; Kotzyba-Hibert, F.; Albrecht-Gary, A. M.; Al Joubbeh, M. *J. Am. Chem. Soc.* 1989, **111**, 8672.

64. Golchini, K.; Mackovic-Basic, M.; Gharib, S. A.; Masilamani, D.; Lucas, M.; Furtz, I. *Am. J. Physiol.* 1990, **285**, F438.

65. He, H.; Mortellaro, M. A.; Leiner, M. J. P.; Fraatz, R. J.; Tusa, J. K. *J. Am. Chem. Soc.* 2003, **125**, 1468.

66. Choy, E. M.; Evans, D. F.; Cussler, E. L. *J. Am. Chem. Soc.* 1974, **96**, 7085.

67. Duax, W. L.; Smith, G. D.; Strong, P. D. *J. Am. Chem. Soc.* 1980, **102**, 6725.

68. Vogtle, F.; Weber, E. *Angew. Chem. Int. Ed. Engl.* 1979, **18**, 753.

69. Tummler, B.; Maass, G.; Weber, E.; Wehner, W.; Vogtle, F. *J. Am. Chem. Soc.* 1977, **99**, 4683.

70. Kakizawa, Y.; Akita, T.; Nakamura, H. *Chem. Lett.* 1993, 1671.

71. Kawakami, J.; Komai, Y.; Sumori, T.; Fukushi, A.; Shimozaki, K.; Ito, S. *J. Photochem. Photobiol. A* 2001, **139**, 71.

72. Kao, J. P. Y.; Harootunian, A. T.; Tsien, R. Y. *J. Biol. Chem.* 1989, **269**, 8179.

73. Tsien, R. Y. *Biochemistry* 1980, **19**, 2396.

74. Tsien, R. Y. *Annu. Rev. Neurosci.* 1989, **12**, 227.

75. Tsien, R. Y. *Am. J. Physiol.* 1992, **263**, C723.

76. de Silva, A. P.; Gunaratne, H. Q. N.; Maguire, G. E. M. *J. Chem. Soc., Chem. Commun.* 1994, 1213.

77. de Silva, A. P.; Gunaratne, H. Q. N. *J. Chem. Soc., Chem. Commun.* 1990, 186.

78. Prodi, L.; Ballardini, R.; Gandolfi, M. T.; Roversi, R. *J. Photochem. Photobiol. A* 2000, **136**, 49.

79. Antonisse, M. M. G.; Reinhoudt, D. N. *Chem. Commun.* 1998, 443.

80. Atwood, J. L.; Holman, K. T.; Steed, J. W. *Chem. Commun.* 1996, 1401.

81. Dietrich, B. *Pure Appl. Chem.* 1993, **65**, 1457.

82. Scheerder, J.; Engbersen, J. F. J.; Reinhoudt, D. N. *Recl.Trav. Chim. Pays-Bas* 1996, **115**, 307.

83. Schmidtchen, F. P.; Berger, M. *Chem. Rev.* 1997, **97**, 1609.

84. Snowden, T. S.; Anslyn, E. V. *Curr. Opin. Chem. Biol.* 1999, **3**, 740.

85. Beer, P. D.; Gale, P. A. *Angew. Chem. Int. Ed. Engl.* 2001, **40**, 486.

86. Shannon, R. D. *Acta Crystallogr., Sect. A: Found. Crystallogr.* 1976, **32**, 751.

87. Dietrich, B.; Hosseini, M. W. *Supramolecular Chemistry of Anions*, Bianchi, A.; Bowman-James, K.; Garcia-Espana, E. Ed.; John Wiley & Sons: New York, 1997.

88. Moyer, B. A.; Bonnesen, P. V. *Supramolecular Chemistry of Anions*, Bianchi, A.; Bowman-James, K.; Garcia-Espana, E. Ed.; John Wiley & Sons: New York, 1997.

89. Hofmeister, F. *Arch. Exp. Pathol. Pharmakol.* 1888, **24**, 247.

90. Buhlmann, P.; Nishizawa, S.; Xiao, K. P.; Umezawa, Y. *Tetrahedron* 1997, **53**, 1647.

91. Beer, P. D.; Cadman, J.; Lloris, J. M.; Martinez-Manez, R.; Padilla, M. E.; Pardo, T.; Smith, D. K.; Soto, J. *J. Chem. Soc. Dalton Trans.* 1999, 127.

92. Dickins, R. S.; Gunnlaugsson, T.; Parker, D.; Peacock, R. D. *Chem. Commun.* 1998, 1643.

93. Yamamoto, M.; Takeuchi, M.; Shinkai, S. *Tetrahedron* 1998, **54**, 3125.

94. Touster, O. *Annu. Rev. Biochem.* 1962, **31**, 407.

95. Weis, W.; Brown, J. H.; Cusack, S.; Paulson, J. C.; Skehel, J. J.; Wiley, D. C. *Nature* 1988, **333**, 426.

96. Sauter, N. K.; Glick, G. D.; Crowther, R. L.; Park, S. J.; Eisen, M. B.; Skehel, J. J.; Knowles, J. R.; Wiley, D. C. *Proc. Nat. Acad. Sci. USA* 1992, **89**, 324.

97. Vance, D. H.; Czarnik, A. W. *J. Am. Chem. Soc.* 1994, **116**, 9397.

98. Kissa, E. *Clin. Chem.* 1987, **33**, 253.

99. Kirk, K. L. *Biochemistry of the Halogens and Inorganic Halides* Plenum Press: New York, 1991.

100. Michigami, Y.; Kuroda, Y.; Ueda, K.; Yamamoto, Y. *Anal. Chim. Acta* 1993, **274**, 299.

101. Rum, G.; Lee, W. Y.; Gardea-Torresdey, J. *J. Chem. Educ.* 2000, **77**, 1604.

102. Sohn, H.; Letant, S.; Sailor, M.; Trogler, W. *J. Am. Chem. Soc.* 2000, **122**, 5399.

103. Noort, D.; Benshop, H. P.; Black, R. M. *Toxicol. Appl. Pharmacol.* 2002, **184**, 116.

104. Frant, M. S.; Ross, J. W. *Science* 1966, **154**, 1533.

105. Black, C. B.; Andrioletti, B.; Try, A. C.; Ruiperez, C.; Sessler, J. L. *J. Am. Chem. Soc.* 1999, **121**, 10438.

106. Anzenbacher, P.; Try, A. C.; Miyaji, H.; Jursikova, K.; Lynch, V. M.; Marquez, M.; Sessler, J. L. *J. Am. Chem. Soc.* 2000, **122**, 10268.

107. Mizuno, T.; Wei, W. H.; Eller, L. R.; Sessler, J. L. *J. Am. Chem. Soc.* 2002, **124**, 1134.

108. Lee, K. H.; Lee, H. Y.; Lee, D. H.; Hong, J. I. *Tetrahedron Lett.* 2001, **42**, 5447.

109. Kim, S. K.; Yoon, J. *Chem. Commun.* 2002, 770.

110. Jimenez, D.; Martanez, R.; Sancenon, F.; Soto, J. *Tetrahedron Lett.* 2002, **43**, 2823.

111. Takeuchi, M.; Shioya, T.; Swager, T. M. *Angew. Chem. Int. Ed. Engl.* 2001, **40**, 3372.

112. Yamaguchi, S.; Akiyama, S.; Tamao, K. *J. Am. Chem. Soc.* 2000, **122**, 6793.

113. Worm, K.; Schmidtchen, F. P.; Schier, A.; Schaefer, A. *Angew. Chem. Int. Ed. Engl.* 1994, **33**, 327.

114. Jacobson, S.; Pizer, R. *J. Am. Chem. Soc.* 1993, **115**, 11216.

115. Paugam, M. F.; Smith, B. D. *Tetrahedron Lett.* 1993, **34**, 3723.

116. Katz, H. E. *J. Org. Chem.* 1985, **50**, 5027.

117. Katz, H. E. *J. Am. Chem. Soc.* 1986, **108**, 7640.

118. Katz, H. E. *J. Am. Chem. Soc.* 1985, **107**, 1420.

119. Katz, H. E. *Organometallics* 1987, **6**, 1134.

120. Reetz, M. T.; Niemeyer, C. M.; Harms, K. *Angew. Chem. Int. Ed. Engl.* 1991, **30**, 1472.

121. Reetz, M. T.; Niemeyer, C. M.; Harms, K. *Angew. Chem. Int. Ed. Engl.* 1991, **30**, 1474.

122. Cooper, C. R.; Spencer, N.; James, T. D. *Chem. Commun.* 1998, 1365.

123. Valeur, B.; Pouget, J.; Bourson, J.; Kaschake, M.; Ernsting, N. P. *J. Phys. Chem.* 1992, **96**, 6545.

124. Farfan, N.; Joseph-Nathan, P.; Chiquete, L. M.; Contreas, R. *J. Organomet. Chem.* 1988, **348**, 149.

125. Ward, C. J.; Patel, P.; Ashton, P. R.; James, T. D. *Chem. Commun.* 2000, 229.

126. Ward, C. J.; Patel, P.; James, T. D. *Chem. Lett.* 2001, 406.

127. DiCesare, N.; Lakowicz, J. R. *Anal. Biochem.* 2002, **301**, 111.

128. Dusemund, C.; Samankumara Sandanayake, K. R. A.; Shinkai, S. *Chem. Commun.* 1995, 333.

129. Yamamoto, H.; Ori, A.; Ueda, K.; Dusemund, C.; Shinkai, S. *Chem. Commun.* 1996, 407.

130. Reetz, M. T.; Johnson, B. M.; Harms, K. *Tetrahedron Lett.* 1994, **35**, 2525.

131. Scheerder, J.; Duynhoven van, J. P. M.; Engbersen, J. F. J.; Reinhoudt, D. N. *Angew. Chem. Int. Ed. Engl.* 1996, **35**, 1090.

132. Scheerder, J.; H., V. R.; Engbersen, J. F. J.; Verboorn, W.; Duynhoven van, J. P. M.; Reinhoudt, D. N. *J. Org. Chem.* 1996, **61**, 3476.

133. de Silva, A. P.; Gunaratne, H. Q. N.; McVeigh, C.; Maguire, G. E. M.; Maxwell, P. R. S.; O'Hanlon, E. *Chem. Commun.* 1996, 2191.

134. Beer, P. D.; Dent, S. W. *Chem. Commun.* 1999, 825.

135. Rudkevich, D. M.; Brzozka, Z.; Palys, M.; Visser, H. C.; Verboom, W.; Reinhoudt, D. N. *Angew. Chem. Int. Ed. Engl.* 1994, **33**, 467.

136. Duff, J. C. *J. Chem. Soc.* 1941, 547.

137. Ogata, Y.; Kawasaki, A.; Sugiura, F. *Tetrahedron* 1968, **24**, 5001.

138. Wada, F.; Hirayama, H.; Namiki, H.; Kikukawa, K.; Matsuda, T. *Bull. Chem. Soc. Jpn.* 1980, **53**, 1473.

139. James, T. D.; Sandanayake, K. R. A. S.; Iguchi, R.; Shinkai, S. *J. Am. Chem. Soc.* 1995, **117**, 8982.

140. Wiskur, S. L.; Lavigne, J. J.; Ait-Haddou, H.; Lynch, V.; Chiu, Y. H.; Canary, J. W.; Anslyn, E. V. *Org. Lett.* 2001, **3**, 1311.

141. Yoon, J.; Czarnik, A. W. *J. Am. Chem. Soc.* 1992, **114**, 5874.

142. Arimori, S.; Bosch, L. I.; Ward, C. J.; James, T. D. *Tetrahedron Lett.* 2002, **43**, 911.

143. Weller, A. *Pure Appl. Chem.* 1968, **58**, 115.

144. Grabowski, Z. R.; Dobkowski, J. *Pure Appl. Chem.* 1983, **55**, 245.

145. Opium. http://www.natur.cuni.cz/~kyvala/opium.html, 2000.

146. Seaman, W.; Johnson, J. R. *J. Am. Chem. Soc.* 1931, **53**, 711.

6 Appendix

6.1 Crystal data

Appendix 1. Crystal structure of compound **11**.

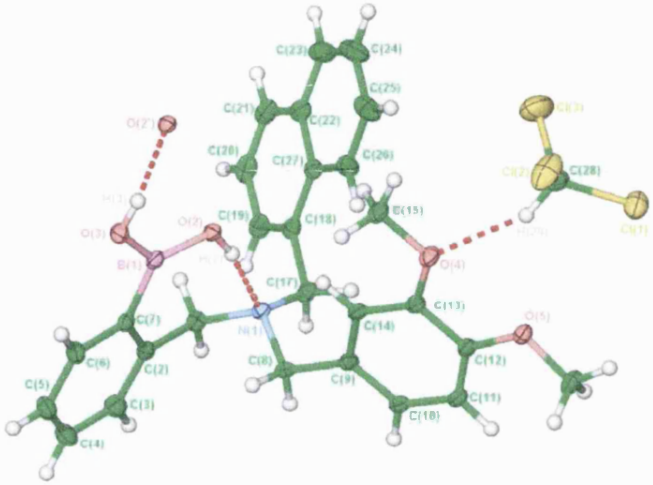

Appendix 2. Crystal structure of dimeric structure of compound **11**.

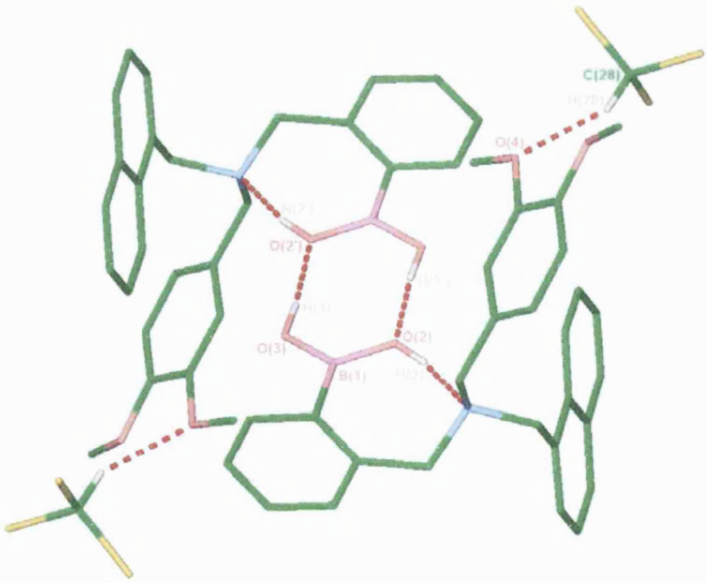

Appendix 3. Crystal data for compound **11.**

Table 11. Crystal data and structure refinement for compound **11.**

Identification code	k02tdj2
Empirical formula	C28 H29 B Cl3 N O4
Formula weight	560.68
Temperature	150(2) K
Wavelength	0.71073 Å
Crystal system	Monoclinic
Space group	P2/n
Unit cell dimensions	a = 12.5810(2)Å $\alpha = 90^\circ$
	b = 11.6210(2)Å $\beta = 101.6170(10)^\circ$
	c = 19.3770(3)Å $\gamma = 90^\circ$
Volume	2774.96(8) $Å^3$
Z	4
Density (calculated)	1.342 Mg/m^3
Absorption coefficient	0.365 mm^{-1}
F(000)	1168
Crystal size	0.30 x 0.20 x 0.08 mm
Theta range for data collection	3.56 to 27.51°
Index ranges	-16<=h<=16; -15<=k<=15; -25<=l<=25
Reflections collected	57325
Independent reflections	6352 [R(int) = 0.0879]
Reflections observed (>2σ)	3635
Data Completeness	0.995
Max. and min. transmission	0.9714 and 0.8985
Refinement method	Full-matrix least-squares on F^2
Data / restraints / parameters	6352 / 2 / 345
Goodness-of-fit on F^2	1.014
Final R indices [I>2σ(I)]	$R_1 = 0.0485$ $wR_2 = 0.1154$
R indices (all data)	$R_1 = 0.1078$ $wR_2 = 0.1400$
Largest diff. peak and hole	0.356 and -0.429 $eÅ^{-3}$

Notes: H2 and H3 located and refined at 0.89Å from relevant oxygens.
C(H…O interaction between hydrogen on chloroform and O4; [O(4)-H(28) 2.18 Å]

Hydrogen bonds with H..A < r(A) + 2.000 Angstroms and <DHA > 110 deg.

D-H	d(D-H)	d(H..A)	<DHA	d(D..A)	A
O2-H2	0.869	1.805	167.99	2.661	N1
O3-H3	0.850	1.923	171.83	2.767	O2 [-x+1, -y, -z]

Table 12. Atomic coordinates ($\times 10^4$) and equivalent isotropic displacement parameters ($Å^2 \times 10^3$) for 1.U(eq) is defined as one third of the trace of the orthogonalized Uij tensor.

Atom	x	y	z	U(eq)
Cl(1)	5219(1)	-3645(1)	4261(1)	67(1)
Cl(2)	6020(1)	-4454(1)	3055(1)	96(1)
Cl(3)	3864(1)	-3580(1)	2863(1)	104(1)
O(2)	4934(1)	1129(1)	617(1)	35(1)
O(3)	5759(1)	1120(1)	-369(1)	42(1)
O(4)	6160(1)	-1564(1)	2582(1)	45(1)
O(5)	6826(1)	-1284(1)	3909(1)	44(1)
N(1)	4883(1)	2597(1)	1664(1)	32(1)
C(1)	4741(2)	3588(2)	1168(1)	37(1)
C(2)	5646(2)	3773(2)	765(1)	35(1)
C(3)	6120(2)	4857(2)	819(1)	49(1)
C(4)	6913(2)	5142(2)	448(1)	57(1)
C(5)	7240(2)	4341(2)	12(1)	54(1)
C(6)	6770(2)	3261(2)	-54(1)	44(1)
C(7)	5967(2)	2942(2)	318(1)	34(1)
C(8)	5958(2)	2641(2)	2144(1)	36(1)
C(9)	6186(2)	1619(2)	2628(1)	33(1)
C(10)	6573(2)	1760(2)	3344(1)	35(1)
C(11)	6824(2)	815(2)	3789(1)	36(1)
C(12)	6657(2)	-283(2)	3522(1)	35(1)
C(13)	6279(2)	-440(2)	2795(1)	35(1)
C(14)	6057(2)	498(2)	2357(1)	35(1)
C(15)	5828(2)	-1778(2)	1844(1)	51(1)
C(16)	7386(2)	-1182(2)	4618(1)	53(1)
C(17)	4019(2)	2655(2)	2090(1)	37(1)
C(18)	2882(2)	2491(2)	1671(1)	38(1)
C(19)	2232(2)	3431(2)	1470(1)	45(1)
C(20)	1158(2)	3320(3)	1097(1)	54(1)
C(21)	728(2)	2261(3)	934(1)	55(1)
C(22)	1348(2)	1255(2)	1135(1)	47(1)
C(23)	924(2)	135(3)	975(1)	62(1)
C(24)	1526(2)	-810(3)	1159(2)	68(1)
C(25)	2598(2)	-708(2)	1526(2)	61(1)
C(26)	3050(2)	344(2)	1694(1)	45(1)
C(27)	2446(2)	1369(2)	1505(1)	38(1)
C(28)	5182(2)	-3455(2)	3358(1)	55(1)
B(1)	5520(2)	1678(2)	194(1)	34(1)

Table 13. Bond lengths [Å] and angles [°] for compound **11**.

Cl(1)-C(28)	1.754(3)	Cl(2)-C(28)	1.747(3)
Cl(3)-C(28)	1.747(3)	O(2)-B(1)	1.367(3)
O(3)-B(1)	1.354(3)	O(4)-C(13)	1.369(2)
O(4)-C(15)	1.427(3)	O(4)-H(28)	2.1842
O(5)-C(12)	1.377(3)	O(5)-C(16)	1.418(3)
N(1)-C(8)	1.481(3)	N(1)-C(1)	1.488(3)
N(1)-C(17)	1.492(2)	C(1)-C(2)	1.519(3)
C(2)-C(3)	1.389(3)	C(2)-C(7)	1.410(3)
C(3)-C(4)	1.382(3)	C(4)-C(5)	1.374(4)
C(5)-C(6)	1.383(3)	C(6)-C(7)	1.403(3)
C(7)-B(1)	1.574(3)	C(8)-C(9)	1.504(3)
C(9)-C(10)	1.384(3)	C(9)-C(14)	1.402(3)
C(10)-C(11)	1.393(3)	C(11)-C(12)	1.376(3)
C(12)-C(13)	1.404(3)	C(13)-C(14)	1.376(3)
C(17)-C(18)	1.507(3)	C(18)-C(19)	1.374(3)
C(18)-C(27)	1.427(3)	C(19)-C(20)	1.404(3)
C(20)-C(21)	1.356(4)	C(21)-C(22)	1.416(4)
C(22)-C(23)	1.418(4)	C(22)-C(27)	1.428(3)
C(23)-C(24)	1.341(4)	C(24)-C(25)	1.397(4)
C(25)-C(26)	1.360(3)	C(26)-C(27)	1.420(3)
C(13)-O(4)-C(15)	117.47(17)	C(13)-O(4)-H(28)	113.8
C(15)-O(4)-H(28)	116.7	C(12)-O(5)-C(16)	116.71(17)
C(8)-N(1)-C(1)	110.77(15)	C(8)-N(1)-C(17)	109.03(15)
C(1)-N(1)-C(17)	108.45(15)	N(1)-C(1)-C(2)	115.92(16)
C(3)-C(2)-C(7)	119.7(2)	C(3)-C(2)-C(1)	116.38(19)
C(7)-C(2)-C(1)	123.81(18)	C(4)-C(3)-C(2)	121.5(2)
C(5)-C(4)-C(3)	119.6(2)	C(4)-C(5)-C(6)	119.7(2)
C(5)-C(6)-C(7)	122.1(2)	C(6)-C(7)-C(2)	117.4(2)
C(6)-C(7)-B(1)	116.12(19)	C(2)-C(7)-B(1)	126.50(18)
N(1)-C(8)-C(9)	113.56(16)	C(10)-C(9)-C(14)	118.49(19)
C(10)-C(9)-C(8)	121.00(18)	C(14)-C(9)-C(8)	120.44(18)
C(9)-C(10)-C(11)	121.1(2)	C(12)-C(11)-C(10)	120.01(19)
C(11)-C(12)-O(5)	125.70(18)	C(11)-C(12)-C(13)	119.47(19)
O(5)-C(12)-C(13)	114.83(18)	O(4)-C(13)-C(14)	124.89(18)
O(4)-C(13)-C(12)	114.94(18)	C(14)-C(13)-C(12)	120.17(19)
C(13)-C(14)-C(9)	120.66(18)	N(1)-C(17)-C(18)	114.51(15)
C(19)-C(18)-C(27)	118.9(2)	C(19)-C(18)-C(17)	119.9(2)
C(27)-C(18)-C(17)	121.14(19)	C(18)-C(19)-C(20)	122.0(2)
C(21)-C(20)-C(19)	120.1(2)	C(20)-C(21)-C(22)	120.9(2)
C(23)-C(22)-C(21)	122.4(2)	C(23)-C(22)-C(27)	118.5(2)
C(21)-C(22)-C(27)	119.1(2)	C(24)-C(23)-C(22)	121.8(3)
C(23)-C(24)-C(25)	120.1(3)	C(26)-C(25)-C(24)	120.8(3)
C(25)-C(26)-C(27)	121.1(2)	C(26)-C(27)-C(18)	123.1(2)
C(26)-C(27)-C(22)	117.7(2)	C(18)-C(27)-C(22)	119.1(2)
Cl(3)-C(28)-Cl(2)	109.29(14)	Cl(3)-C(28)-Cl(1)	111.60(16)
Cl(2)-C(28)-Cl(1)	110.79(14)	O(3)-B(1)-O(2)	119.7(2)
O(3)-B(1)-C(7)	116.03(19)	O(2)-B(1)-C(7)	124.30(19)

Symmetry transformations used to generate equivalent atoms:

Table 14. Anisotropic displacement parameters ($Å^2 \times 10^3$) for compound **11**. The anisotropic displacement factor exponent takes the form: $-2\ gpi^2\ [h^2\ a^{*2}\ U11 + ... + 2\ h\ k\ a^*\ b^*\ U]$

Atom	U11	U22	U33	U23	U13	U12
Cl(1)	81(1)	63(1)	56(1)	2(1)	13(1)	4(1)
Cl(2)	145(1)	76(1)	63(1)	-16(1)	10(1)	42(1)
Cl(3)	85(1)	108(1)	100(1)	10(1)	-30(1)	-16(1)
O(2)	37(1)	40(1)	27(1)	-6(1)	8(1)	-6(1)
O(3)	53(1)	44(1)	31(1)	-5(1)	16(1)	-8(1)
O(4)	63(1)	39(1)	31(1)	-5(1)	3(1)	-3(1)
O(5)	51(1)	45(1)	31(1)	2(1)	0(1)	-4(1)
N(1)	30(1)	36(1)	28(1)	-3(1)	5(1)	1(1)
C(1)	40(1)	36(1)	35(1)	-1(1)	7(1)	5(1)
C(2)	35(1)	34(1)	33(1)	5(1)	-1(1)	0(1)
C(3)	56(2)	37(1)	51(1)	2(1)	5(1)	-3(1)
C(4)	62(2)	43(1)	64(2)	12(1)	7(1)	-15(1)
C(5)	49(2)	60(2)	54(2)	16(1)	13(1)	-11(1)
C(6)	43(1)	48(1)	41(1)	9(1)	10(1)	-3(1)
C(7)	33(1)	41(1)	27(1)	6(1)	2(1)	0(1)
C(8)	32(1)	38(1)	36(1)	-5(1)	1(1)	-4(1)
C(9)	27(1)	39(1)	32(1)	-4(1)	5(1)	-2(1)
C(10)	31(1)	41(1)	33(1)	-7(1)	6(1)	-3(1)
C(11)	30(1)	51(1)	26(1)	-5(1)	3(1)	-3(1)
C(12)	31(1)	42(1)	30(1)	2(1)	5(1)	0(1)
C(13)	34(1)	39(1)	32(1)	-4(1)	5(1)	-2(1)
C(14)	30(1)	44(1)	27(1)	-2(1)	2(1)	-3(1)
C(15)	74(2)	47(1)	31(1)	-8(1)	4(1)	-9(1)
C(16)	67(2)	56(2)	32(1)	3(1)	-2(1)	9(1)
C(17)	37(1)	48(1)	28(1)	-7(1)	8(1)	4(1)
C(18)	37(1)	51(1)	27(1)	-1(1)	13(1)	6(1)
C(19)	44(1)	53(1)	41(1)	1(1)	16(1)	9(1)
C(20)	43(2)	78(2)	45(1)	11(1)	15(1)	19(1)
C(21)	34(1)	94(2)	39(1)	3(1)	11(1)	4(1)
C(22)	36(1)	74(2)	35(1)	-5(1)	17(1)	-5(1)
C(23)	42(2)	88(2)	59(2)	-18(2)	20(1)	-22(2)
C(24)	61(2)	66(2)	84(2)	-18(2)	33(2)	-26(2)
C(25)	60(2)	51(2)	79(2)	-5(1)	34(2)	-8(1)
C(26)	37(1)	52(2)	49(1)	-3(1)	18(1)	-4(1)
C(27)	36(1)	53(1)	29(1)	-2(1)	16(1)	-1(1)
C(28)	67(2)	43(1)	49(2)	-4(1)	-4(1)	-5(1)
B(1)	30(1)	44(1)	27(1)	0(1)	2(1)	1(1)

Table 15. Hydrogen coordinates ($\times 10^4$) and isotropic displacement parameters ($Å^2 \times 10^3$) for compound **11**.

Atom	x	y	z	U(eq)
H(1A)	4668	4297	1438	44
H(1B)	4053	3482	823	44
H(3A)	5894	5415	1117	59
H(4)	7230	5887	494	68
H(5)	7787	4530	-243	65
H(6)	6997	2718	-361	52
H(8A)	6002	3349	2433	43
H(8B)	6527	2688	1859	43
H(10)	6669	2514	3535	42
H(11)	7110	927	4276	43
H(14)	5814	384	1864	41
H(15A)	5125	-1411	1668	77
H(15B)	5764	-2609	1762	77
H(15C)	6369	-1461	1596	77
H(16A)	8114	-871	4630	80
H(16B)	7446	-1942	4842	80
H(16C)	6986	-663	4872	80
H(17A)	4062	3412	2327	45
H(17B)	4166	2057	2460	45
H(19)	2517	4179	1587	54
H(20)	732	3987	959	65
H(21)	1	2193	680	66
H(23)	193	51	731	74
H(24)	1223	-1550	1040	81
H(25)	3016	-1382	1660	73
H(26)	3780	395	1943	54
H(28)	5456	-2665	3286	66
H(2)	4850(20)	1550(20)	974(11)	62(8)
H(3)	5550(20)	423(16)	-402(14)	62(8)

6.2 Tetrabutylammonium halide fluorescence titrations

Pyrene series

Appendix 4: Fluorescence Intensity (I_F) of sensor **1** (5×10^{-7} M) with increasing concentration of nBu_4NF in $CHCl_3$. λ_{ex} = 345 nm.

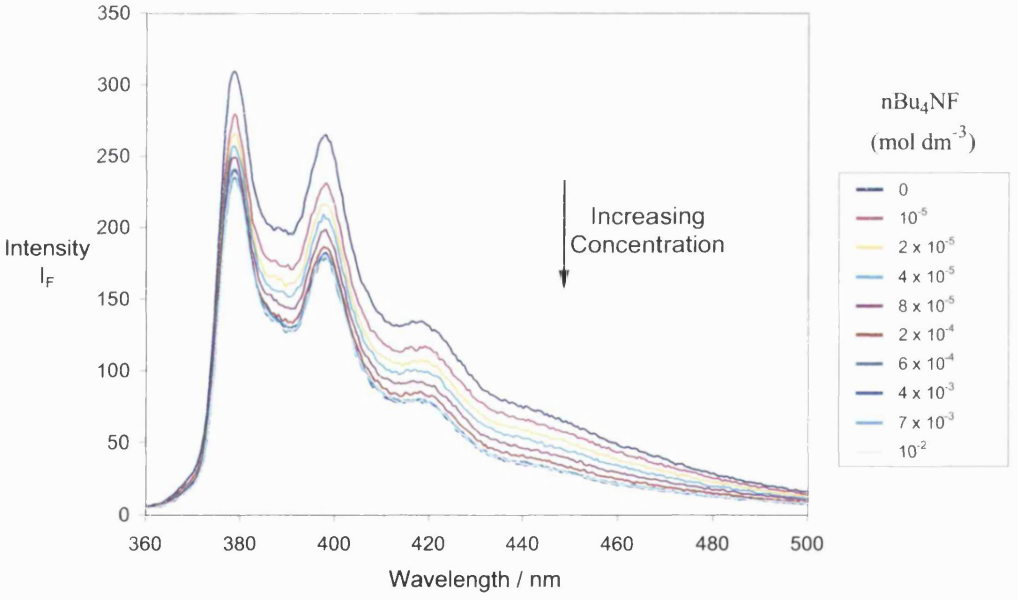

Appendix 5: Fluorescence Intensity (I_F) of sensor **2** (5×10^{-7} mol dm^{-3}) with increasing concentration of nBu_4NF in $CHCl_3$. λ_{ex} = 347 nm.

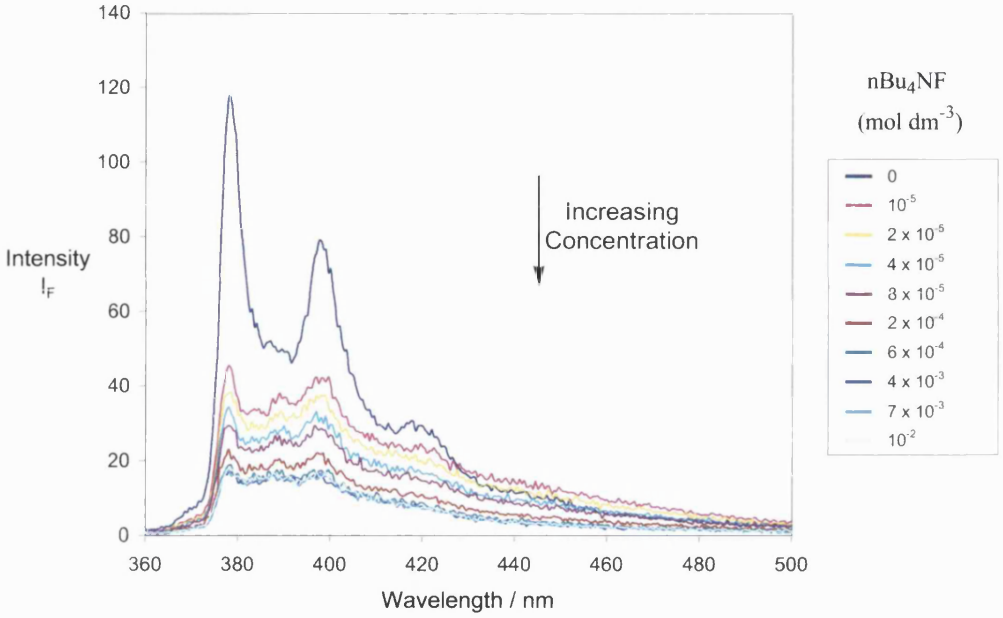

Appendix 6: Fluorescence Intensity (I_F) of sensor **7** (5×10^{-7} mol dm^{-3}) with increasing concentration of nBu_4NF in $CHCl_3$. λ_{ex} = 343 nm.

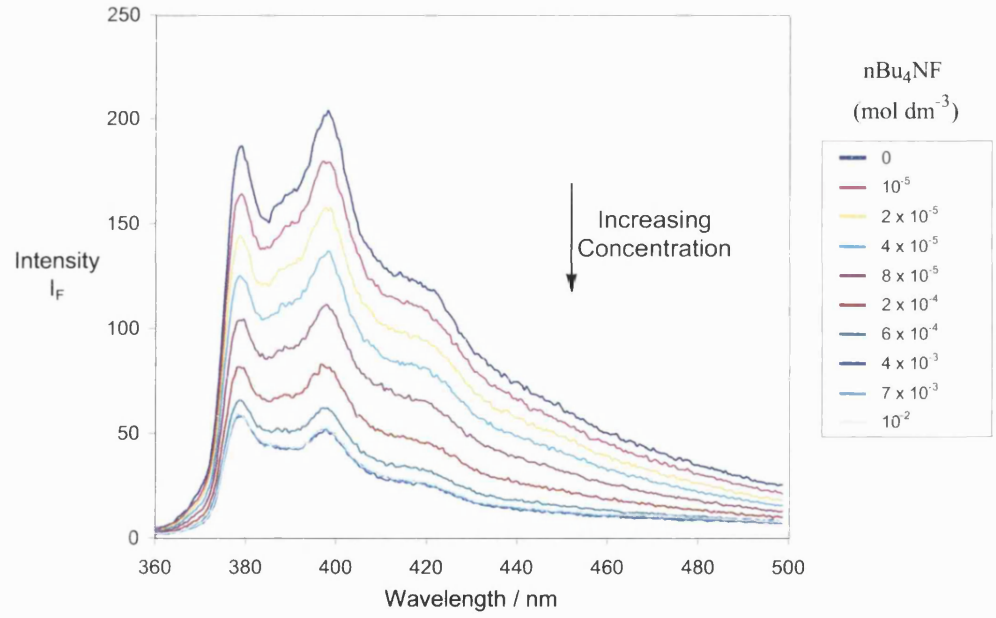

Appendix 7: Fluorescence Intensity (I_F) of sensor **8** (5×10^{-7} mol dm^{-3}) with increasing concentration of nBu_4NF in $CHCl_3$. λ_{ex} = 343 nm.

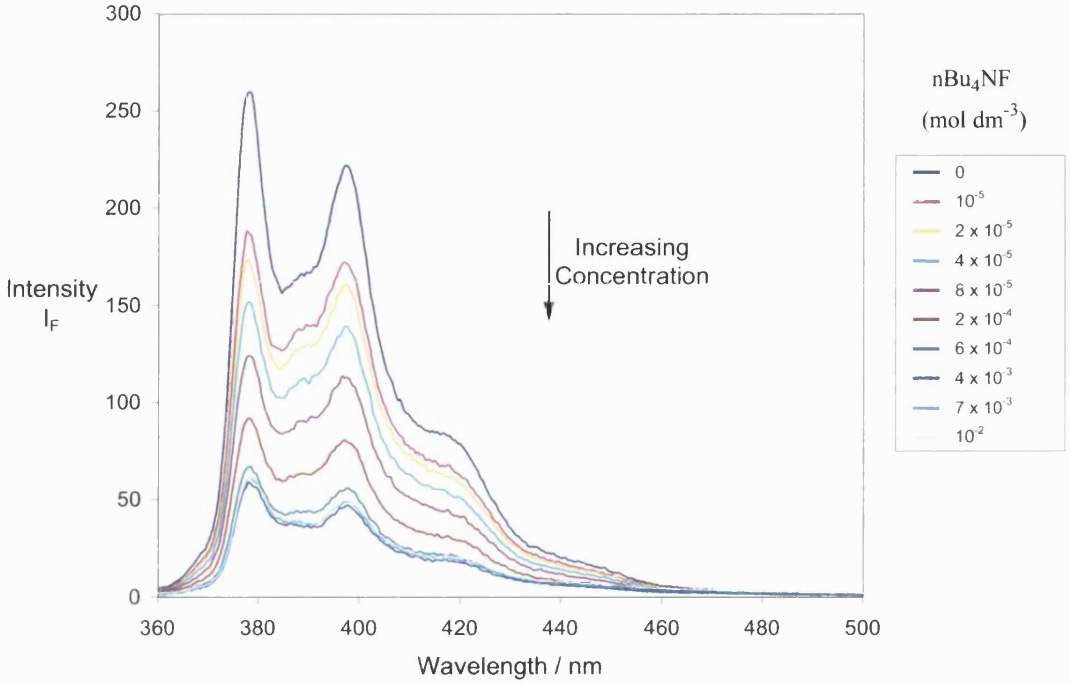

Appendix 8. Relative Fluorescence Intensity (I / I_0) of sensor **1** (5×10^{-7} M) *versus* nBu_4NF (○), nBu_4NCl (Δ) and nBu_4NBr (□) at 25 °C in chloroform; λ_{ex} = 345 nm, λ_{em} = 397 nm.

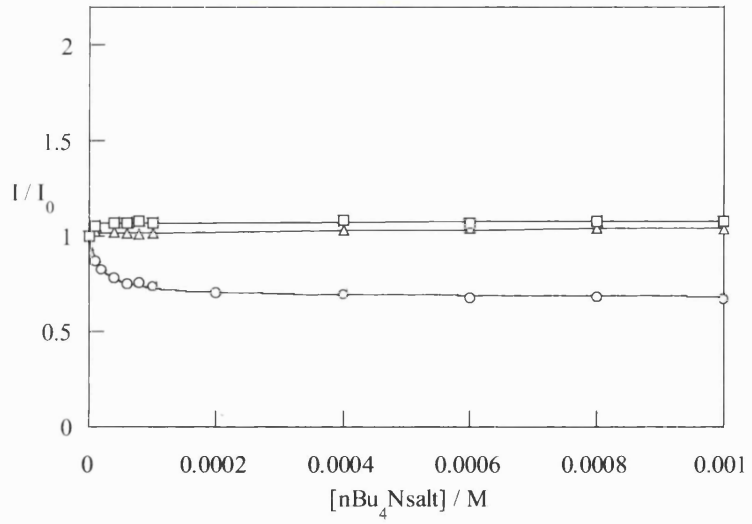

Appendix 9. Relative Fluorescence Intensity (I / I_0) of sensor **2** (5×10^{-7} M) *versus* nBu_4NF (○), nBu_4NCl (Δ) and nBu_4NBr (□) at 25 °C in chloroform; $\lambda_{ex} = 347$ nm, $\lambda_{em} = 397$ nm.

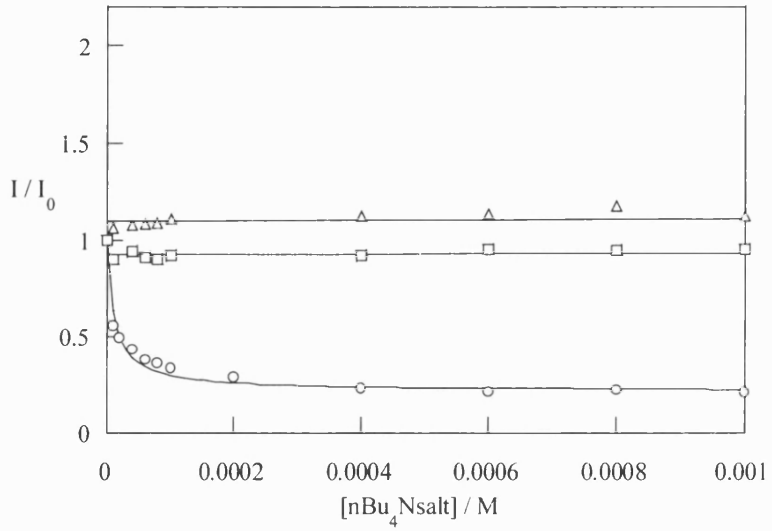

Appendix 10. Relative Fluorescence Intensity (I / I_0) of sensor **7** (5×10^{-7} M) *versus* nBu_4NF (○), nBu_4NCl (Δ) and nBu_4NBr (□) at 25 °C in chloroform; $\lambda_{ex} = 343$ nm, $\lambda_{em} = 397$ nm.

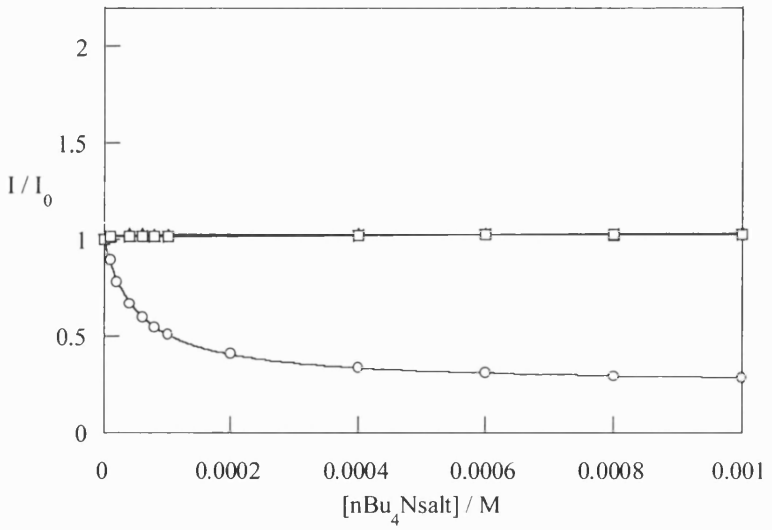

Appendix 11. Relative Fluorescence Intensity (I / I_0) of sensor **8** (5×10^{-7} M) *versus* nBu_4NF (○), nBu_4NCl (Δ) and nBu_4NBr (□) at 25 °C in chloroform; $\lambda_{ex} = 342$ nm, $\lambda_{em} = 397$ nm.

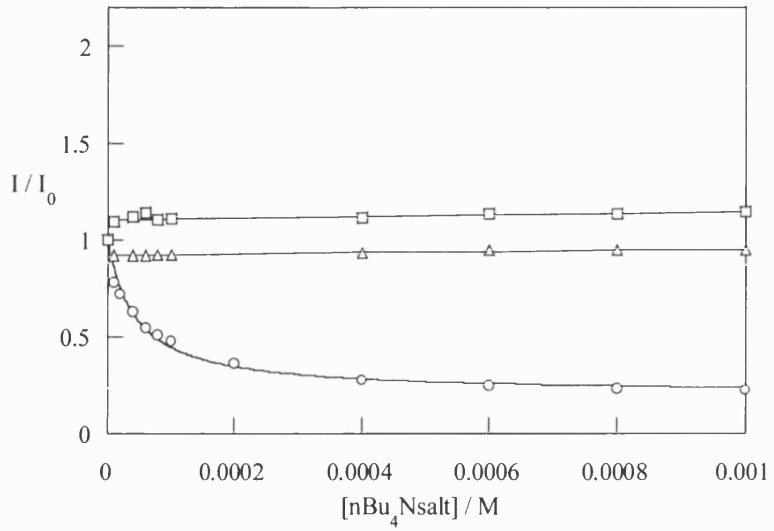

Appendix 12. Relative Fluorescence Intensity (I / I_0) of sensor **5** (5×10^{-7} M) *versus* nBu_4NF (○), nBu_4NCl (Δ) and nBu_4NBr (□) at 25 °C in chloroform; $\lambda_{ex} = 341$ nm, $\lambda_{em} = 397$ nm.

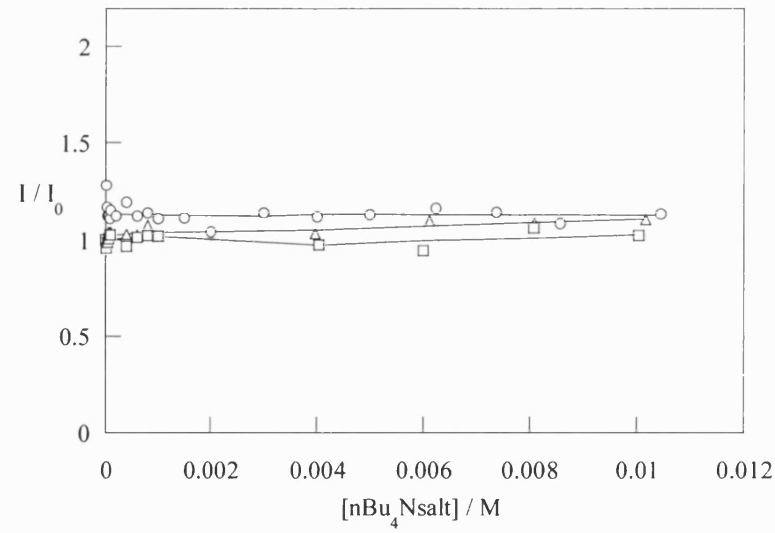

Appendix 13. Relative Fluorescence Intensity (I / I_0) of sensor **6** (5×10^{-7} M) *versus* nBu_4NF (○), nBu_4NCl (Δ) and nBu_4NBr (□) at 25 °C in chloroform; $\lambda_{ex} = 347$ nm, $\lambda_{em} = 397$ nm.

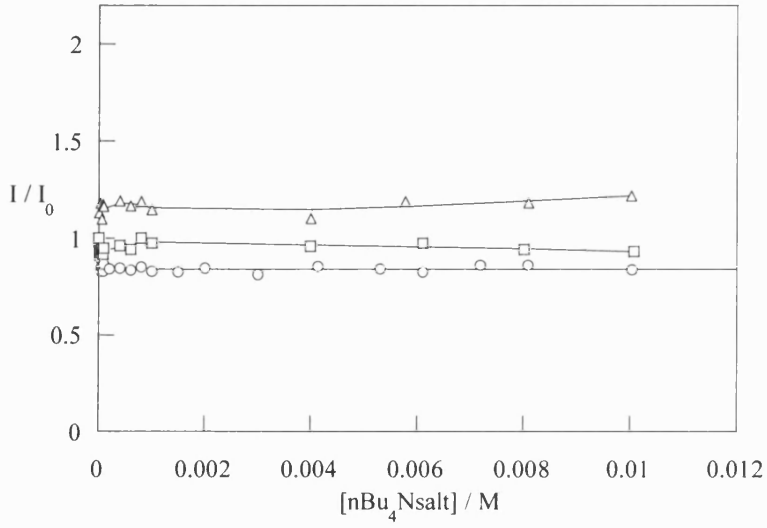

Naphthalene series

Appendix 14: Fluorescence Intensity (I_F) of sensor **3** (5×10^{-7} mol dm^{-3}) with increasing concentration of nBu_4NF in $CHCl_3$. λ_{ex} = 288 nm.

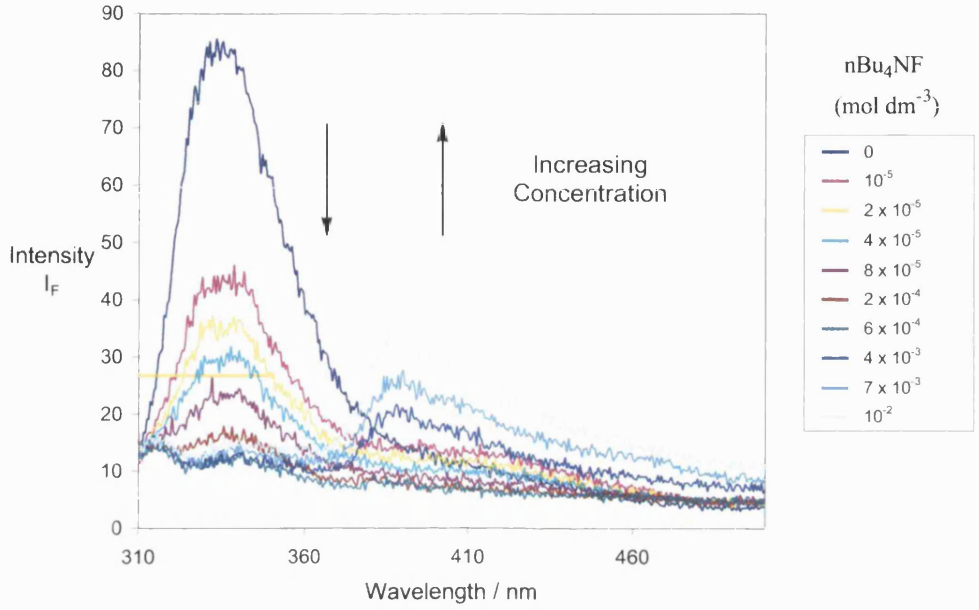

Appendix 15: Fluorescence Intensity (I_F) of sensor **4** (5×10^{-7} mol dm^{-3}) with increasing concentration of nBu_4NF in $CHCl_3$. λ_{ex} = 288 nm.

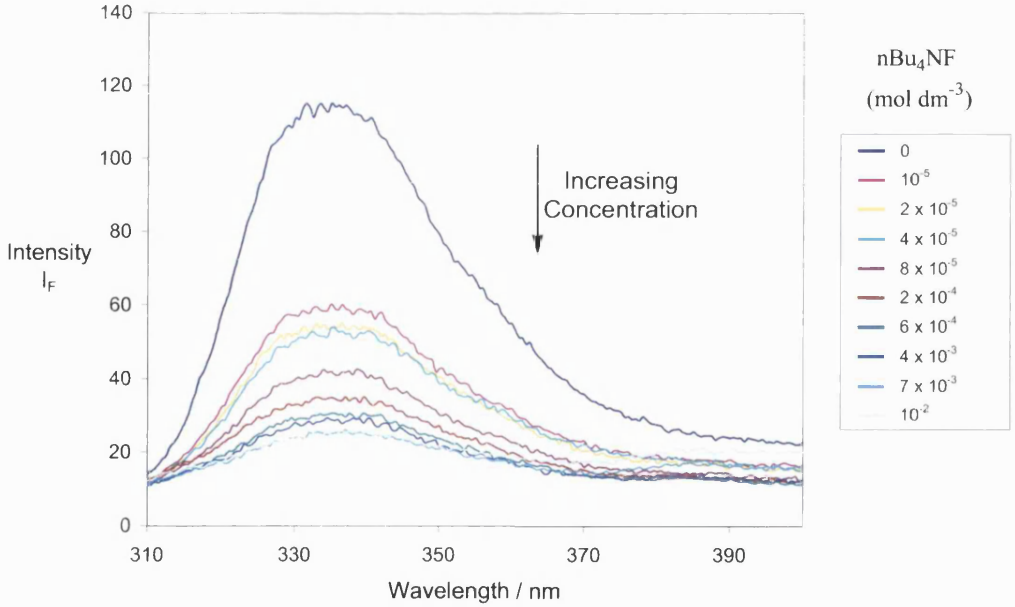

Appendix 16: Fluorescence Intensity (I_F) of sensor **11** (5×10^{-7} mol dm^{-3}) with increasing concentration of nBu_4NF in $CHCl_3$. λ_{ex} = 288 nm.

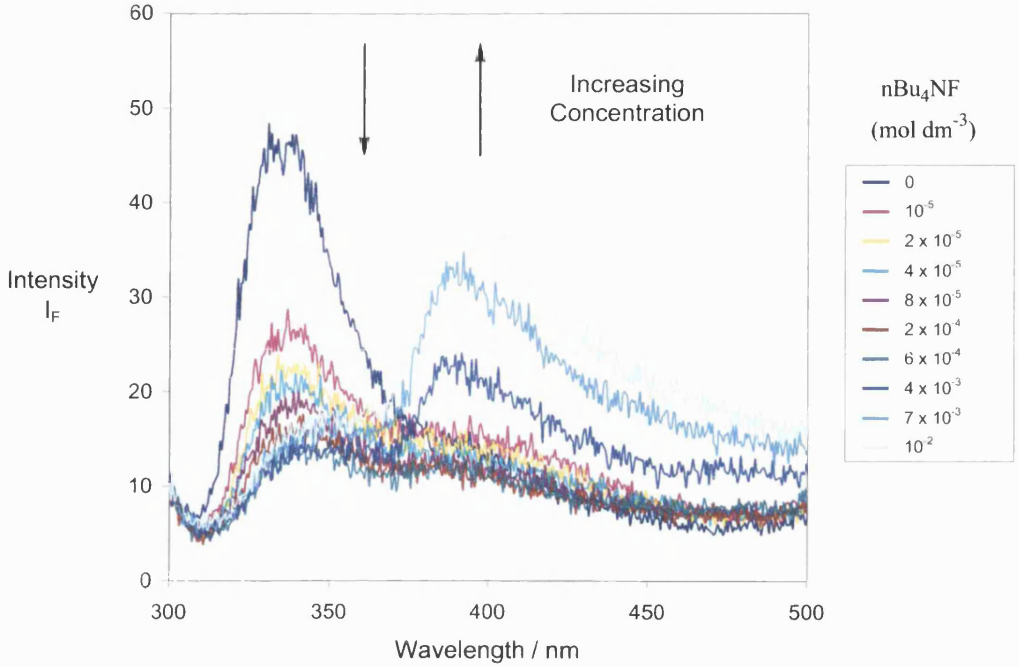

Appendix 17: Fluorescence Intensity (I_F) of sensor **12** (5×10^{-7} mol dm^{-3}) with increasing concentration of nBu_4NF in $CHCl_3$. λ_{ex} = 288 nm.

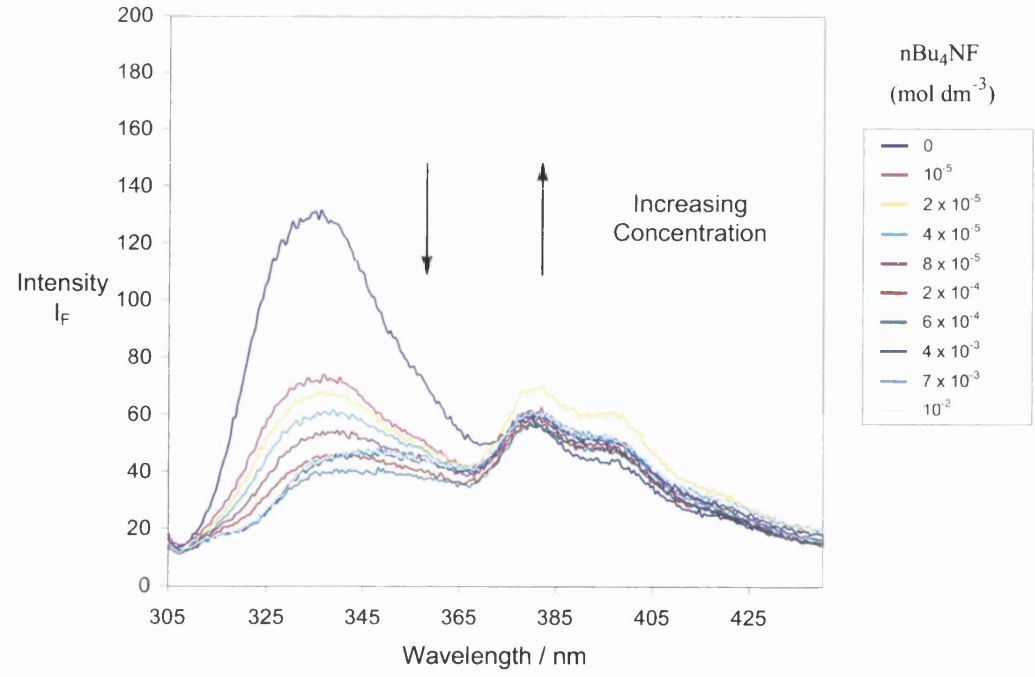

Appendix 18. Relative Fluorescence Intensity (I / I_0) of sensor **3** (5×10^{-7} M) *versus* nBu_4NF (○), nBu_4NCl (Δ) and nBu_4NBr (□) at 25 °C in chloroform; $\lambda_{ex} = 343$ nm, $\lambda_{em} = 397$ nm.

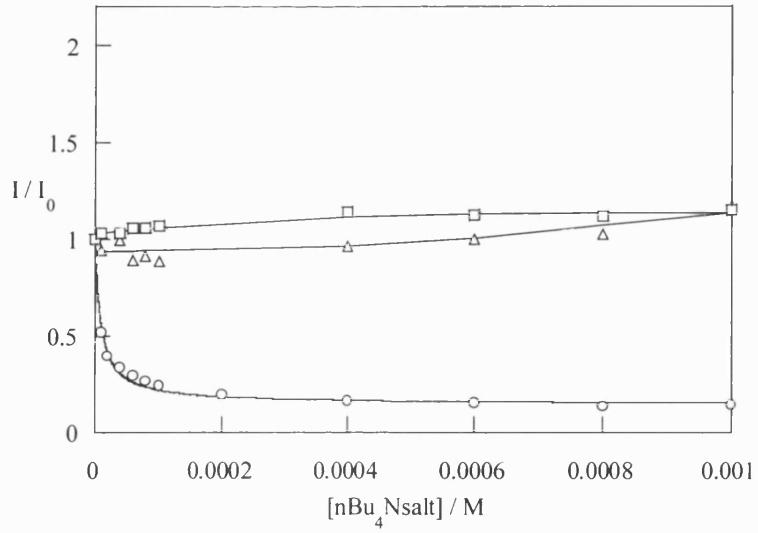

Appendix 19. Relative Fluorescence Intensity (I / I_0) of sensor **4** (5×10^{-7} M) *versus* nBu_4NF (○), nBu_4NCl (Δ) and nBu_4NBr (□) at 25 °C in chloroform; $\lambda_{ex} = 343$ nm, $\lambda_{em} = 397$ nm.

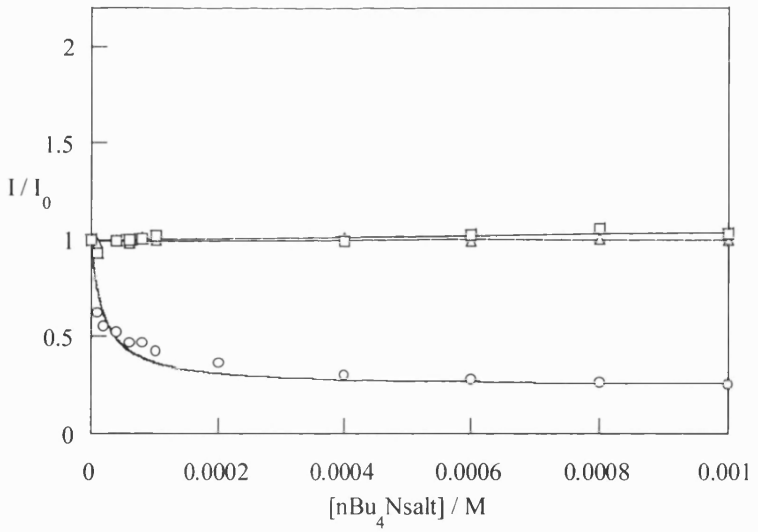

Appendix 20. Relative Fluorescence Intensity (I / I_0) of sensor **11** (5×10^{-7} M) *versus* nBu_4NF (○), nBu_4NCl (Δ) and nBu_4NBr (□) at 25 °C in chloroform; $\lambda_{ex} = 343$ nm, $\lambda_{em} = 397$ nm.

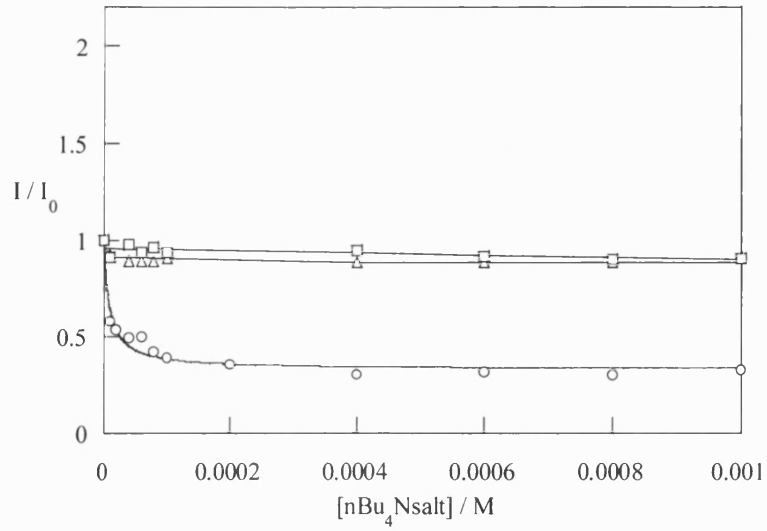

Appendix 21. Relative Fluorescence Intensity (I / I_0) of sensor **12** (5×10^{-7} M) *versus* nBu_4NF (○), nBu_4NCl (Δ) and nBu_4NBr (□) at 25 °C in chloroform; $\lambda_{ex} = 343$ nm, $\lambda_{em} = 397$ nm.

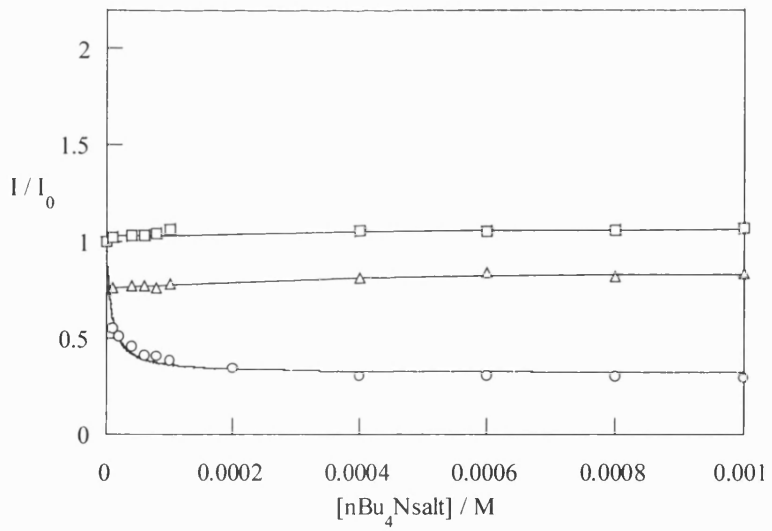

Appendix 22. Relative Fluorescence Intensity (I / I_0) of sensor **9** (5×10^{-7} M) *versus* nBu_4NF (○), nBu_4NCl (Δ) and nBu_4NBr (□) at 25 °C in chloroform; $\lambda_{ex} = 343$ nm, $\lambda_{em} = 397$ nm.

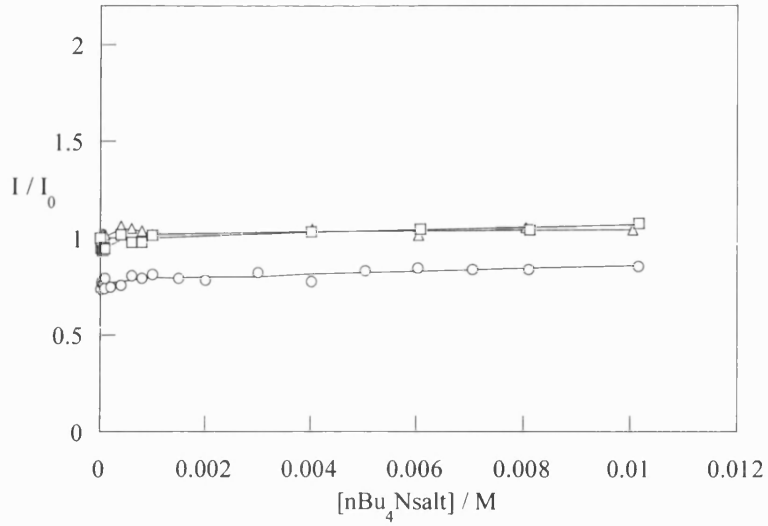

Appendix 23. Relative Fluorescence Intensity (I / I_0) of sensor **10** (5×10^{-7} M) *versus* nBu_4NF (○), nBu_4NCl (Δ) and nBu_4NBr (□) at 25 °C in chloroform; $\lambda_{ex} = 343$ nm, $\lambda_{em} = 397$ nm.

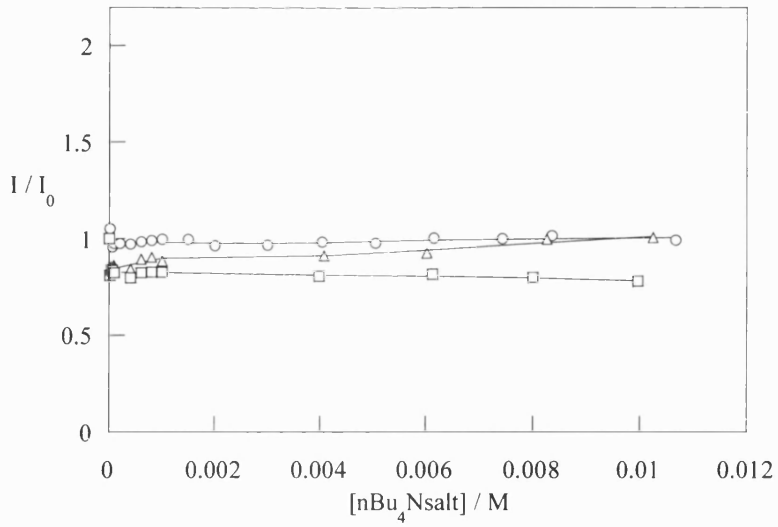

6.3 Potassium halide fluorescence titrations

Appendix 24: Fluorescence Intensity (I_F) of sensor **1** (5×10^{-7} mol dm^{-3}) with increasing concentration of KF in MeOH. λ_{ex} = 345 nm.

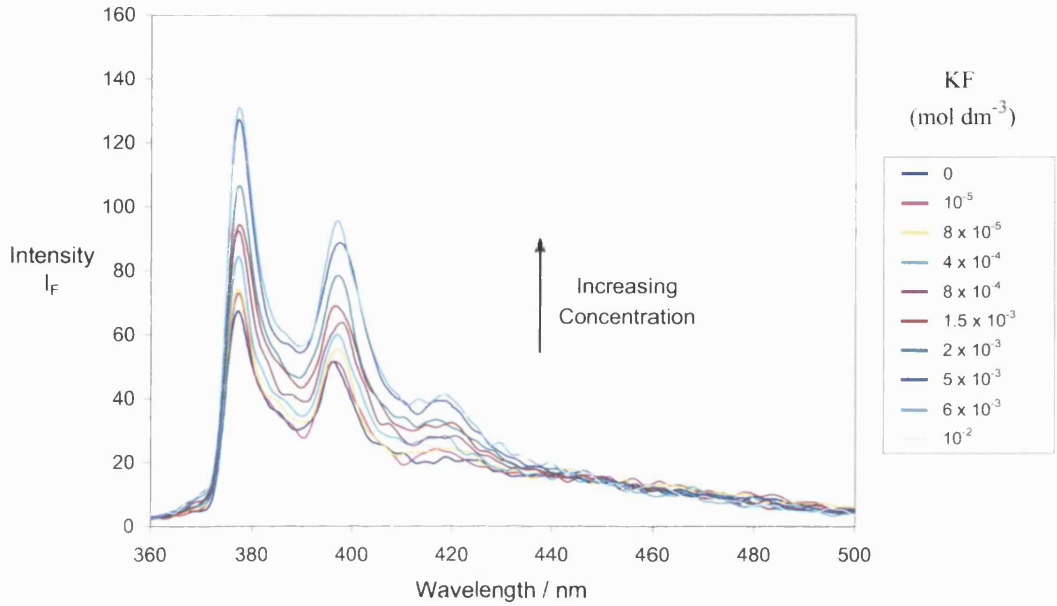

Appendix 25: Fluorescence Intensity (I_F) of sensor **2** (5×10^{-7} mol dm^{-3}) with increasing concentration of KF in MeOH. λ_{ex} = 347 nm.

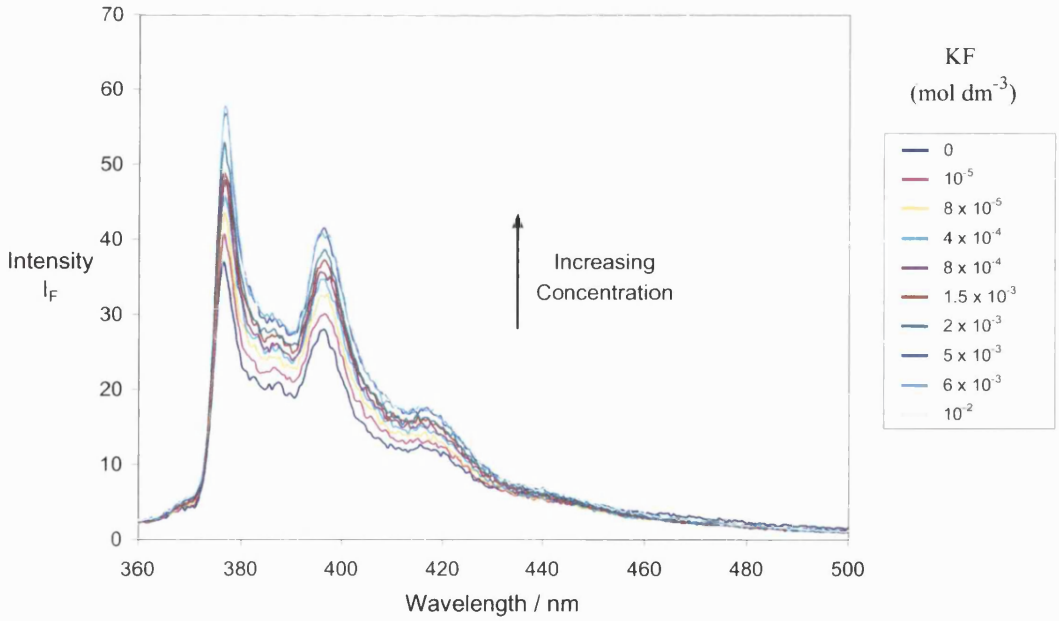

Appendix 26. Relative Fluorescence Intensity (I / I_0) of sensor **1** (5×10^{-7} M) *versus* KF (○), KCl (Δ) and KBr (□) at 25 °C in methanol; $\lambda_{ex} = 345$ nm, $\lambda_{em} = 397$ nm.

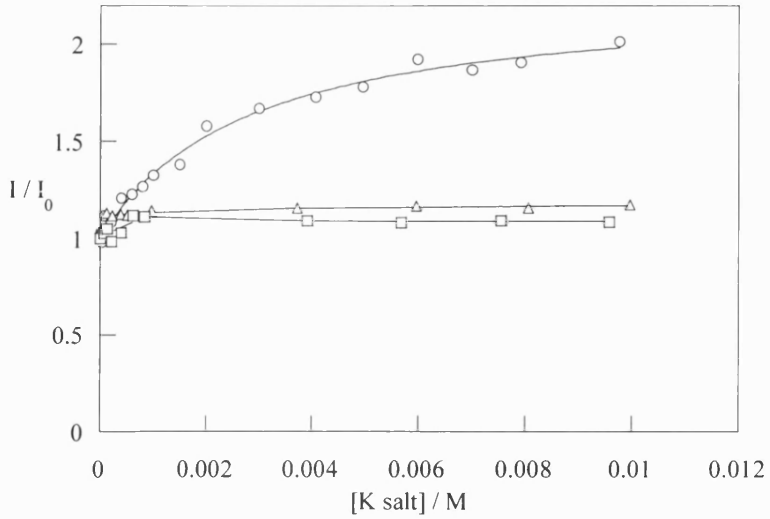

Appendix 27. Relative Fluorescence Intensity (I / I_0) of sensor **2** (5×10^{-7} M) *versus* KF (○), KCl (Δ) and KBr (□) at 25 °C in methanol; $\lambda_{ex} = 347$ nm, $\lambda_{em} = 397$ nm.

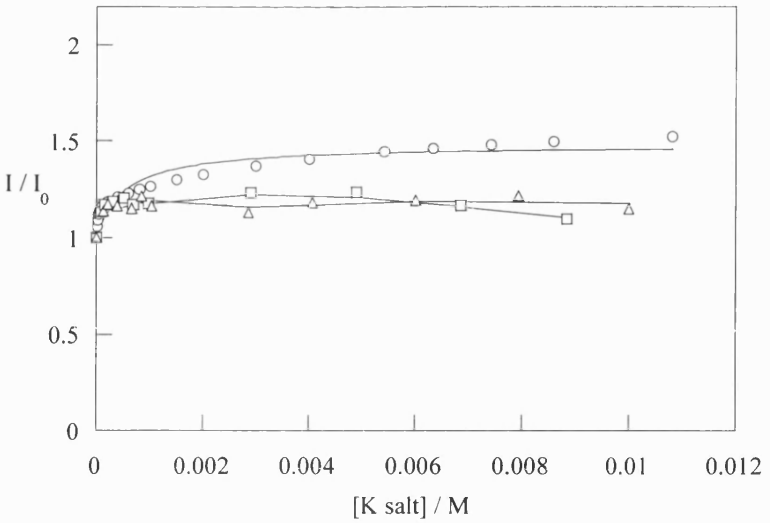

Appendix 28. Relative Fluorescence Intensity (I / I_0) of sensor **5** (5×10^{-7} M) *versus* KF (○), KCl (Δ) and KBr (□) at 25 °C in methanol; $\lambda_{ex} = 341$ nm, $\lambda_{em} = 397$ nm.

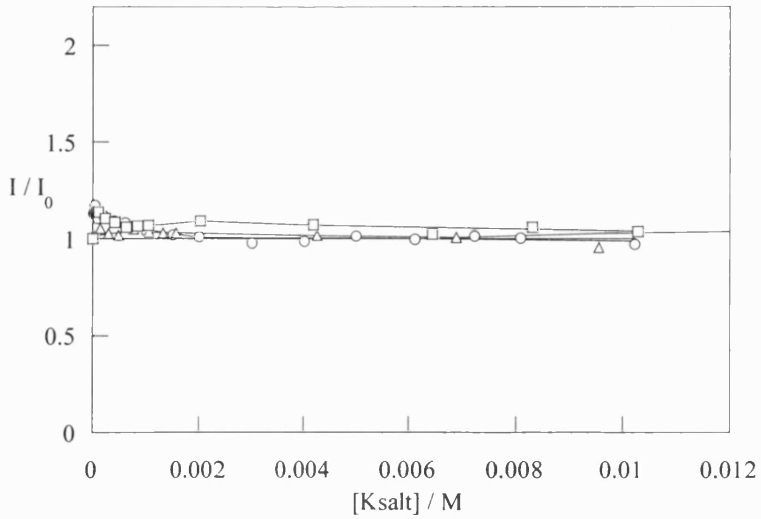

Appendix 29. Relative Fluorescence Intensity (I / I_0) of sensor **6** (5×10^{-7} M) *versus* KF (○), KCl (Δ) and KBr (□) at 25 °C in methanol; $\lambda_{ex} = 341$ nm, $\lambda_{em} = 397$ nm.

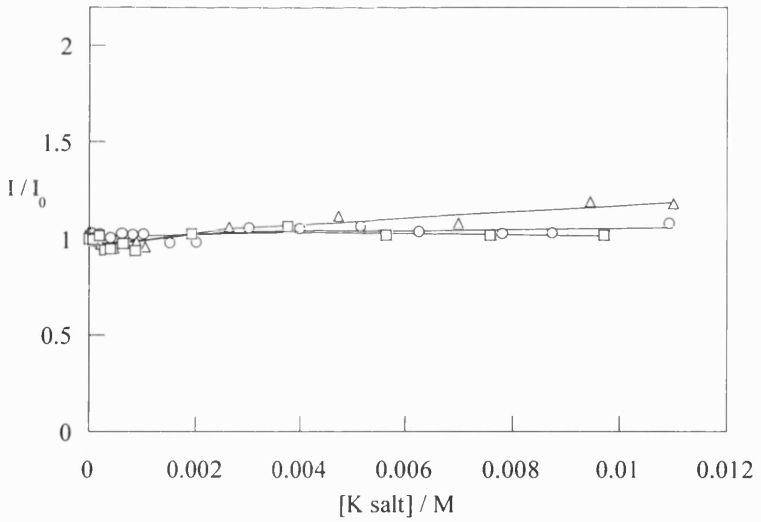

Appendix 30. Relative Fluorescence Intensity (I / I_0) of sensor **7** (5×10^{-7} M) *versus* KF (○), KCl (Δ) and KBr (□) at 25 °C in methanol; $\lambda_{ex} = 343$ nm, $\lambda_{em} = 397$ nm.

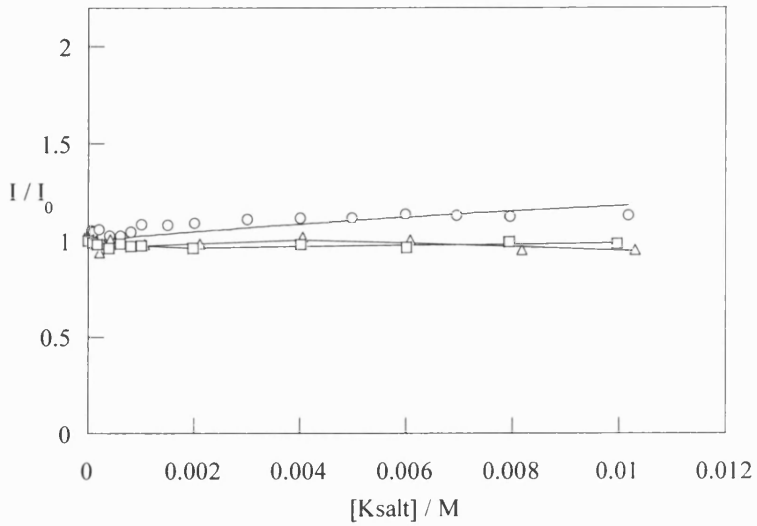

Appendix 31. Relative Fluorescence Intensity (I / I_0) of sensor **8** (5×10^{-7} M) *versus* KF (○), KCl (Δ) and KBr (□) at 25 °C in methanol; $\lambda_{ex} = 342$ nm, $\lambda_{em} = 397$ nm.

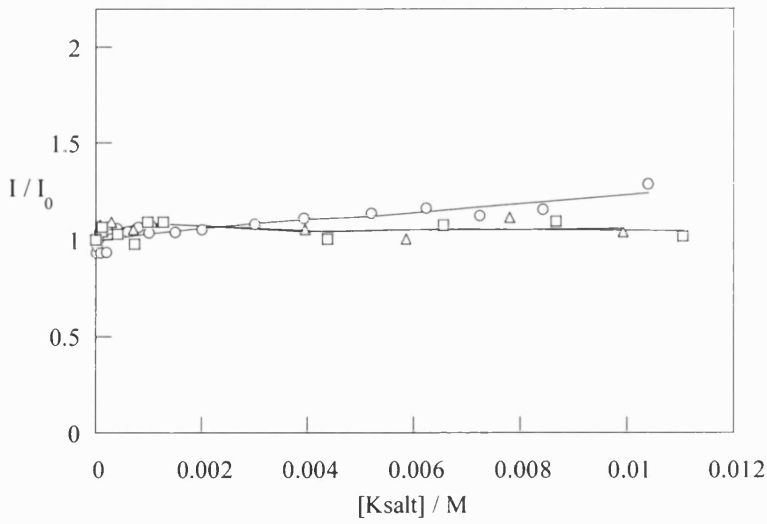

6.4 Caesium halide fluorescence titrations

Appendix 32. Fluorescence Intensity (I_F) of sensor **1** (5×10^{-7} mol dm^{-3}) with increasing concentration of CsF in MeOH. λ_{ex} = 230 nm, λ_{em} = 335 nm.

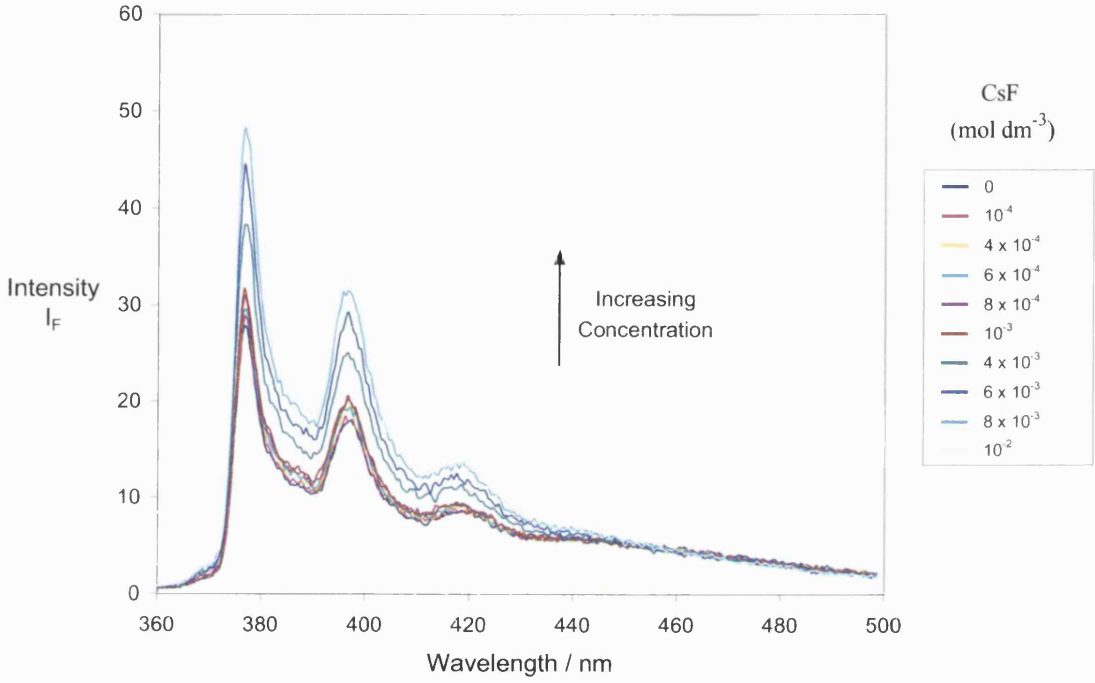

Appendix 33. Fluorescence Intensity (I_F) of sensor **2** (5×10^{-7} mol dm^{-3}) with increasing concentration of CsF in MeOH. λ_{ex} = 230 nm, λ_{em} = 335 nm.

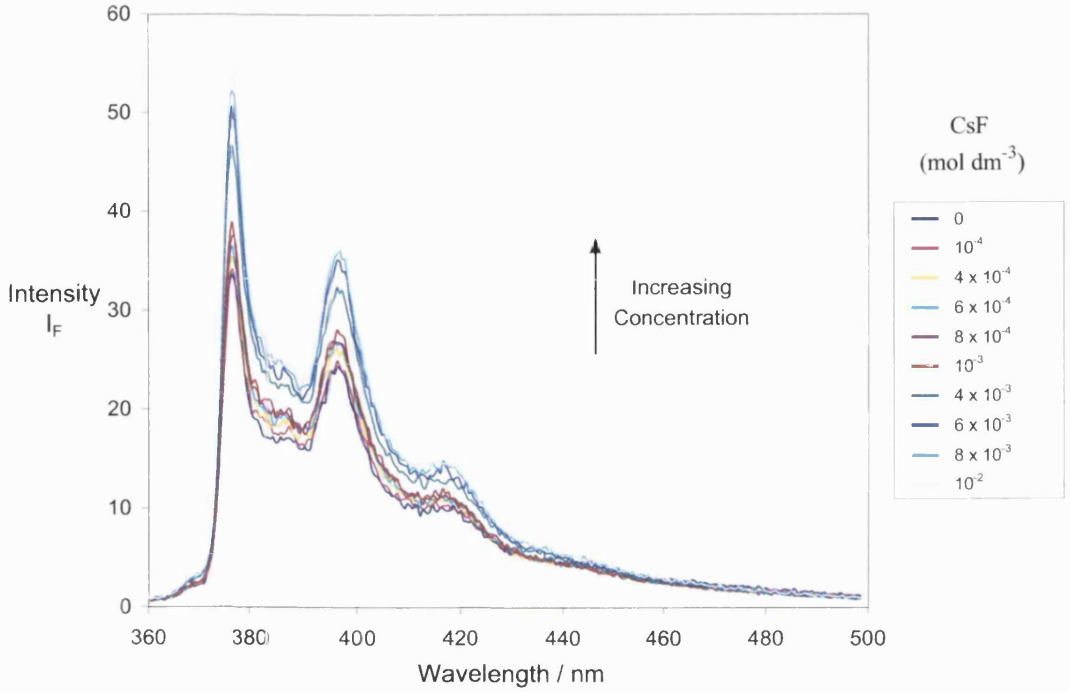

Appendix 34. Relative Fluorescence Intensity (I / I_0) of sensor **1** (5×10^{-7} M) *versus* CsF (○), CsCl (Δ) and CsBr (□) at 25 °C in methanol; λ_{ex} = 342 nm, λ_{em} = 397 nm.

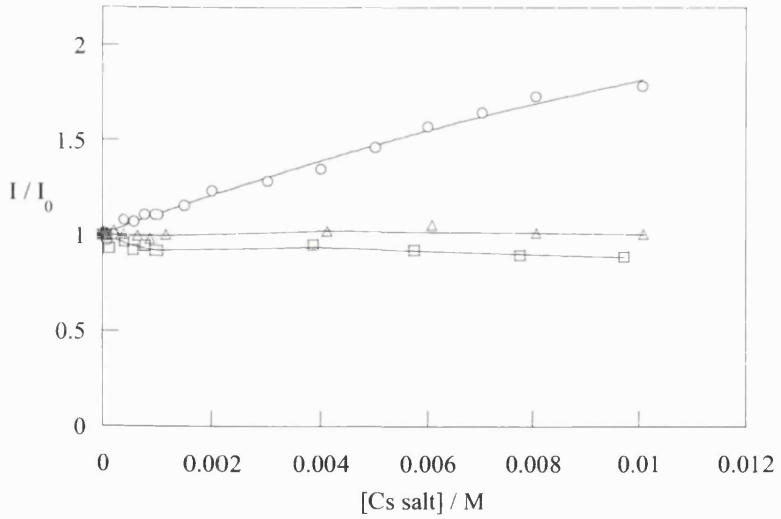

Appendix 35. Relative Fluorescence Intensity (I / I_0) of sensor **2** (5×10^{-7} M) *versus* CsF (○), CsCl (Δ) and CsBr (□) at 25 °C in methanol; $\lambda_{ex} = 342$ nm, $\lambda_{em} = 397$ nm.

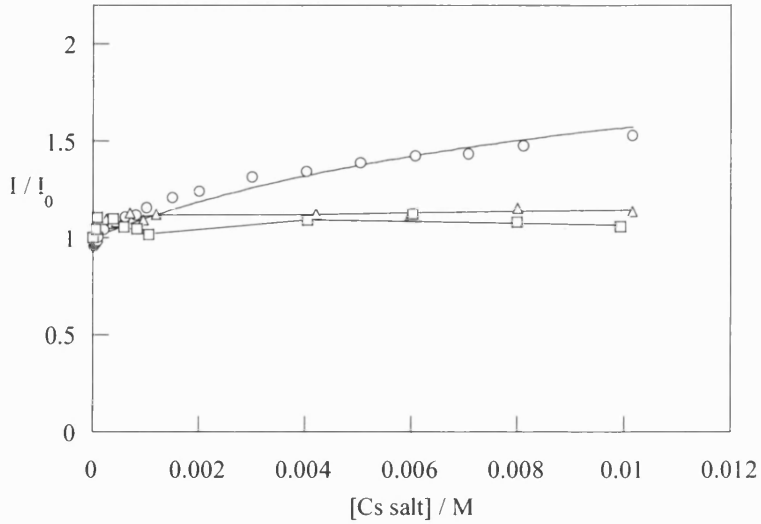

Appendix 36. Relative Fluorescence Intensity (I / I_0) of sensor **5** (5×10^{-7} M) *versus* CsF (○), CsCl (Δ) and CsBr (□) at 25 °C in methanol; $\lambda_{ex} = 342$ nm, $\lambda_{em} = 397$ nm.

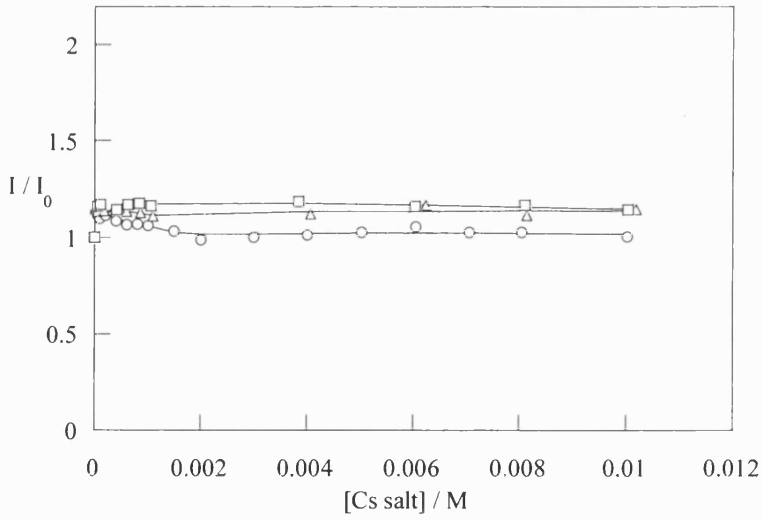

Appendix 37. Relative Fluorescence Intensity (I / I_0) of sensor **6** (5×10^{-7} M) *versus* CsF (○), CsCl (Δ) and CsBr (□) at 25 °C in methanol; $\lambda_{ex} = 342$ nm, $\lambda_{em} = 397$ nm.

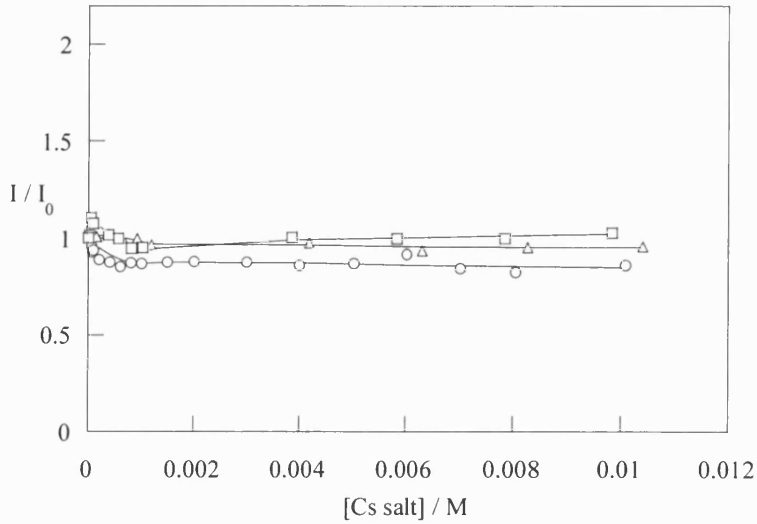

Appendix 38. Relative Fluorescence Intensity (I / I_0) of sensor **7** (5×10^{-7} M) *versus* CsF (○), CsCl (Δ) and CsBr (□) at 25 °C in methanol; $\lambda_{ex} = 342$ nm, $\lambda_{em} = 397$ nm.

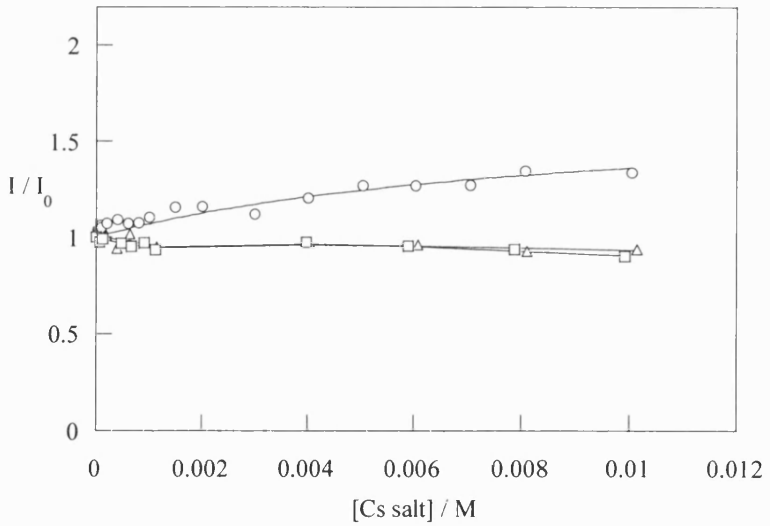

Appendix 39. Relative Fluorescence Intensity (I / I_0) of sensor **8** (5×10^{-7} M) *versus* CsF (○), CsCl (Δ) and CsBr (□) at 25 °C in methanol; λ_{ex} = 342 nm, λ_{em} = 397 nm.

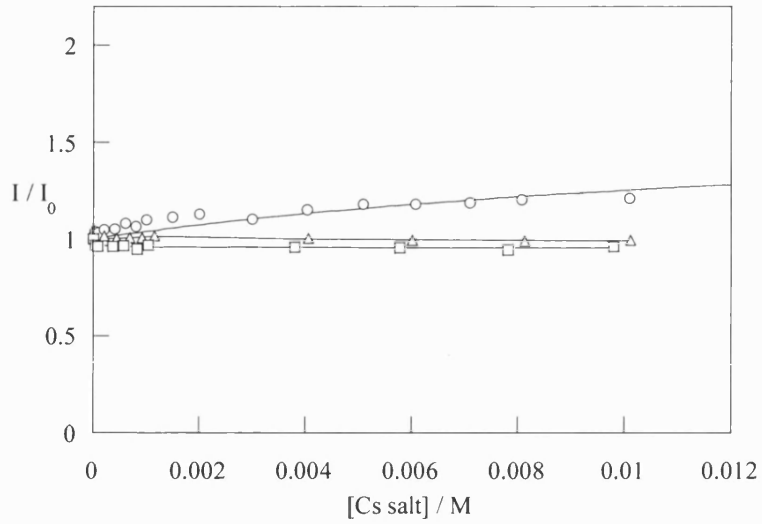

6.5 Potassium fluoride titrations with Naphthalene series

Appendix 40. Fluorescence Intensity (I_F) of sensor **3** (5×10^{-7} mol dm^{-3}) with increasing concentration of KF in MeOH. λ_{ex} = 230 nm, λ_{em} = 335 nm.

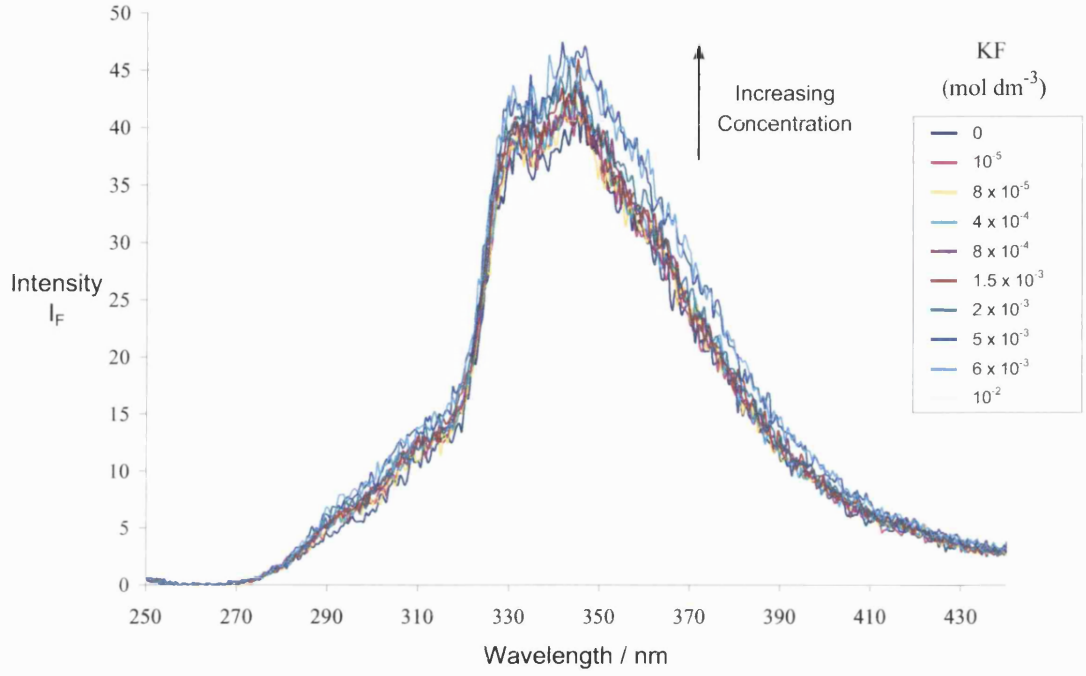

Appendix 41. Relative Fluorescence Intensity (I / I_0) of sensor **3** (5×10^{-7} M) *versus* KF (○), KCl (Δ) and KBr (□) at 25 °C in methanol; λ_{ex} = 230 nm, λ_{em} = 335 nm.

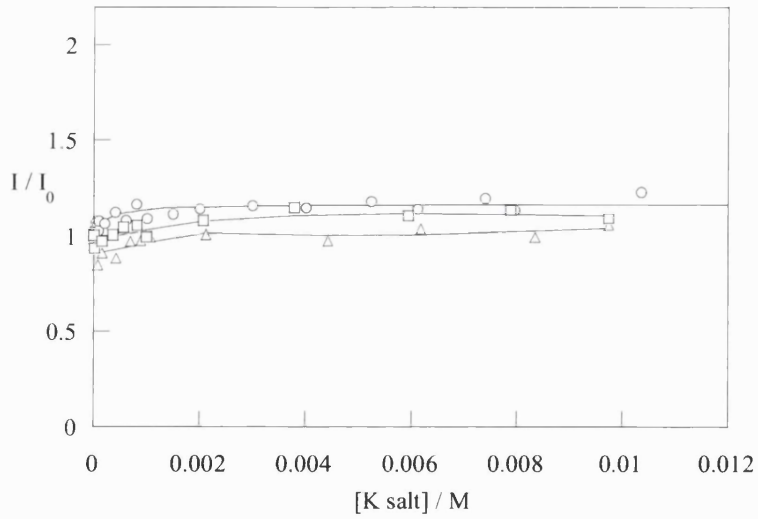

Appendix 42. Relative Fluorescence Intensity (I / I_0) of sensor **4** (5×10^{-7} M) *versus* KF (○), KCl (Δ) and KBr (□) at 25 °C in methanol; $\lambda_{ex} = 288$ nm, $\lambda_{em} = 335$ nm.

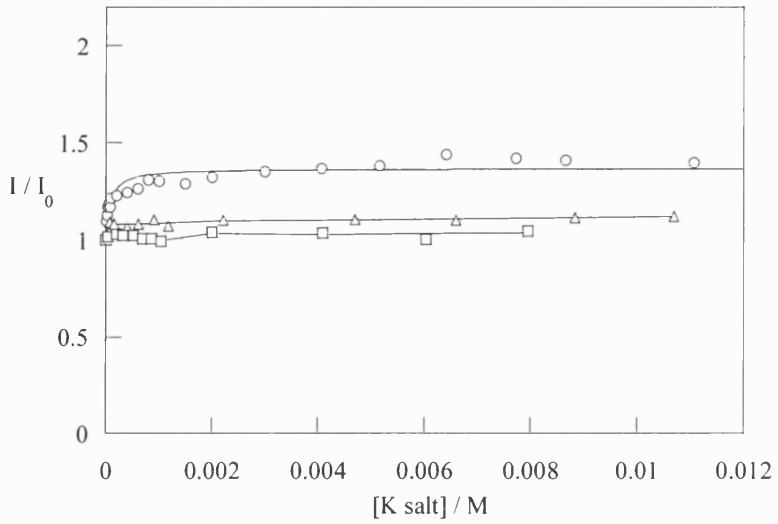

Appendix 43. Relative Fluorescence Intensity (I / I_0) of sensor **9** (5×10^{-7} M) *versus* KF (○), KCl (Δ) and KBr (□) at 25 °C in methanol; $\lambda_{ex} = 310$ nm, $\lambda_{em} = 335$ nm.

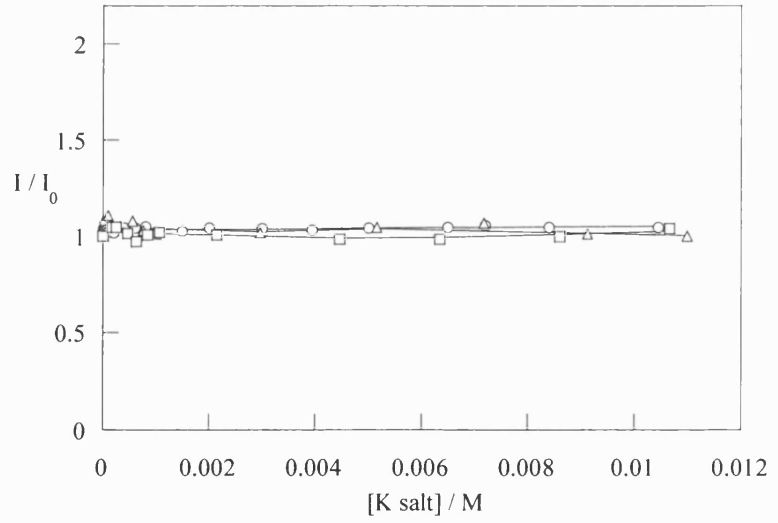

Appendix 44. Relative Fluorescence Intensity (I / I_0) of sensor **10** (5×10^{-7} M) *versus* KF (○), KCl (Δ) and KBr (□) at 25 °C in methanol; $\lambda_{ex} = 288$ nm, $\lambda_{em} = 335$ nm.

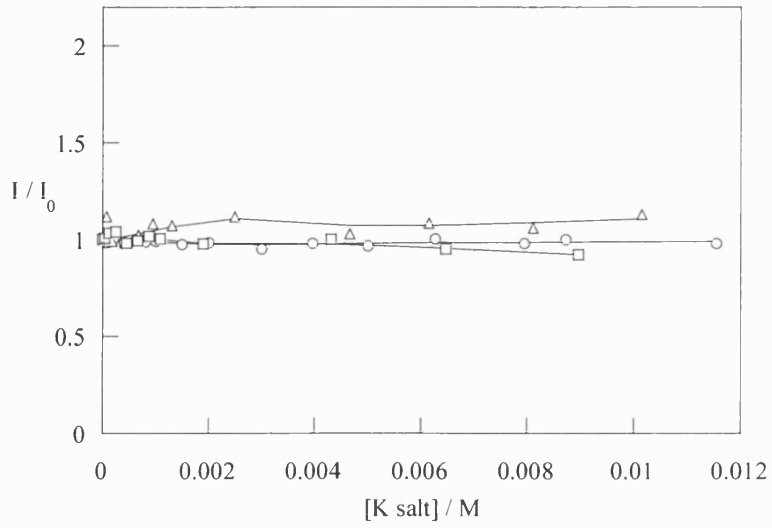

Appendix 45. Relative Fluorescence Intensity (I / I_0) of sensor **11** (5×10^{-7} M) *versus* KF (○), KCl (Δ) and KBr (□) at 25 °C in methanol; $\lambda_{ex} = 230$ nm, $\lambda_{em} = 335$ nm.

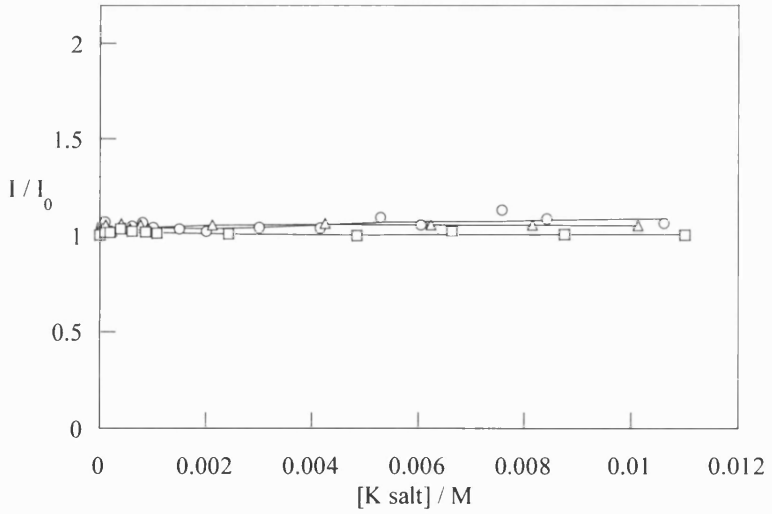

Appendix 46. Relative Fluorescence Intensity (I / I_0) of sensor **12** (5×10^{-7} M) *versus* KF (○), KCl (Δ) and KBr (□) at 25 °C in methanol; $\lambda_{ex} = 288$ nm, $\lambda_{em} = 335$ nm.

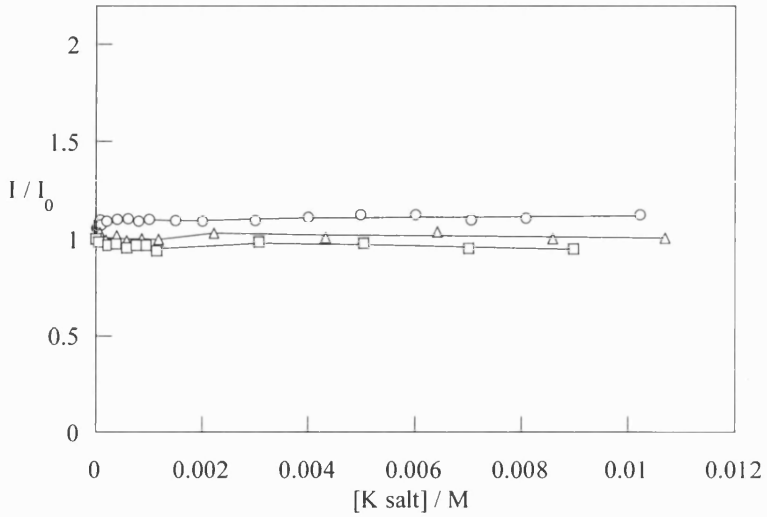

6.6 Sodium halide fluorescence titrations

Appendix 47. Relative Fluorescence Intensity (I / I_0) of sensor **1** (5×10^{-7} M) *versus* NaF (○), NaCl (Δ) and NaBr (□) at 25 °C in methanol; $\lambda_{ex} = 230$ nm, $\lambda_{em} = 335$ nm.

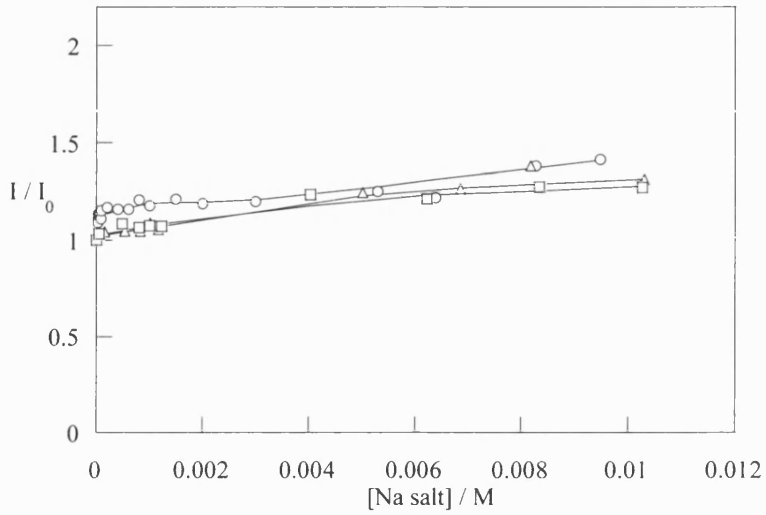

Appendix 48. Relative Fluorescence Intensity (I / I_0) of sensor **2** (5×10^{-7} M) *versus* NaF (○), NaCl (Δ) and NaBr (□) at 25 °C in methanol; $\lambda_{ex} = 288$ nm, $\lambda_{em} = 335$ nm.

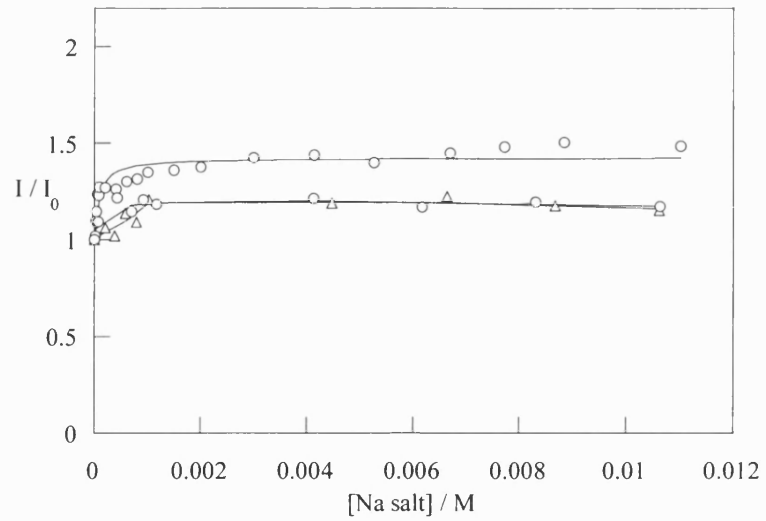

6.7 'Off-On' action

Appendix 49. Fluorescence Intensity (I_F) of sensor **1** (5×10^{-7} mol dm^{-3}) with added guests in MeOH. λ_{ex} = 345 nm, λ_{em} = 397 nm.

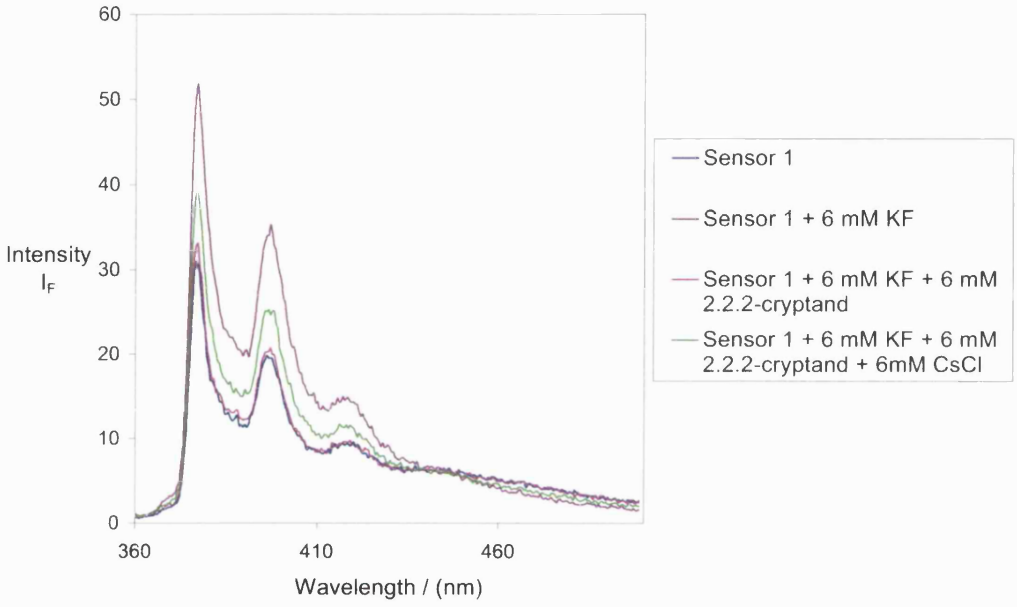

Appendix 50. Fluorescence Intensity (I_F) of sensor **1** (5×10^{-7} mol dm^{-3}) with added guests in MeOH. λ_{ex} = 345 nm, λ_{em} = 397 nm.

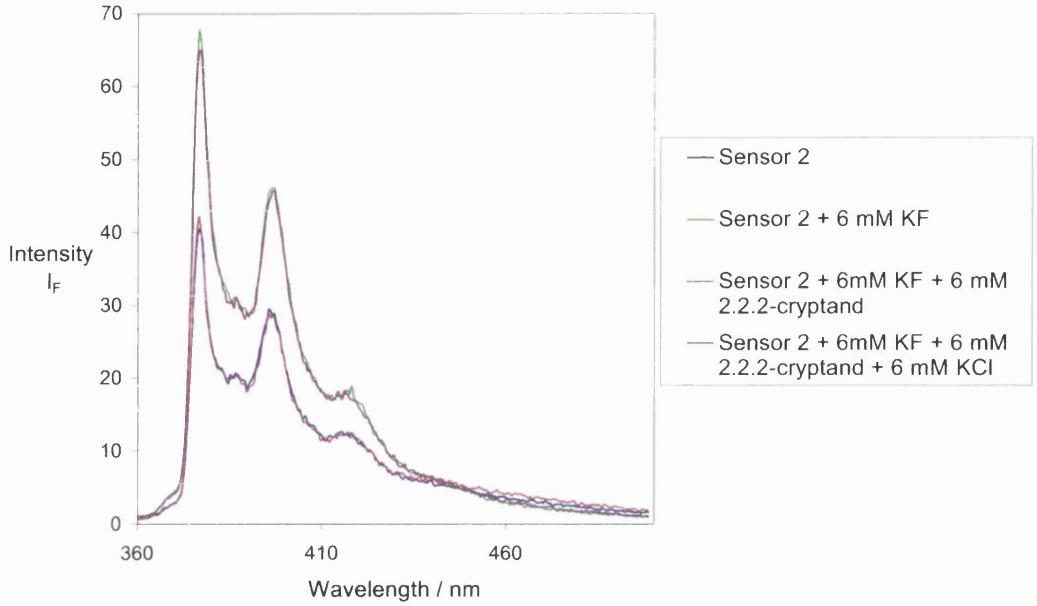

Appendix 51. Fluorescence Intensity (I_F) of sensor 1 (5×10^{-7} mol dm^{-3}) with added guests in MeOH. λ_{ex} = 345 nm, λ_{em} = 397 nm.